Otranto School

XXXII International Seminar of Nuclear and Subnuclear Physics
“Francesco Romano”

Gravitational Waves
part 3: observatory and results

Giovanni A. Prodi, Università di Trento and INFN-TIFPA, Trento

giovanniandrea.prodi@unitn.it

UNIVERSITÀ DI TRENTO

INFN Istituto Nazionale di Fisica Nucleare

TIFPA Trento Institute for Fundamental Physics and Applications

Directional Sensitivity of Detectors

Each interferometer senses only one of the two GW polarizations:

- measures the linear combination

$$h_{det} = F_+ h_+ + F_\times h_\times$$

$$F_{+,\times}(\text{sky direction})$$

antenna patterns for + and x

- misses the orthogonal combination

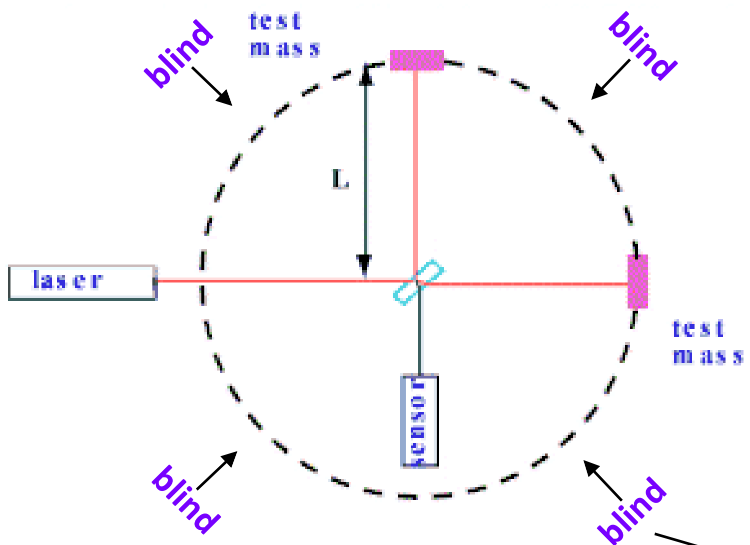

Broad directional sensitivity:

LIGO Livingston

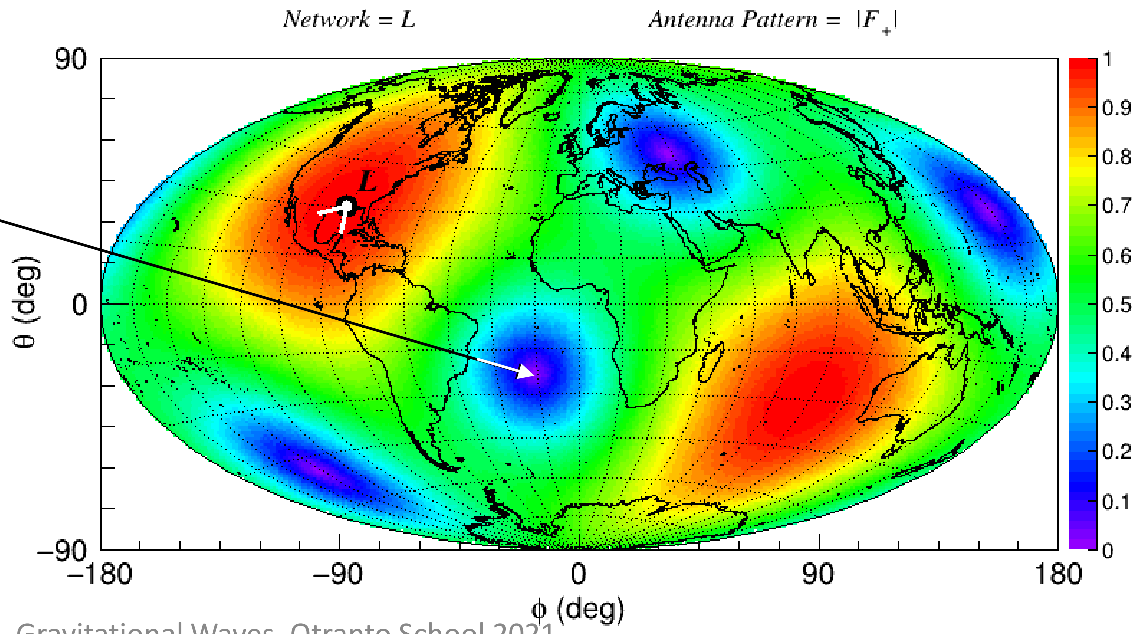

Antenna pattern

- the “scalar input” of the detector for a GW wavefront of generic direction:

  $h(t) = D_{ij} h_{ij}(t)$ where D_{ij} is the detector tensor
- for an IFO with arms aligned with the $\hat{x}$ and $\hat{y}$ axes (lab frame) is:

$$D_{ij} = \frac{1}{2}\left(\hat{x}_i \hat{x}_j - \hat{y}_i \hat{y}_j\right) \Rightarrow h(t) = \frac{1}{2}\left(h_{xx} - h_{yy}\right)$$

- A generic impinging GW wave h'_{kl} transforms by rotation

$$R = \begin{pmatrix} \cos\phi & \sin\phi & 0 \\ -\sin\phi & \cos\phi & 0 \\ 0 & 0 & 0 \end{pmatrix} \begin{pmatrix} \cos\theta & 0 & \sin\theta \\ 0 & 0 & 0 \\ -\sin\theta & 0 & \cos\theta \end{pmatrix}$$

- Thus, since $h_{ij} = (R^T h' R)ij = R_{ik}\, R_{jl} h'_{kl}$:

$$h_{xx} = h_+\left(\cos^2\theta\cos^2\phi - \sin^2\phi\right) + 2h_\times \cos\theta \sin\phi\cos\phi$$
$$h_{yy} = h_+\left(\cos^2\theta\cos^2\phi - \cos^2\phi\right) - 2h_\times \cos\theta \sin\phi\cos\phi \quad \Rightarrow$$

Remember: $\cos^2 x = \frac{1+\cos 2x}{2}, \sin^2 x = \frac{1-\cos 2x}{2}$

$$\Rightarrow h(t) = F_+(\theta,\phi) h_+ + F_\times(\theta,\phi) h_\times, \begin{cases} F_+(\theta,\phi) = \frac{1}{2}\left(1+\cos^2\theta\right)\cos 2\phi \\ F_\times(\theta,\phi) = \cos\theta\sin 2\phi \end{cases}$$

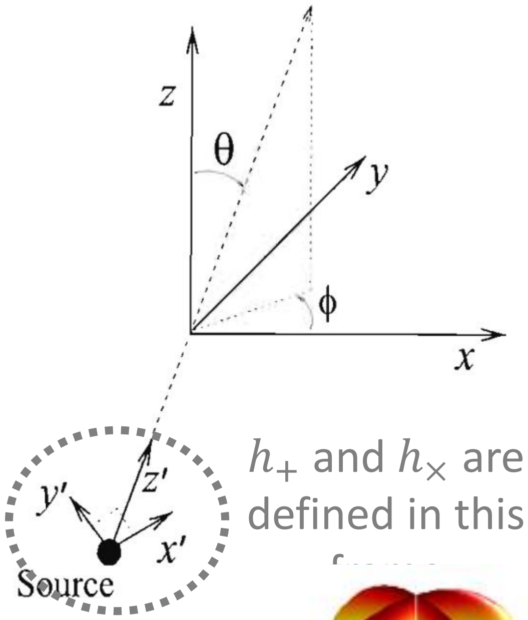

h_+ and $h_\times$ are defined in this

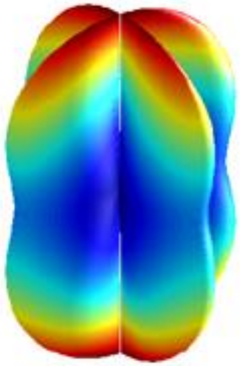

$F_+(\theta,\phi)$

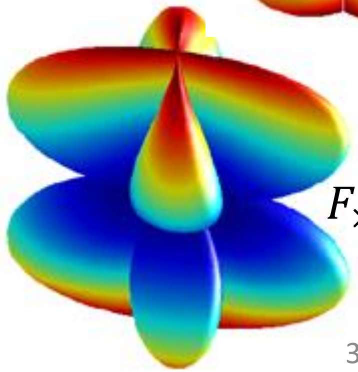

$F_\times(\theta,\phi)$

The LIGO network of two detectors

- **Detection confidence: discriminate GW candidates from noise fluctuations**
  - ✓ **At least two detectors in coincidence observation are required**
    unless for searches of persistent and/or well parametrized signals, e.g. periodic GWs or strong Compact Binary Coalescences
  - ✓ multimessenger searches with other detectors can help

LIGOs arms are almost aligned

- **Sky coverage of LIGOs is very similar to that of a single detector**

$\Rightarrow$ **almost blind to one GW polarization per each direction:**

$|\vec{F}_{+}|$ LIGO Hanford + LIGO Livingston $|\vec{F}_{\times}|$

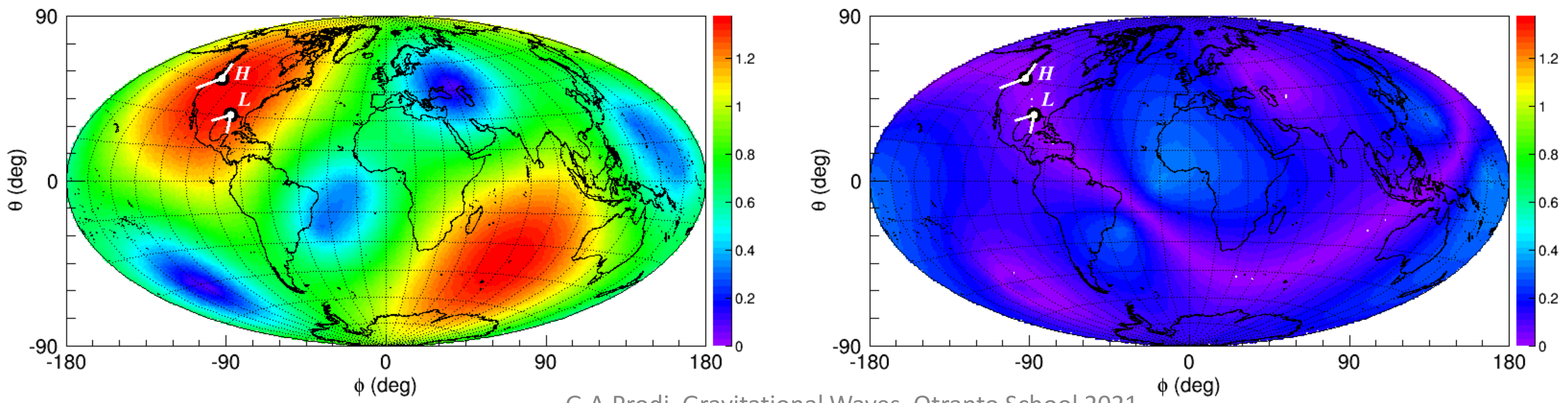

Benefits of adding Virgo detector

- **sky localization of the source**:
triangulation by arrival times at detectors + amplitude consistency

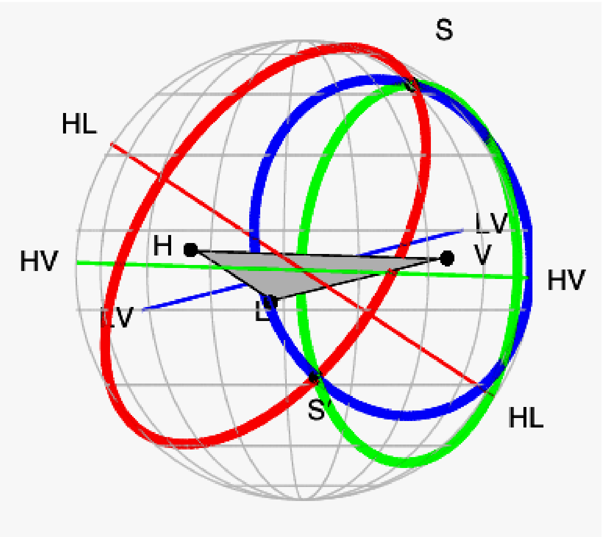

- Increased **time coverage of the survey** by detector pairs

LIGO H1 + LIGO L1

$|\vec{F}_{+}|$

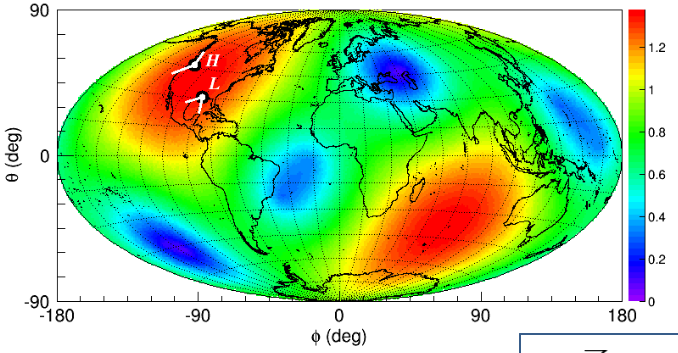

$|\vec{F}_{\times}|$

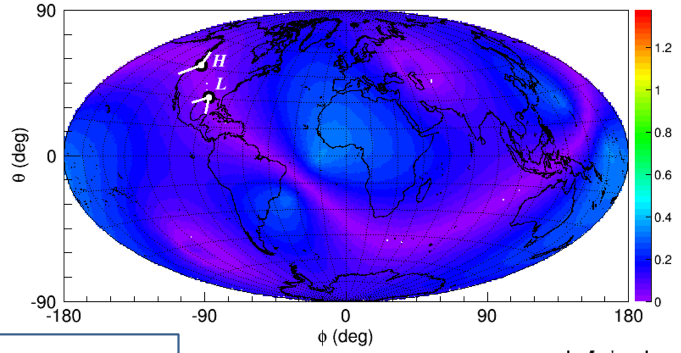

LIGO H1 + LIGO L1 **+ Virgo**

$|\vec{F}_{+}|$

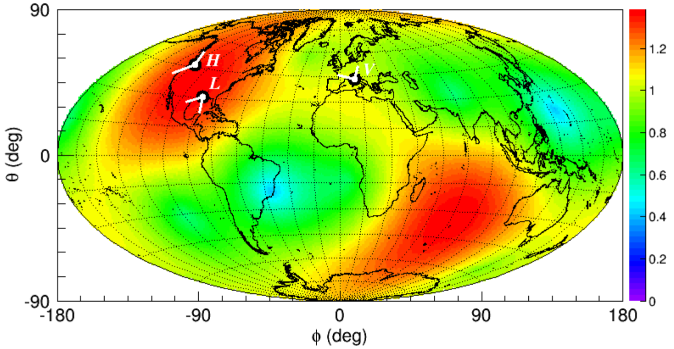

assuming same spectral sensitivity

$|F'_{\times}|$

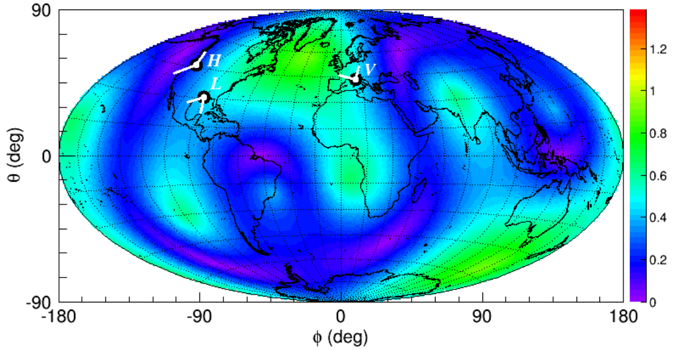

- **coverage of sky and both GW polarizations**: better waveform reconstruction

GW170817 : The best to date 3D Sky Localization

- Rapid Localization results 90% confidence (within hours)
  - **Only LIGO = 190 deg²**
  - **LIGO+Virgo = 31 deg²**
- **Refined localization** (days)
  - **LIGO+Virgo = 28 deg²**
- **Source distance** $\approx 40^{+8}_{-14}$ Mpc
- **Localization volume** $\approx$ 380 Mpc³

  containing about 50 known galaxies

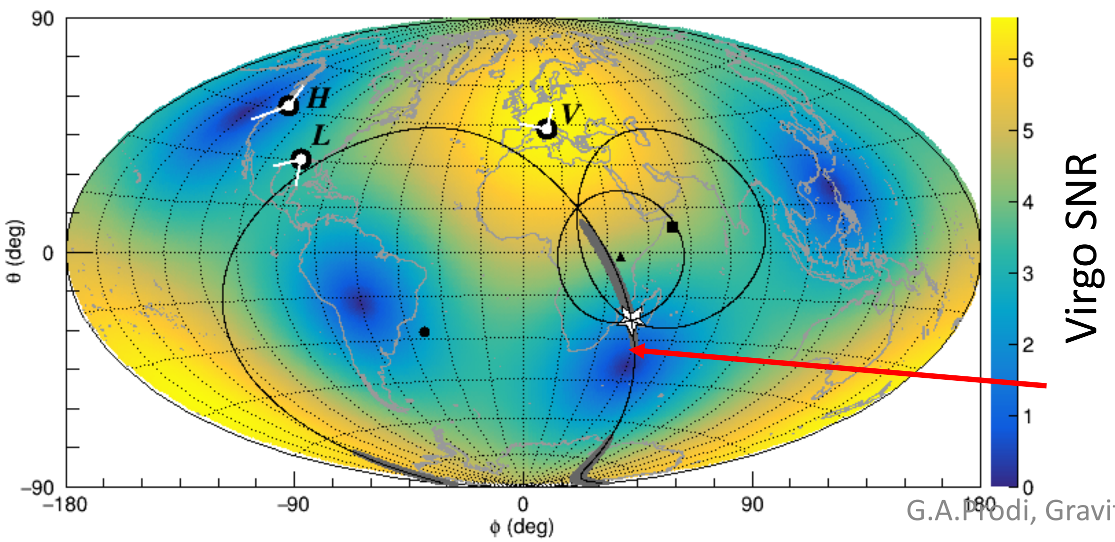

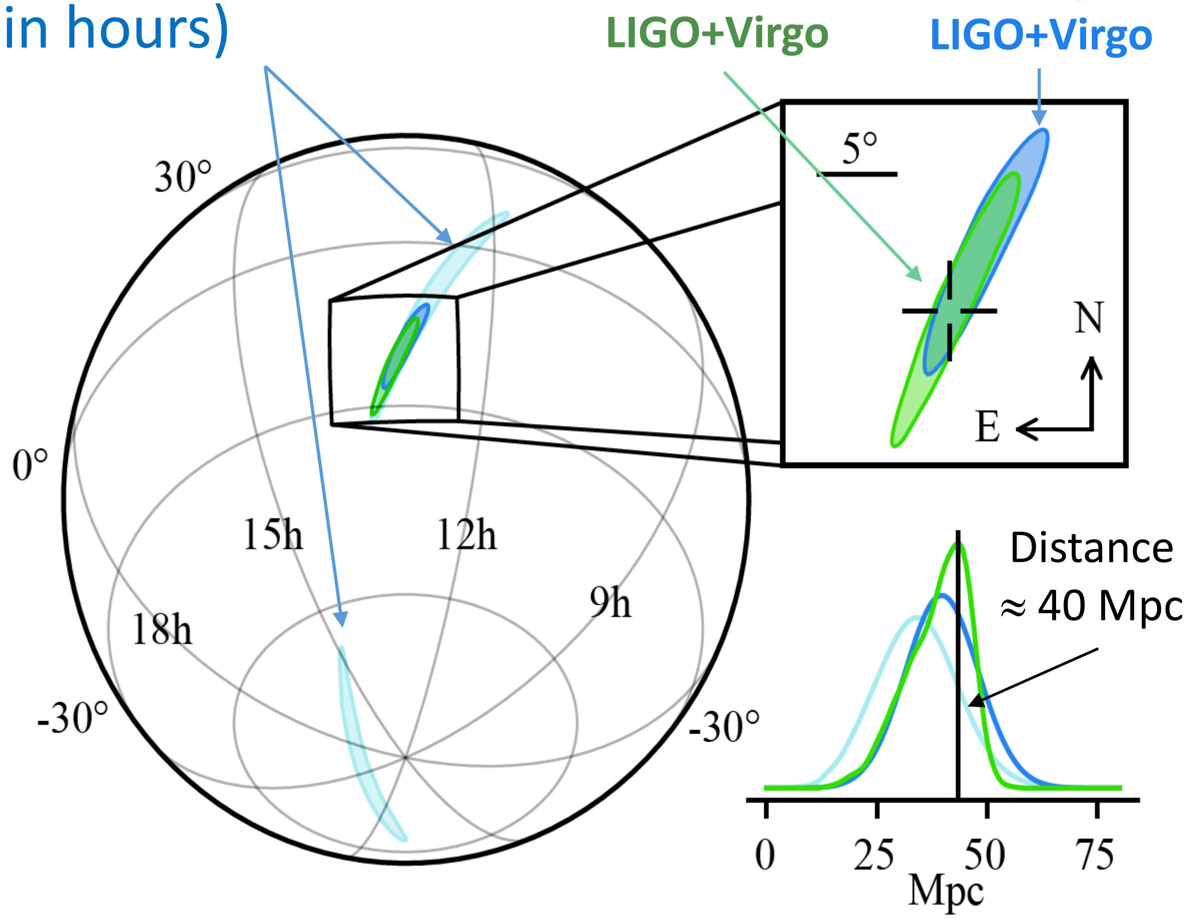

How Virgo Contribute ?

Amplitude consistency of measured signal

The Network of Gravitational Wave Detectors

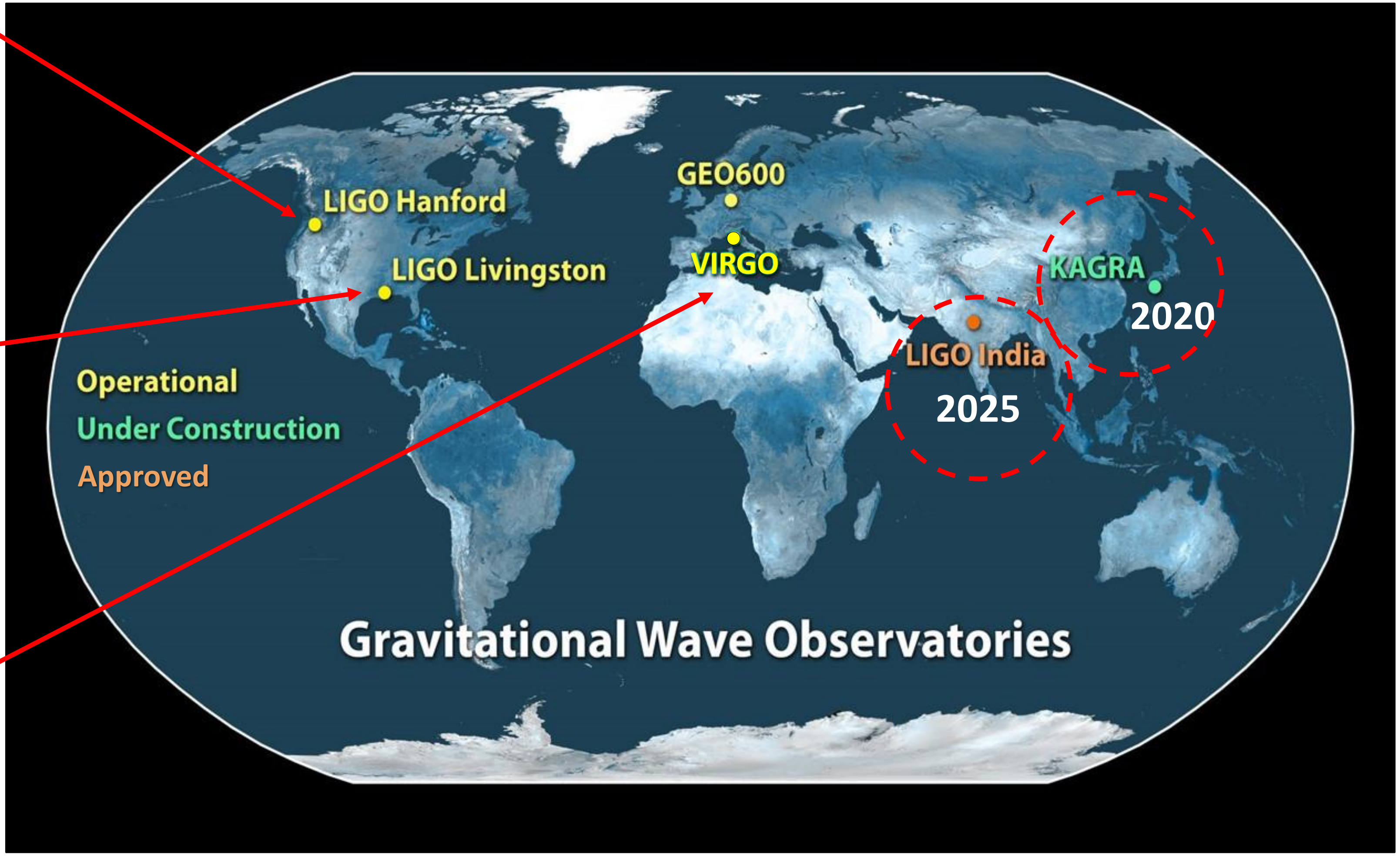

Increase detection confidence

Better source localization

Enhance sky coverage

Reduce downtime

More reliable source parameter estimation

GLOBAL 2019+ NETWORK

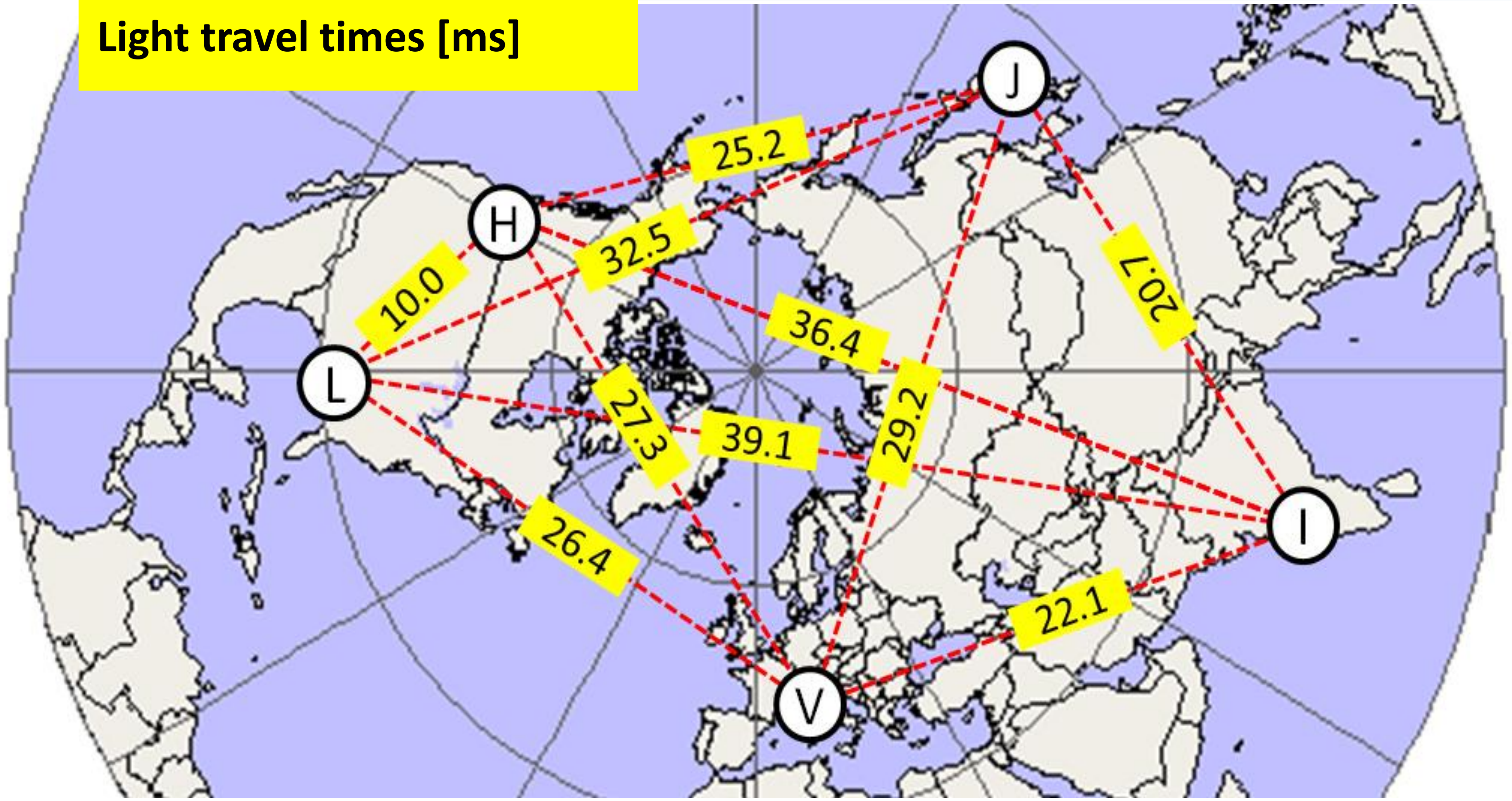

single detector triggers:

- confident multimessenger association with a different astrophysical event (e.g. GRBs, galactic SN neutrinos…)
- strong and well fitted by known signal models (e.g. Compact Binary Coalescences…)

network enables coherent analyses (aperture synthesis):

- background noise reduction
- GW source localization by phase and amplitude consistency
- GW waveform reconstruction

2 GW polarization amplitudes

+

1 incoherent noise residuals

L LIGO Livingston
H LIGO Hanford
V Virgo

3 amplitude stream measurements

Two more interferometers will join:
J KAGRA (Japan, end 2020+)
I LIGO India (A+ timescale and A+ detector class)

GLOBAL 2025+ NETWORK

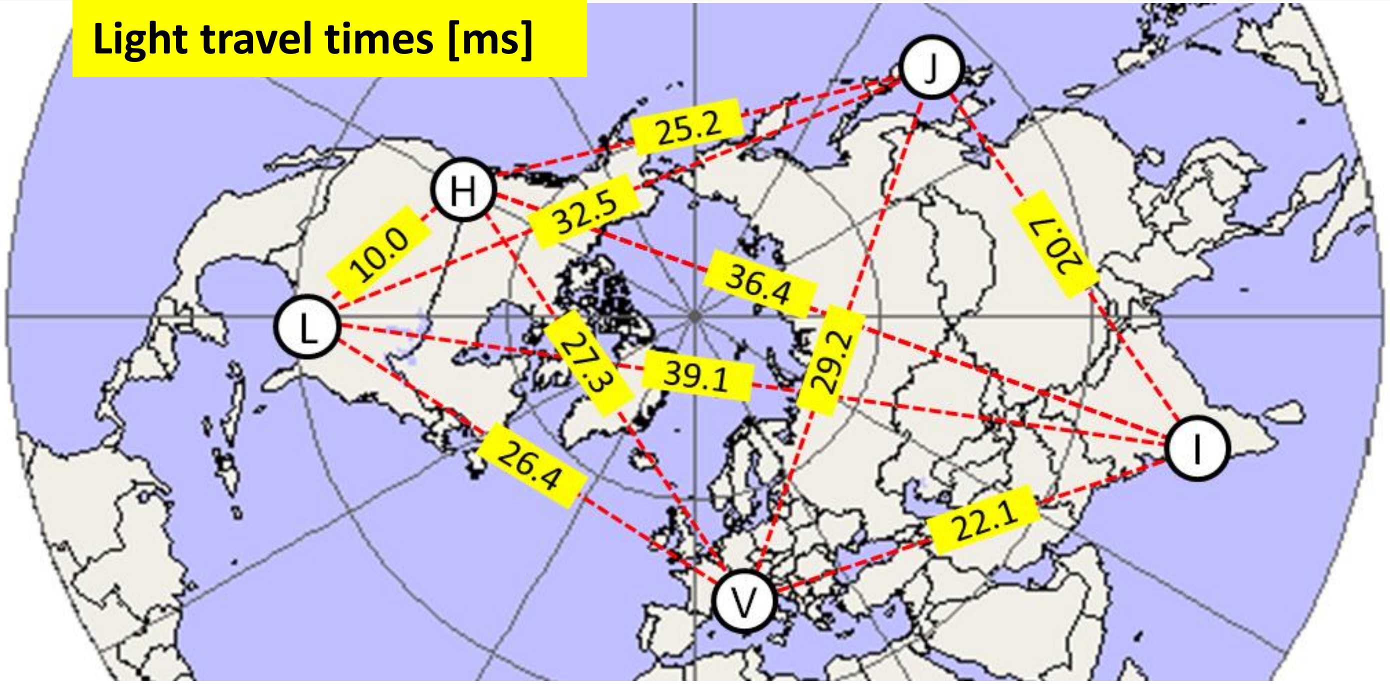

$|\vec{F}_+|$ **sky coverage of the whole observatory** $|\vec{F}_\times|$

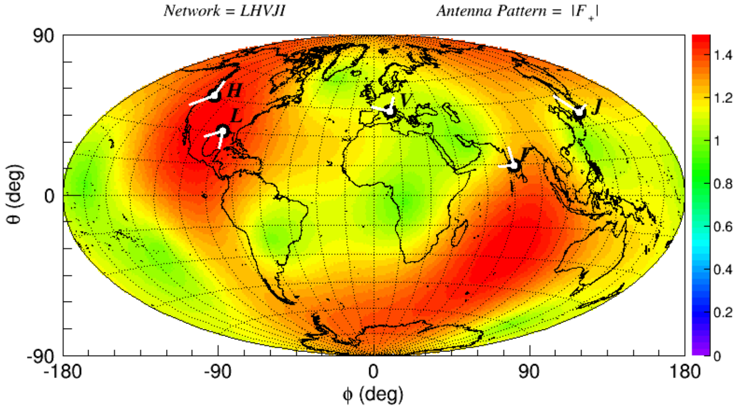

almost omni-directional observatory

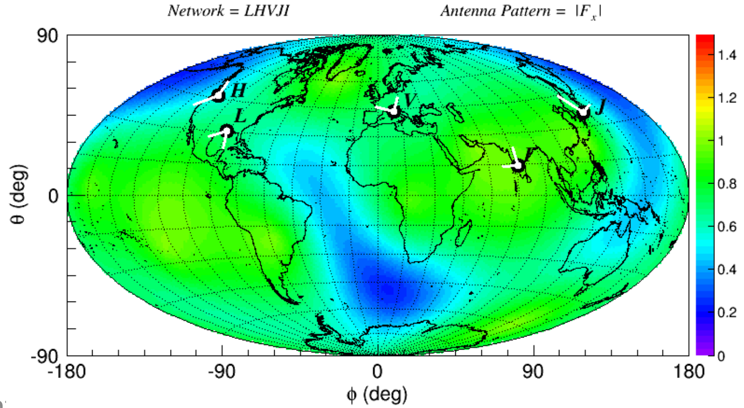

ENSURED SIGNALS

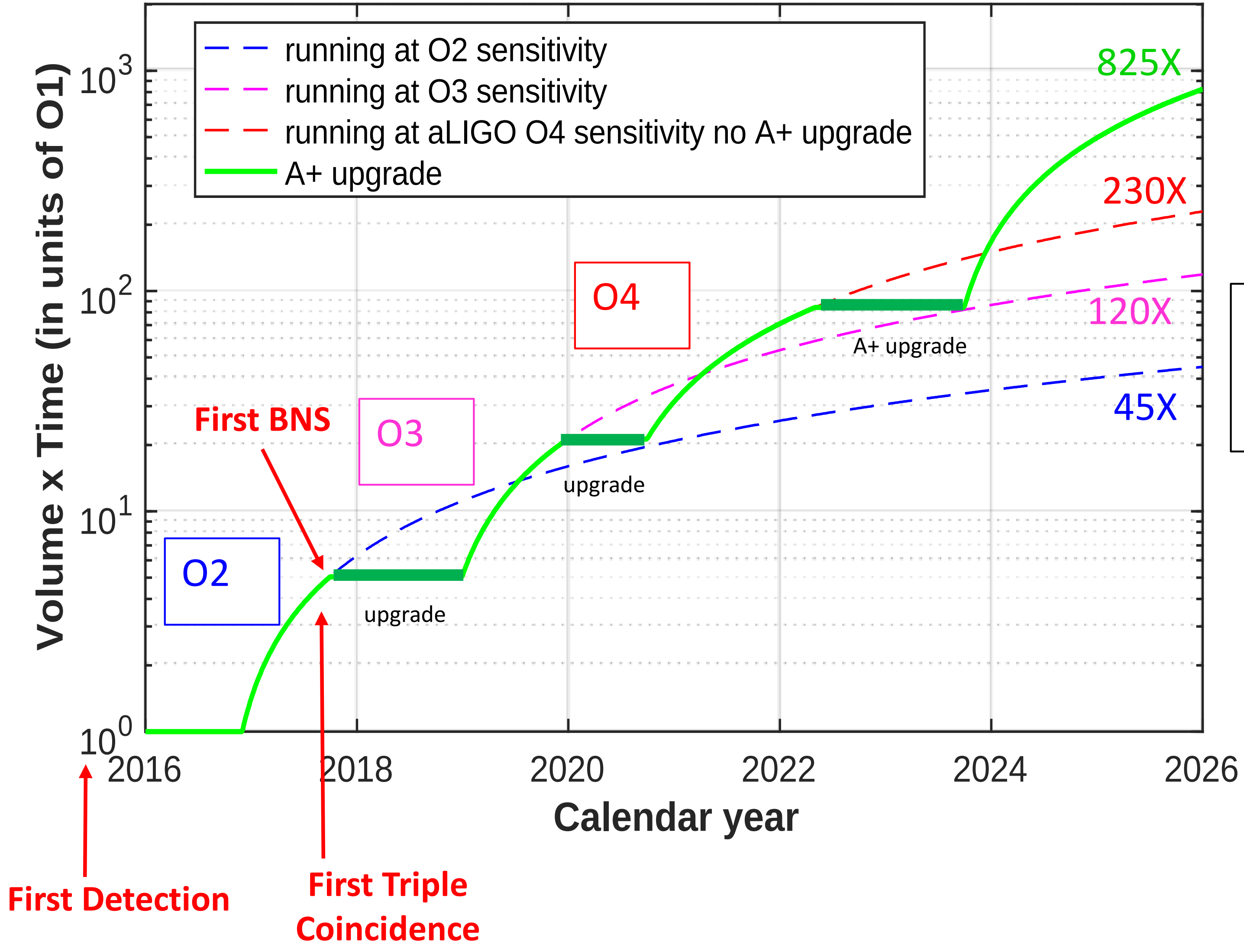

plotted values based on Binary Neutron Stars mergers

similar evolution for other compact object coalescences

N_{events} = <R>**VT** **VT *PRODUCTIVITY***

- <R> average astrophysical rate
- V volume of the universe probed → $(\text{Range})^3$
- T coincident observing time

a step-wise approach of upgrades interleaved by observation runs is the wisest strategy for exploiting the current infrastructures

sources published to date

GWTC 2, Phys. Rev. X 11, 021053 (2021)

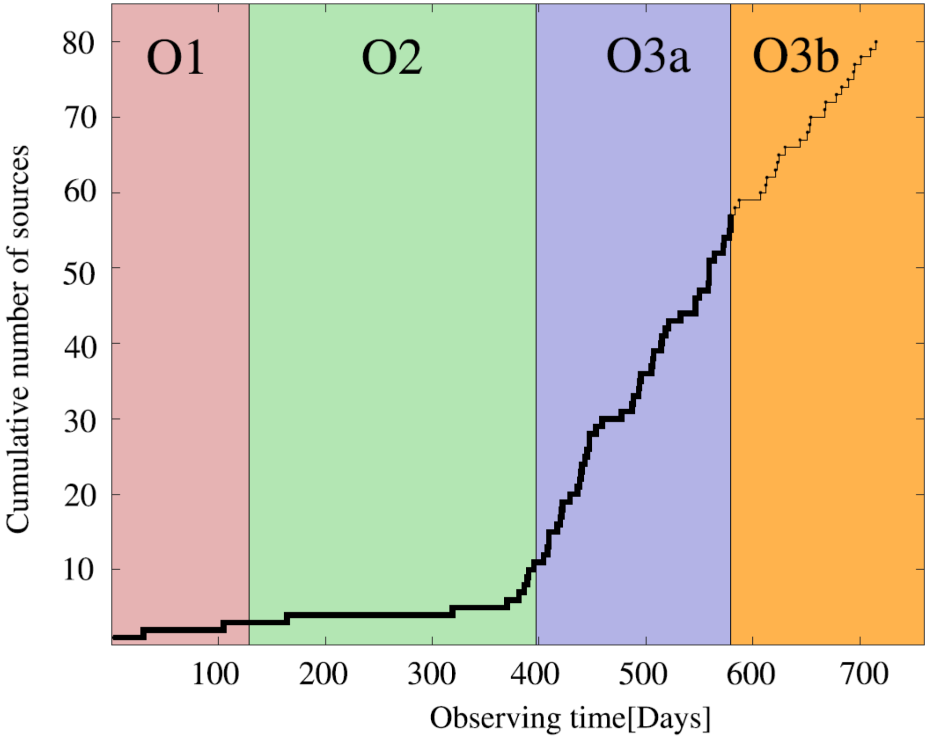

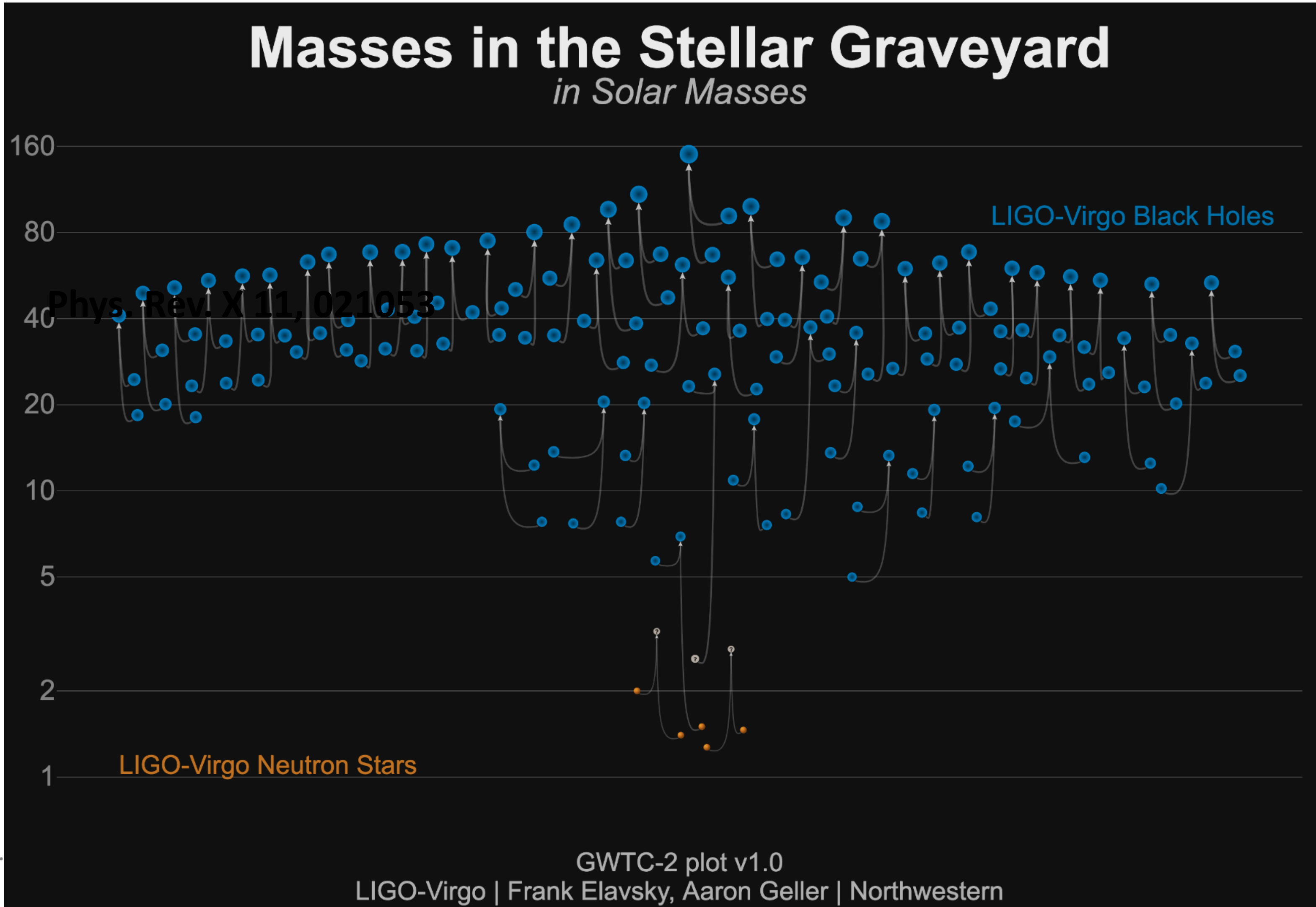

G.A.

latest published source catalog

GWTC 2, Phys. Rev. X 11, 021053 (2021)

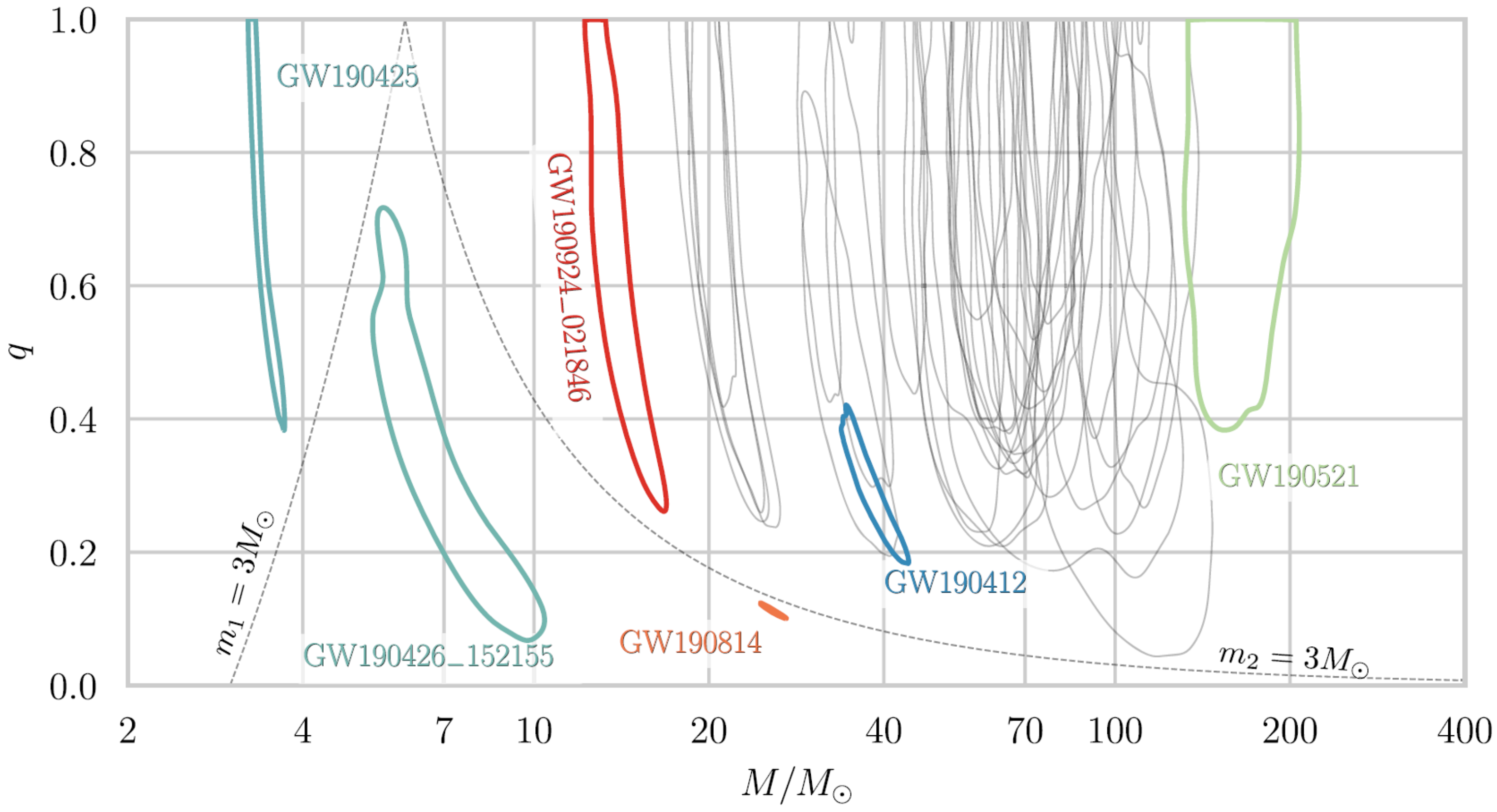

FIG. 6. Credible region contours for all candidate events in the plane of total mass M and mass ratio q. Each contour represents the 90% credible region for a different event. We highlight the previously published candidate events: GW190412, GW190425, GW190521, and GW190814, the potential NSBH GW190426_152155, and, finally, GW190924_021846, which is most probably the least massive system with both masses $> 3\ M_\odot$. The dashed lines delineate regions where the primary or secondary can have a mass below $3\ M_\odot$. For the region above the $m_2 = 3\ M_\odot$ line, both objects in the binary have masses above $3\ M_\odot$.

ENSURED TRANSIENT GW SIGNALS

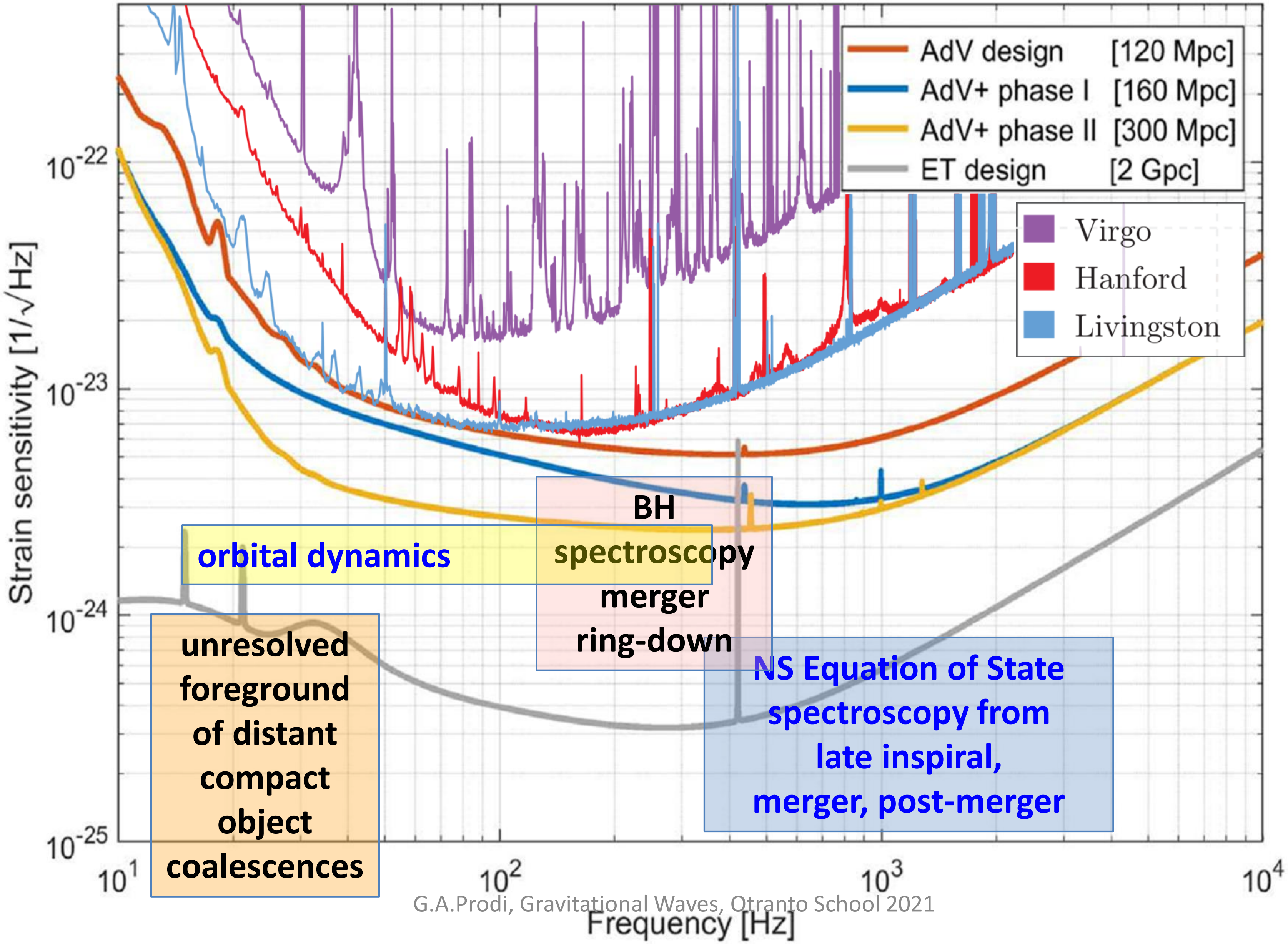

POSSIBLE TRANSIENT GW SIGNALS

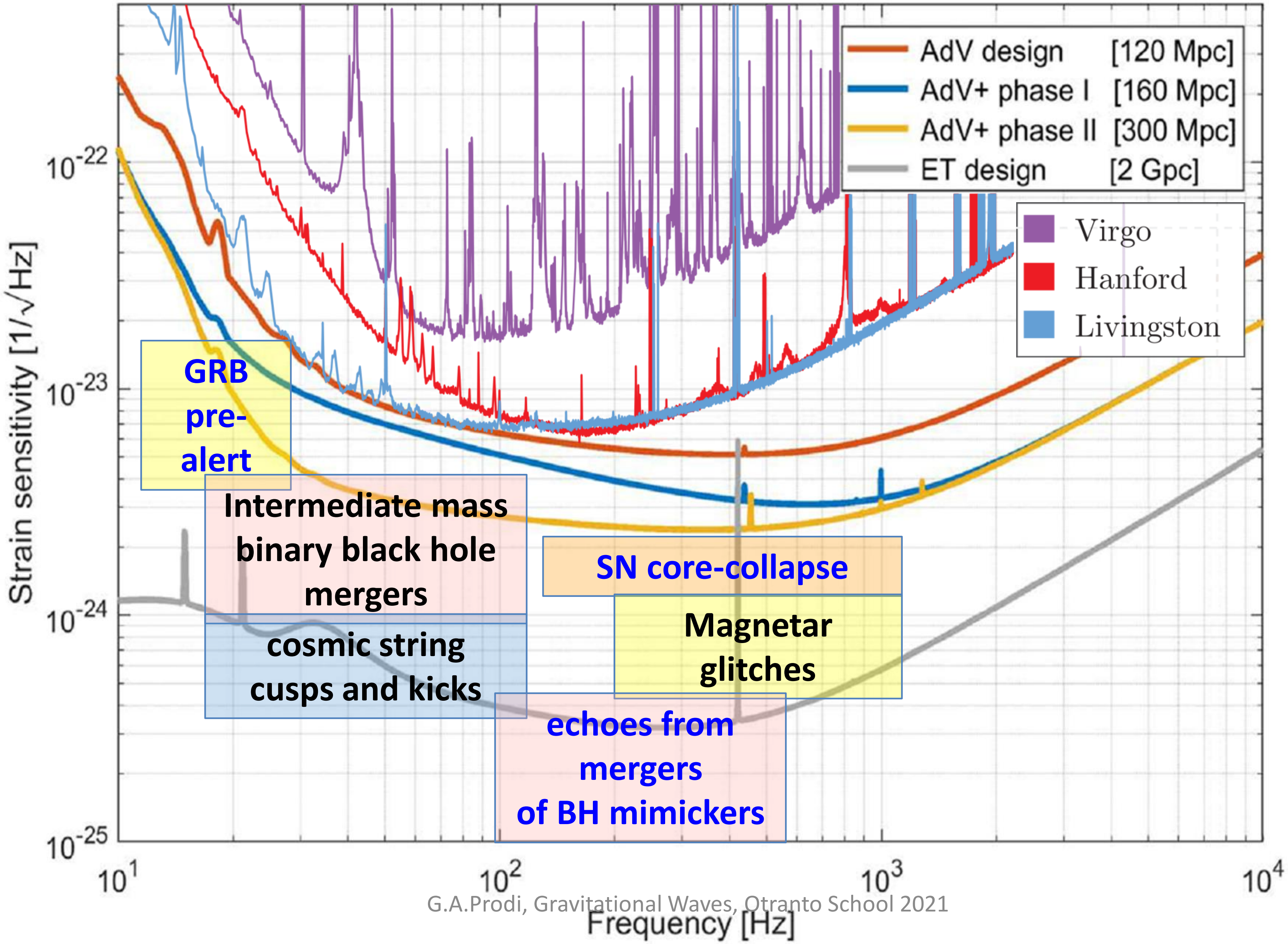

GW signal vs Noise Separation

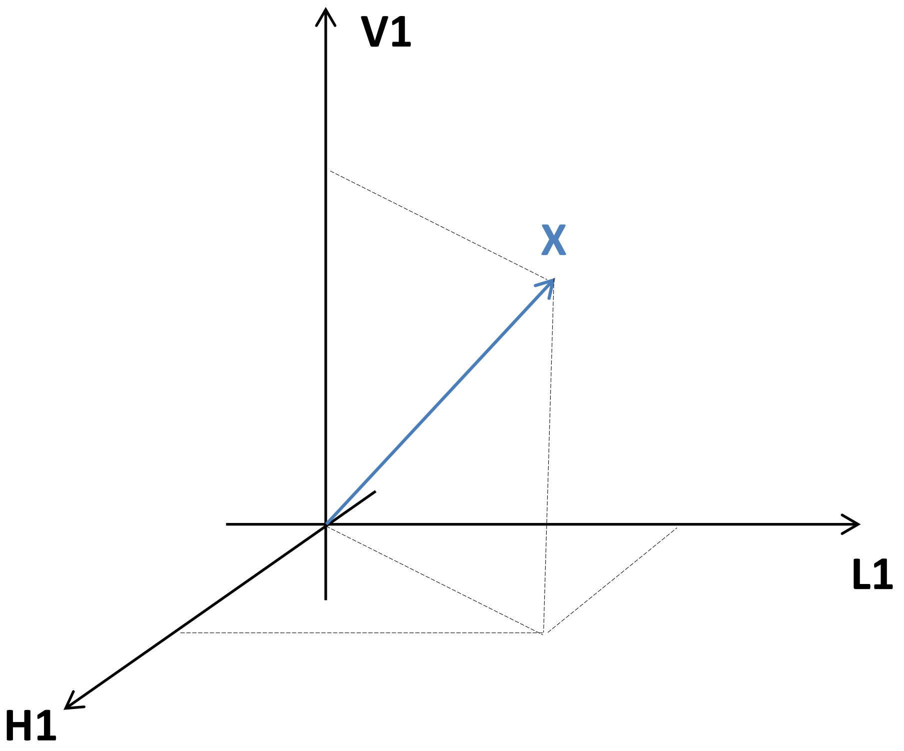

Basic principles of a

Coherent Network Data Analysis:

- **H1,L1,V1,** … is the detector frame
- **X** is the data vector (H1,L1,V1, …) e.g. a time-frequency pixel
- **F_{+}, F_{x}** are the antenna pattern of the network of detectors for a given sky direction and spectral range, i.e.
- **F_{+}, F_{x}** define the **GW Plane** of all possible network responses to a GW from a given direction and at a given frequency
- **Null Space** is the noise contribution to the data **X** and is $\perp$ to **GW Plane**

Each data X = S + n — **GW signal component S $\in$ GW Plane**
noise component n $\perp$ GW Plane , i.e. n $\in$ Null Space

this decomposition is a function of sky direction and frequency through the spectral and directional sensitivities of the detectors in the newtork.

With at least 3 detectors we can separate noise from signal components without relying on signal models

GW signal vs Noise Separation

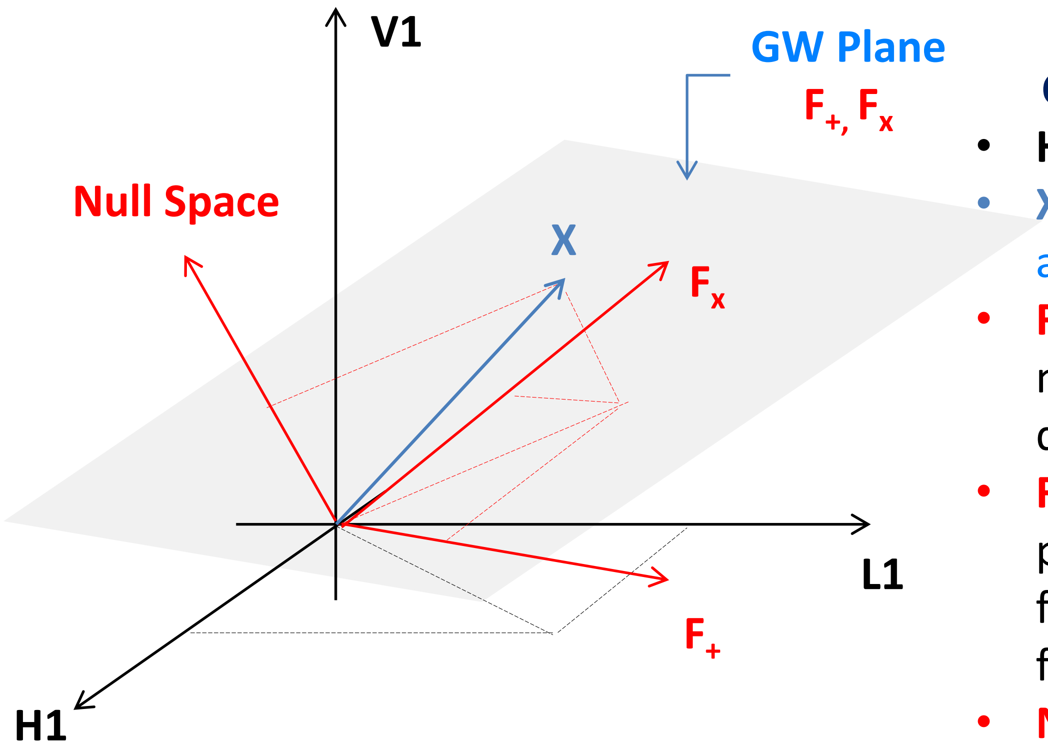

Basic principles of a **Coherent Network Data Analysis**:

- **H1,L1,V1,** … is the detector frame
- **X** is the data vector (H1,L1,V1, …) e.g. a time-frequency pixel
- F_+, F_x are the antenna pattern of the network of detectors for a given sky direction and spectral range, i.e.
- F_+, F_x define the **GW Plane** of all possible network responses to a GW from a given direction and at a given frequency
- **Null Space** is the noise contribution to the data **X** and is ⊥ to **GW Plane**

Each data X = S + n

- **GW signal component S ∈ GW Plane**
- **noise component n ⊥ GW Plane , i.e. n ∈ Null Space**

this decomposition is a function of sky direction and frequency through the spectral and directional sensitivities of the detectors in the newtork.

With at least 3 detectors we can separate noise from signal components without relying on signal models

GW signal vs Noise Separation

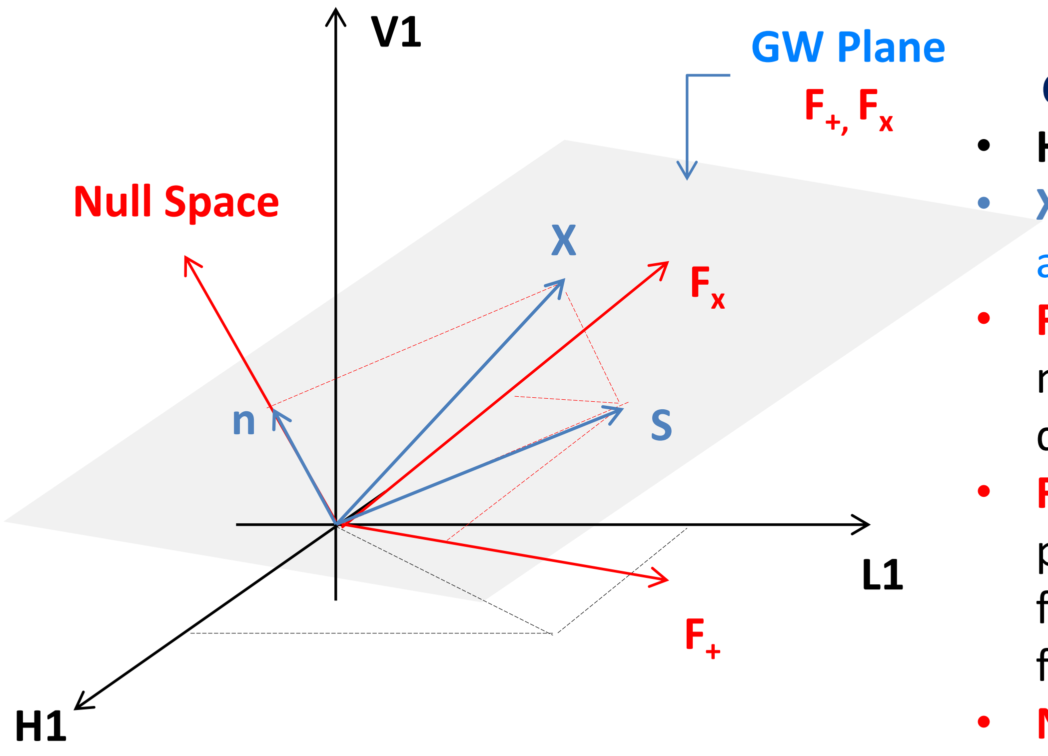

Basic principles of a
Coherent Network Data Analysis:

- **H1,L1,V1,** … is the detector frame
- **X** is the data vector (H1,L1,V1, …) e.g. a time-frequency pixel
- **F_+,F_x** are the antenna pattern of the network of detectors for a given sky direction and spectral range, i.e.
- **F_+,F_x** define the **GW Plane** of all possible network responses to a GW from a given direction and at a given frequency
- **Null Space** is the noise contribution to the data **X** and is ⊥ to **GW Plane**

Each data X = S + n
- **GW signal component S ∈ GW Plane**
- **noise component n ⊥ GW Plane , i.e. n ∈ Null Space**

this decomposition is a function of sky direction and frequency through the spectral and directional sensitivities of the detectors in the newtork.

With at least 3 detectors we can separate noise from signal components without relying on signal models

data analysis in a nutshell

Matched filter for one template

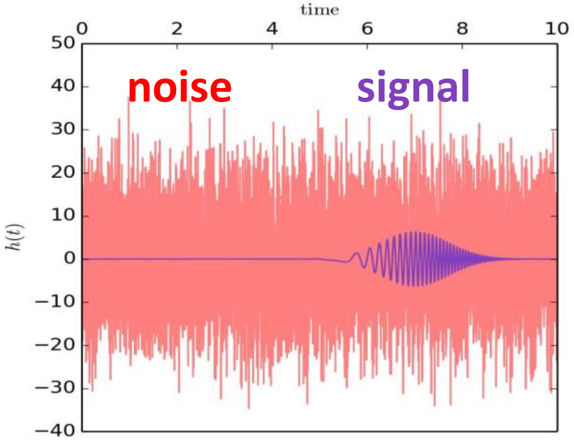

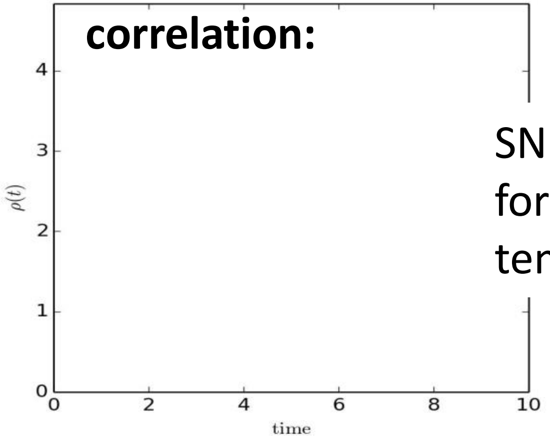

SNR time series for that template

Template Searches

bank of predicted templates function of (limited) source parameters

find template that fits data best

- confident detection & parameter estimation
- need exact source model, may fail if theory does not match Nature

Burst Searches

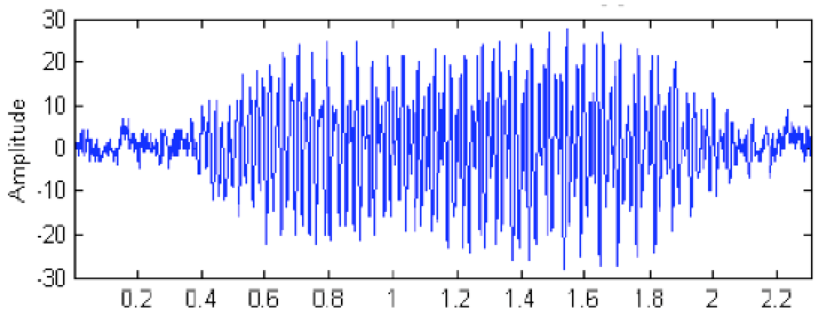

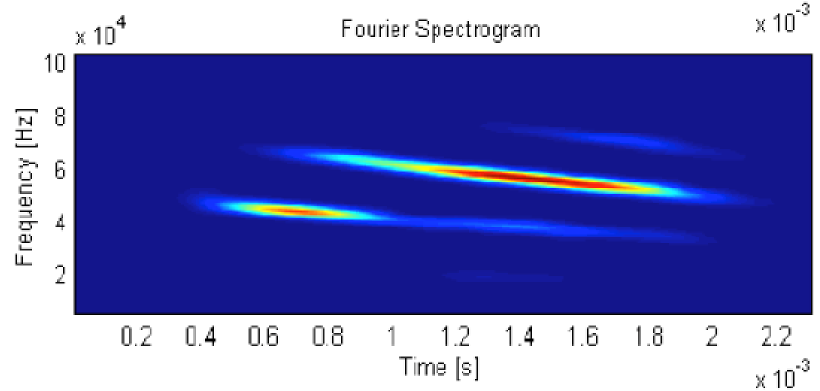

- detects excess power in time – frequency consistent/coherent in multiple detectors
- can search for un-modeled & un-expected sources

Uncorrelated noise across distant detectors

- **Anthropogenic noise**: human activity or infrequent ground motion. *Monitored by accelerometers, seismometers, microphones, power line meters ...*
- **Earthquakes**: can make detectors inoperable or inducing low frequency motion. *Monitored by seismometers*
- **instrumental origin in the interferometer**: controls/actuators. *Vetoed.*

Class.Quant.Grav. 33, 134001 (2016)

- **“Blip” transients**: show as a symmetric teardrop shape in time-frequency. *No hint yet to the cause.*

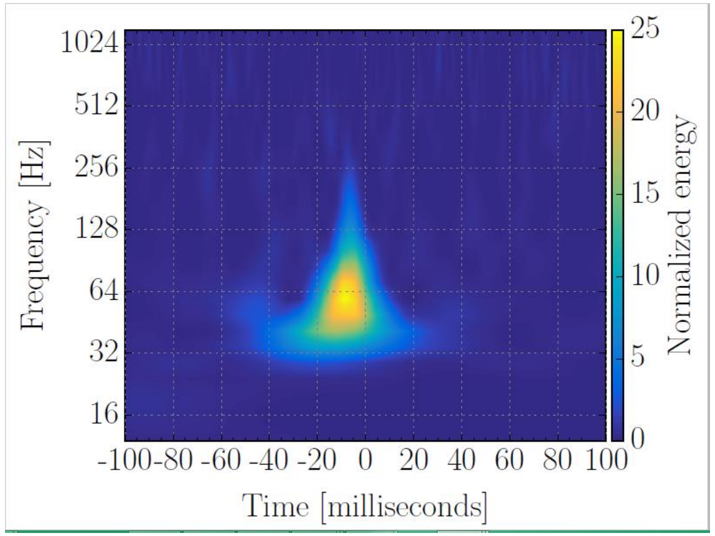

- *There are also some correlated noises e.g. lightning and magnetic resonances*

GW170817 detection

- identified by **on-line analysis as a single-detector event** at LIGO-Hanford
  - alert for human evaluation
- LIGO-Livingston affected by a loud ***"glitch"*** 1.1s before merger
  - prevented on-line analysis to consider its data
  - data checked off-line and cleaned:
    - zeroing for the glitch duration
    - subtraction of the glitch model
- **event significance** estimated using LIGOs data
  - against 5.9 days of coincident observation (Aug.13-21)
  - false alarm rate, **FAR < 1 / 8.0 x10^4 years**

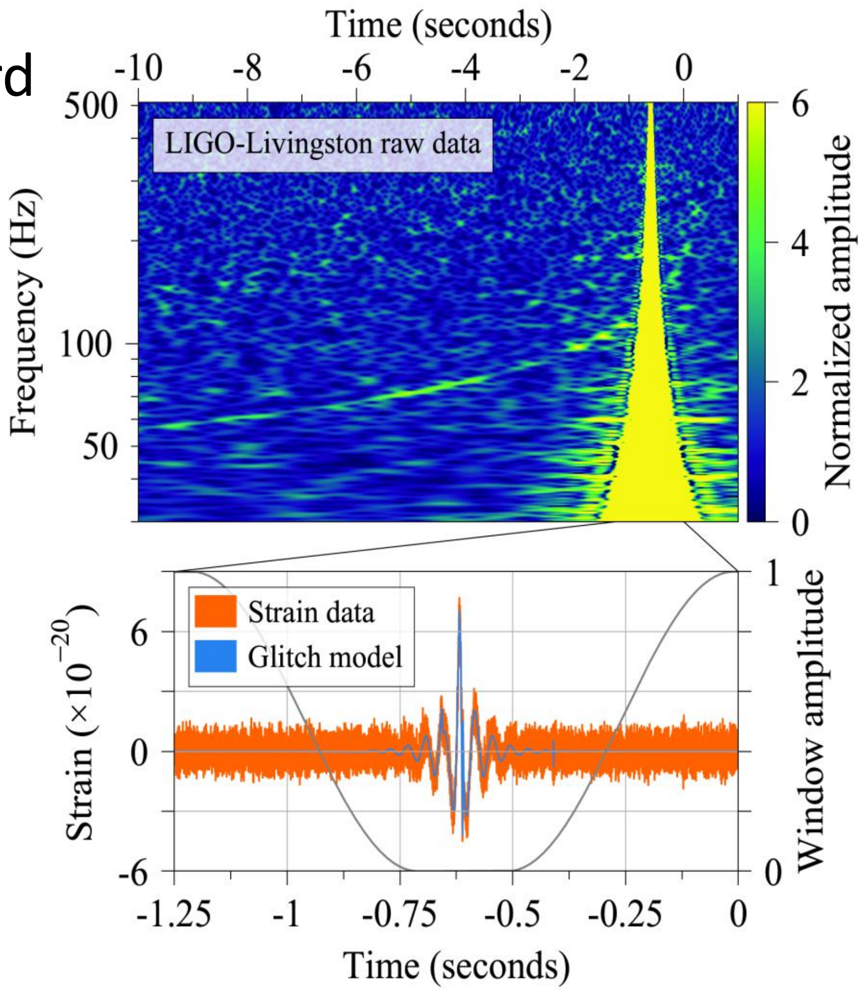

GW170817 morphology

- neat **chirping morphology** from binary inspiral
  - ≈ 100s duration within LIGOs' bandwidth
  - ≈ 3000 cycles
  - SNR collected in [24, ≈ 300]Hz
- **BNS horizon,** max distance for SNR=8 in single detector
  - LIGO-Livingston **218 Mpc**,
  - LIGO-Hanford **107 Mpc**,
  - Virgo **58Mpc**.
- **matched-filter** binary-coalescence searches
  - searched total mass ∈ [2, 500] M_{sun}
  - SNR: LIGO-H **19**, LIGO-L **26**, Virgo **2**
- waveform-agnostic searches recover a fraction of the chirp, ≈ 15s

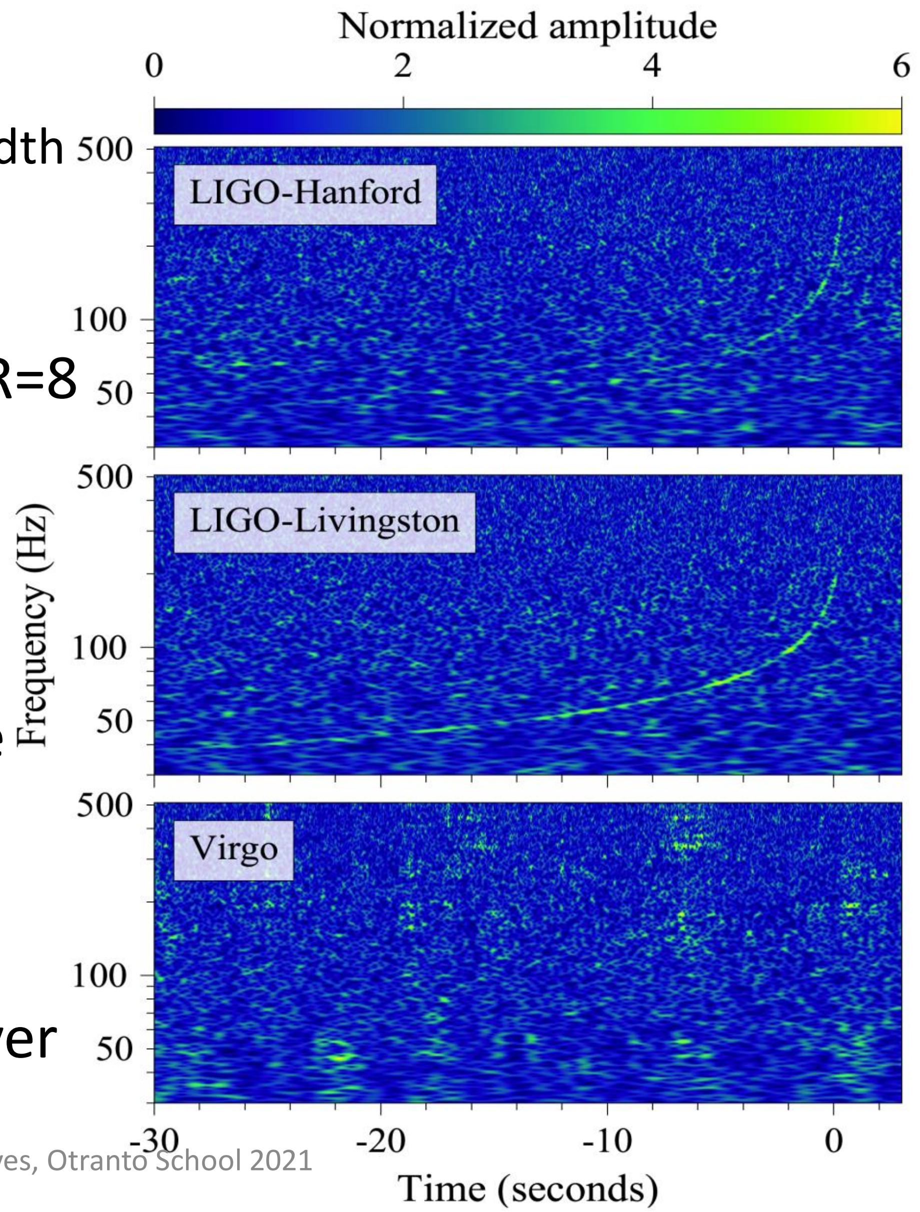

GW170817 : The best to date 3D Sky Localization

- Rapid Localization results 90% confidence (within hours)
  - **Only LIGO = 190 deg^2**
  - **LIGO+Virgo = 31 deg^2**
- **Refined localization** (days)
  - **LIGO+Virgo = 28 deg^2**
- **Source distance** $\approx 40^{+8}_{-14}$ Mpc
- **Localization volume** $\approx$ 380 Mpc^3
  containing about 50 known galaxies

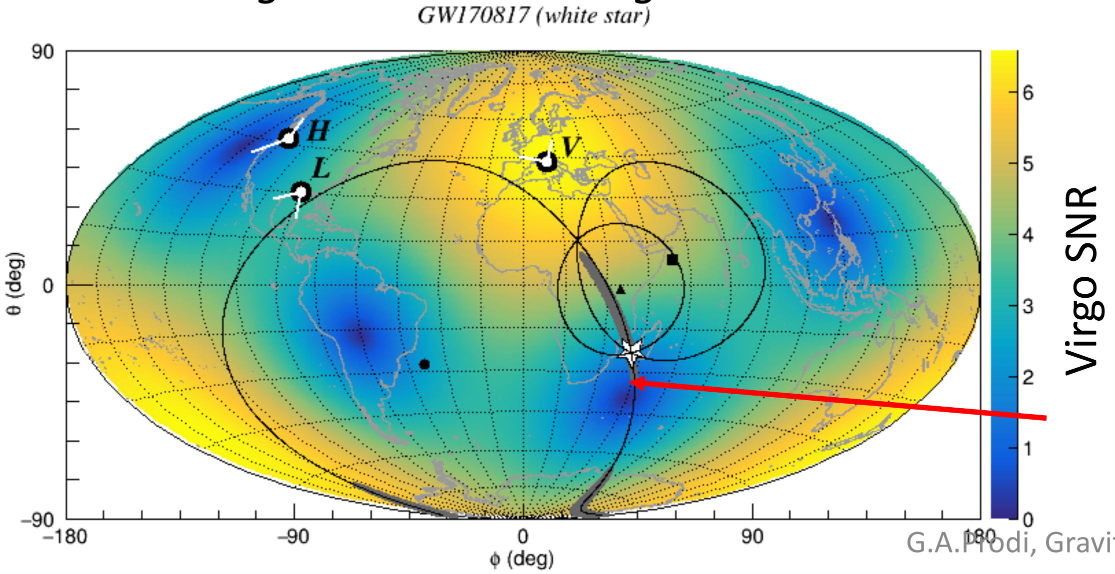

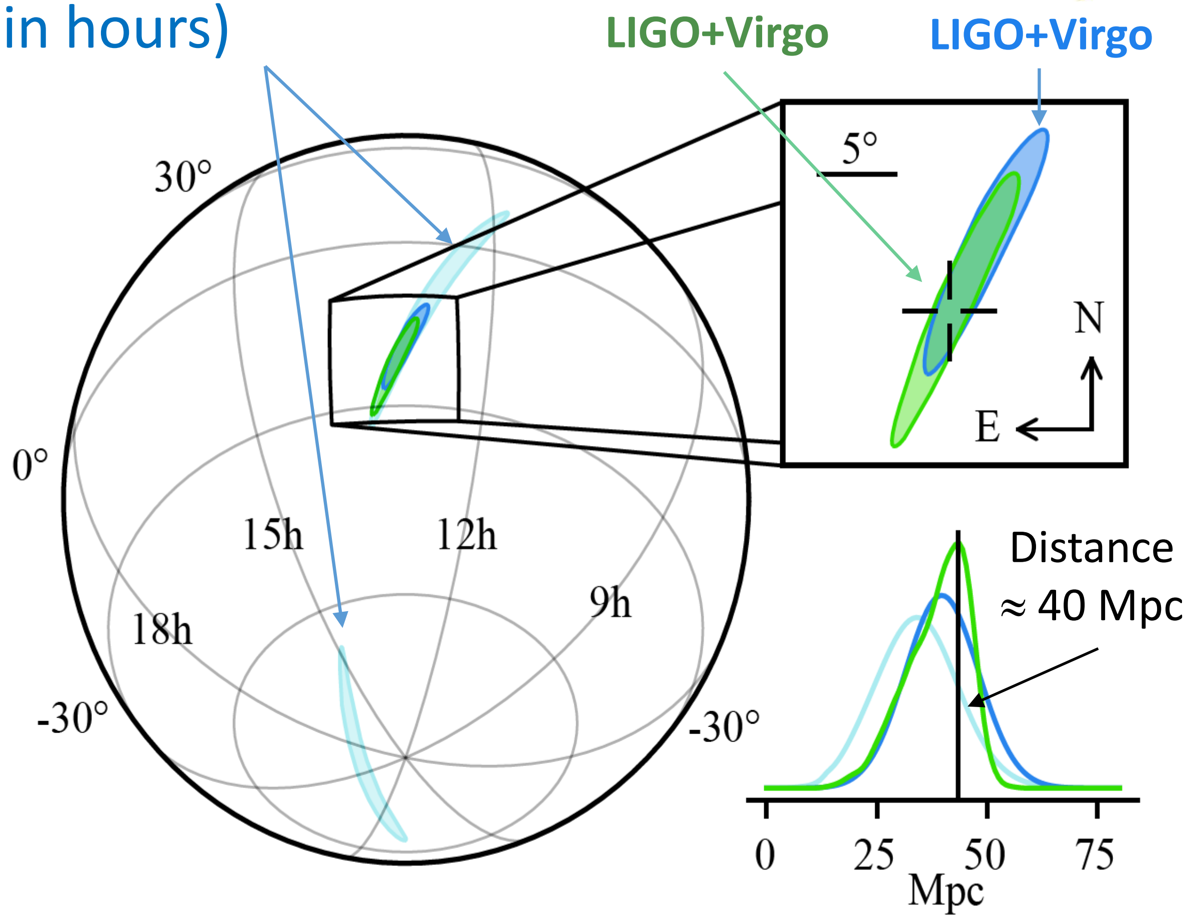

How Virgo Contribute ?

Amplitude consistency of measured signal

Ready ? GOOO ! Aug.17, 2017, h12:41:04 UTC

about 60 groups/collaborations participated to the investigations of

GRB170817A – GW170817 – AT2017fgo

- **a multimessenger coordination for rapid followup of triggers was fully operational** agreements with about 90 partners https://gw-astronomy.org/wiki/LV_EM/PublicParticipatingGroups coverage of the electromagnetic spectrum (earth and space telescopes) and High Energy Neutrinos

The Astrophysical Journal Letters, 848:L12 (59pp), 2017 October 20 https://doi.org/10.3847/2041-8213/aa91c9

OPEN ACCESS

CrossMark

Multi-messenger Observations of a Binary Neutron Star Merger

LIGO Scientific Collaboration and Virgo Collaboration, Fermi GBM, INTEGRAL, IceCub…
Telluride Imager Team, IPN Collaboration, The Insight-Hxmt Collaboratio…
Team, The 1M2H Team, The Dark Energy Camera GW…
GRAWITA: GRAvitational Wave Inaf T…
Array, ASKAP: Australi…
and CA…
…, Caltech-
…, KU Collaboration, Nordic
… Transient Robotic Observatory of the South
…Array, The CALET Collaboration, IKI-GW Follow-up
…oration, LWA: Long Wavelength Array, HAWC Collaboration, The Pierre Auger
… VLBI Team, Pi of the Sky Collaboration, The Chandra Team at McGill University, DFN:
…, ATLAS, High Time Resolution Universe Survey, RIMAS and RATIR, and SKA South Africa/MeerKAT

LIGO-Virgo indica la direzione e la distanza
i telescopi trovano la luce dei resti della collisione

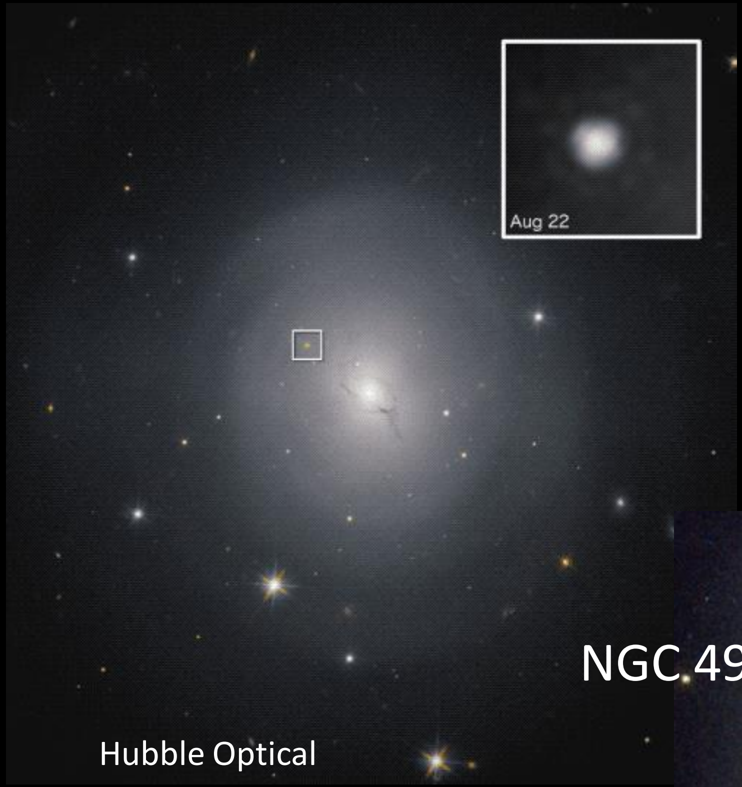

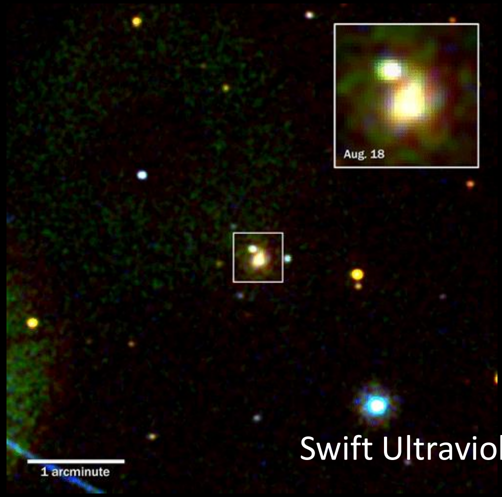

NGC 4993

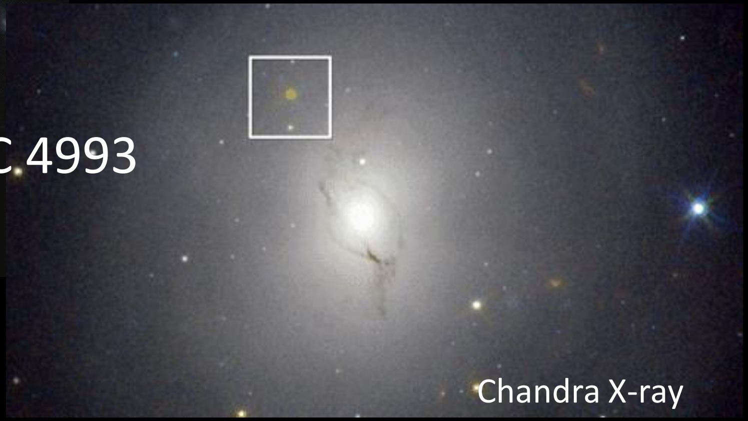

Images courtesy of NASA / ESA

Chronicles of the dawn of multimessenger astronomy

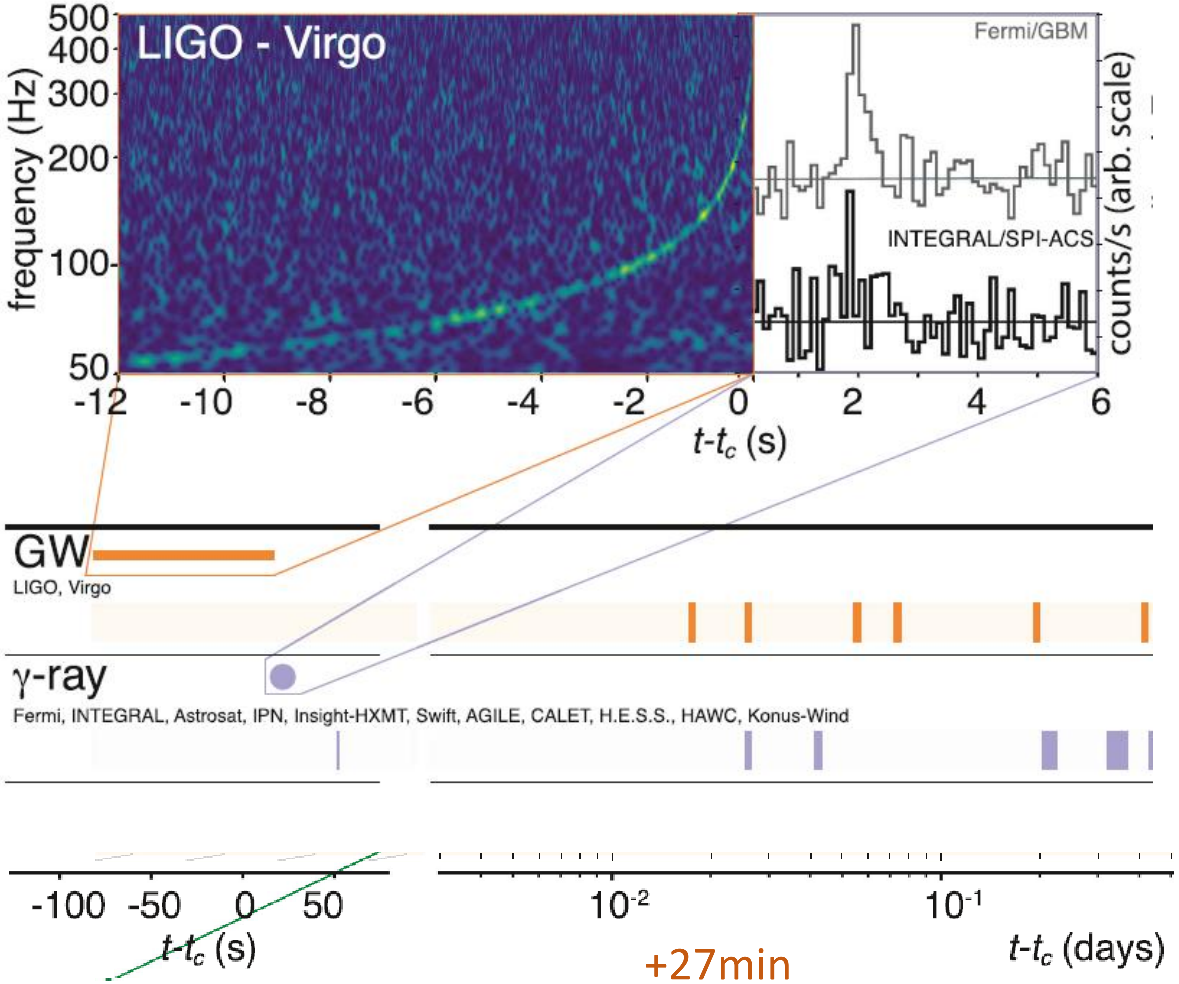

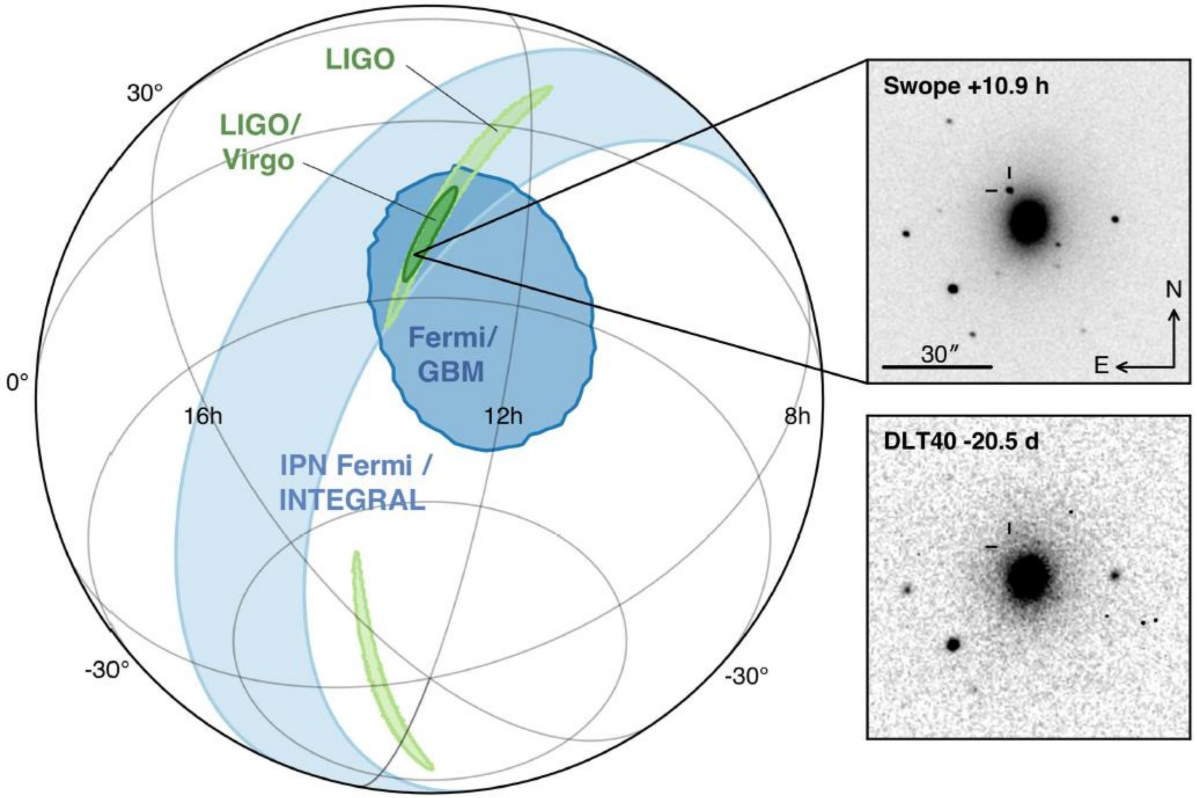

+14s
GRB170817A GNC Notice
FERMI GBM

+27min
GW170817 GNC Notice

+5h
GW170817 GNC Circular
sky map 31 deg^2

IPN localization
FERMI GBM – INTEGRAL SPI ACS

+12h
SSS17a GCN Circular
IM2H Swope
OPTICAL TRANSIENT
-> AT2017fgo

Chronicles …

- Optical: more identifications of the transient in a few hours
- early photometric data UV-OPT-IR
- rapid dimming of UV (day)
- unusual brightness in IR

  not a SN
- No prompt X-ray
- No prompt radio
- X counterpart at 9d
- Radio counterpart at 16.4d
- No neutrinos

Source was occulted by the Sun in Nov.

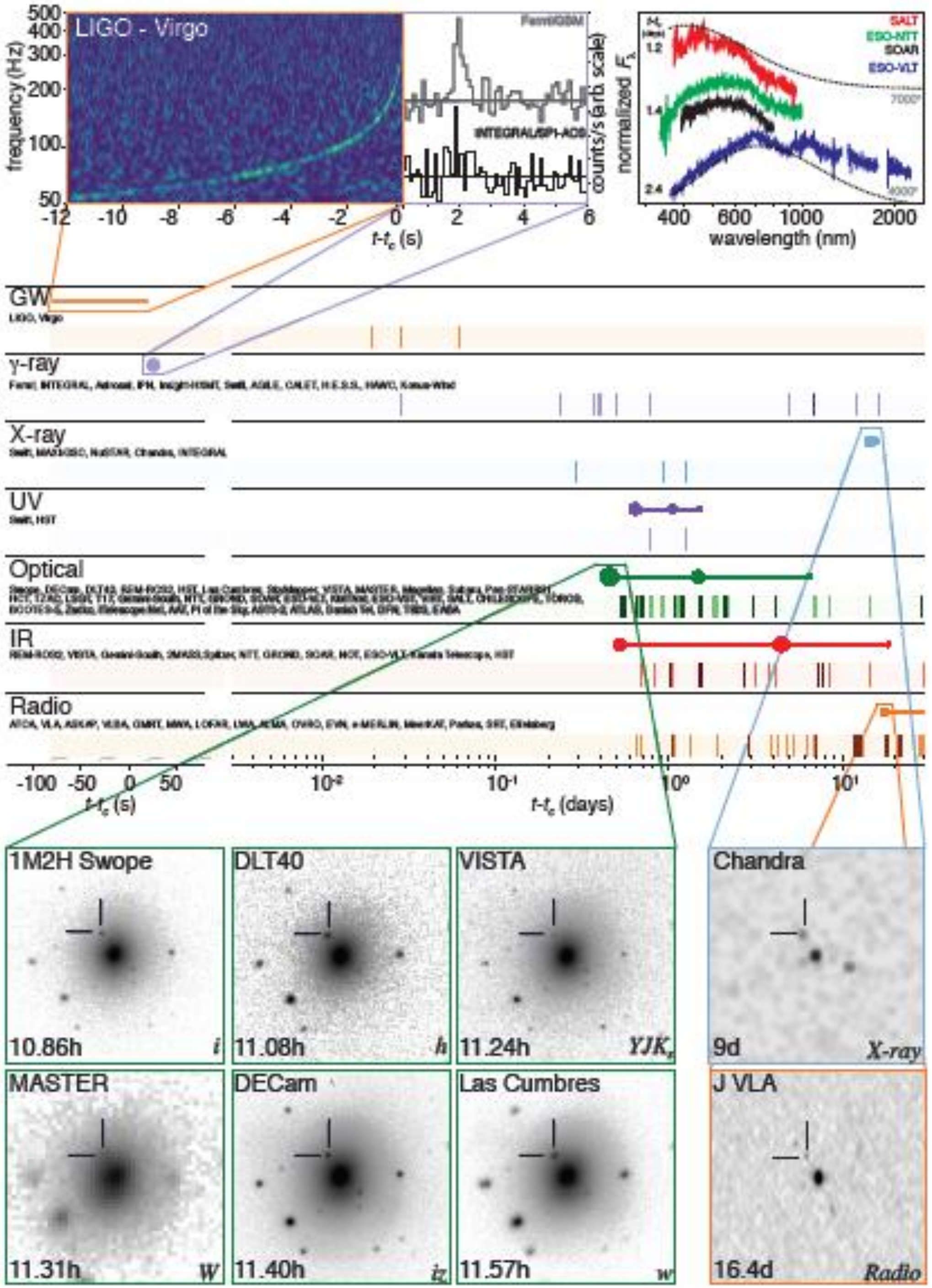

Association of GW170817 and GRB170817A & Fundamental Physics

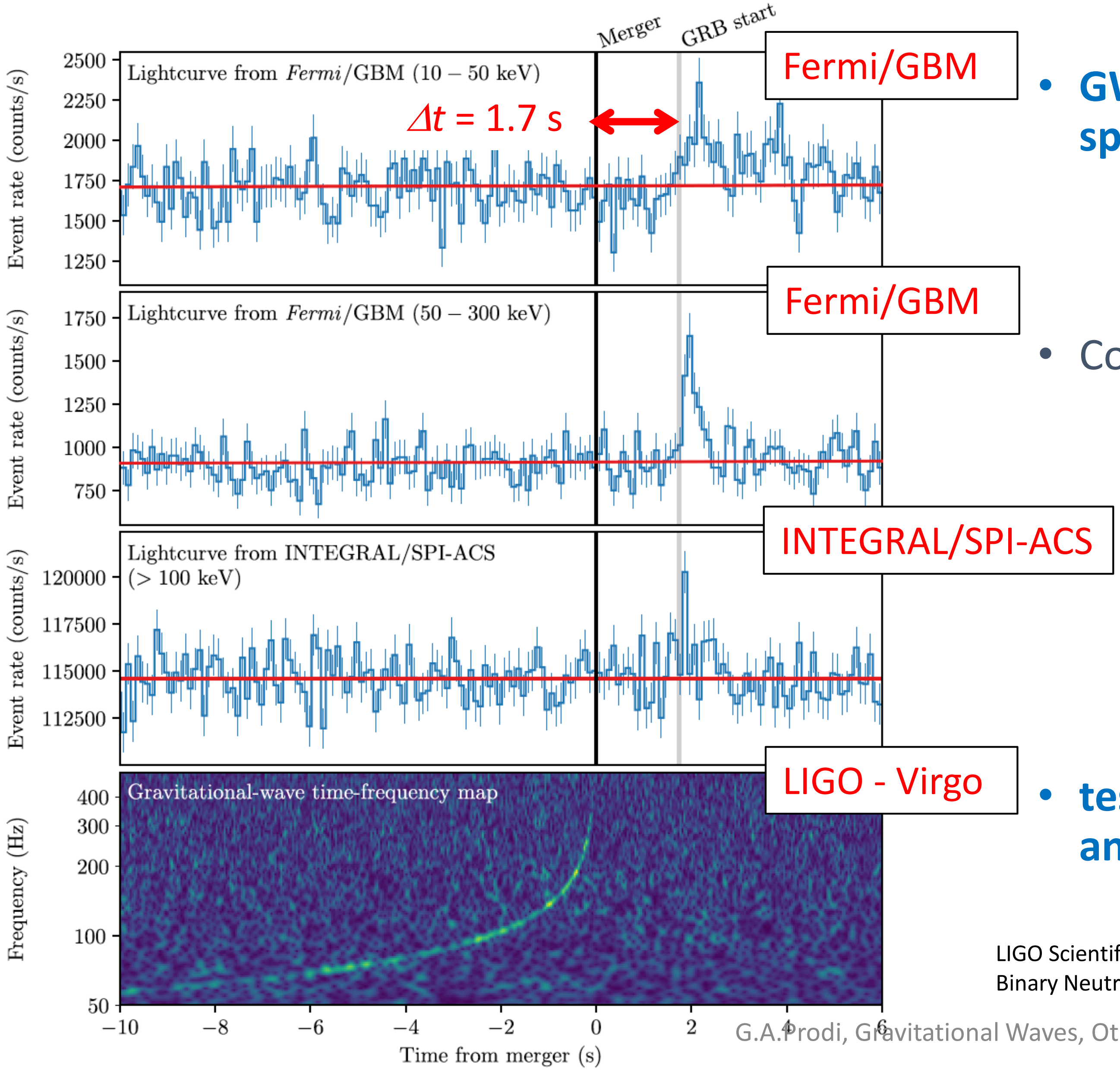

- **GW170817 provides a stringent test of the speed of gravitational waves**

$$\frac{v_{GW} - c}{c} \approx \frac{c\Delta t}{D}$$

- Conservative assumptions
  - t_{GW} - t_{EM} at emission in [-10, 0] sec
  - $D \approx 26$ Mpc
    - Conservative limit – use 90% confidence level lower limit on GW source from parameter estimation

$$-3 \times 10^{-15} \leq \frac{\Delta v}{v_{\mathrm{EM}}} \leq +7 \times 10^{-16}$$

- ***testing violations of local Lorentz Invariance and Equivalence Principle***

LIGO Scientific Collaboration and Virgo Collaboration, Gravitational Waves and Gamma-Rays from a Binary Neutron Star Merger: GW170817 and GRB 170817A" Astrophys. J. Lett., 848:L13, (2017)

COSMOGRAPHY

Direct measurement of Luminosity distance:

Compact Binary Coalescences GWs $$h_+ \propto \frac{(\cos\iota + 1)^2}{2D_L} \qquad h_\times \propto \frac{\cos\iota}{D_L}$$

degeneracy with orbital inclination angle

plus one of the following:

- direct measurement of EM host galaxy red-shift (BNS and possibly more distant NS-BH)

Sathyaprakash+ CQG 27 215006, Nissanke+ 1307.2638

- detailed knowledge of galaxy catalogs within LIGO-Virgo source localization (use BBHs !)

Schutz Nature 1986, Del Pozzo PRD 86 043011

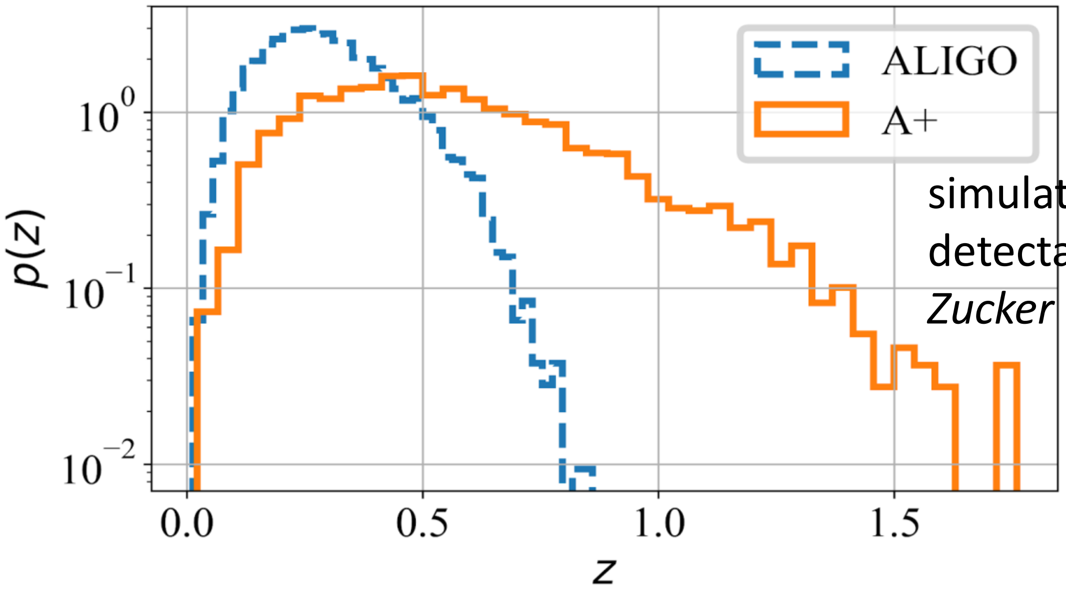

simulated distribution of detectable BBH mergers *Zucker LIGO-G1800514*

simulated distribution of detectable BBH mergers *Hall, Miller*

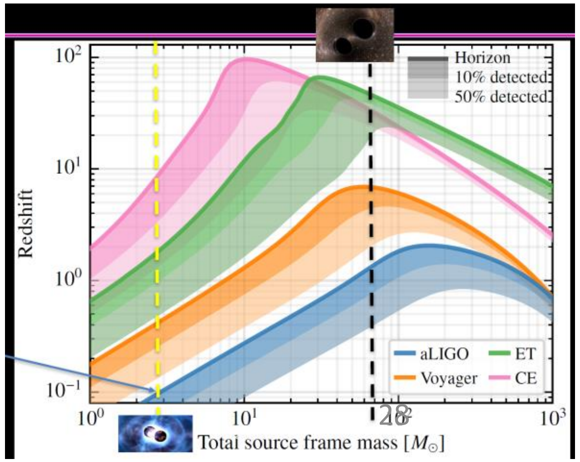

GW170817: Implications

Nature 551, 85 (2017)

Cosmology:

association with host galaxy NGC 4993 & luminosity distance directly measured from the Gravitational wave signal, the Hubble constant is inferred to be

$$H_0 = 70^{+12}_{-8}\ \mathrm{kms^{-1}Mpc^{-1}}$$

(most probable value and minimum 68.3% probability range, which can be compared to the value from Planck $H_0 = 67 \pm 0.55\ \mathrm{kms^{-1}Mpc^{-1}}$

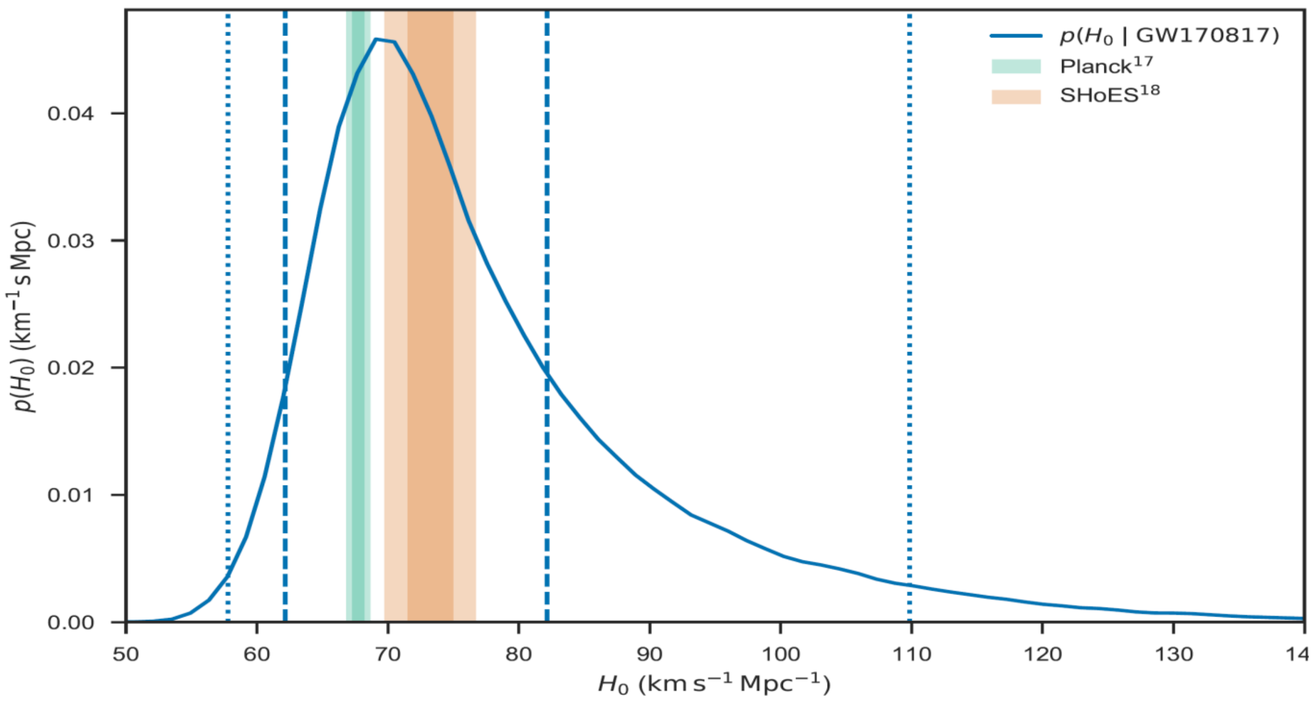

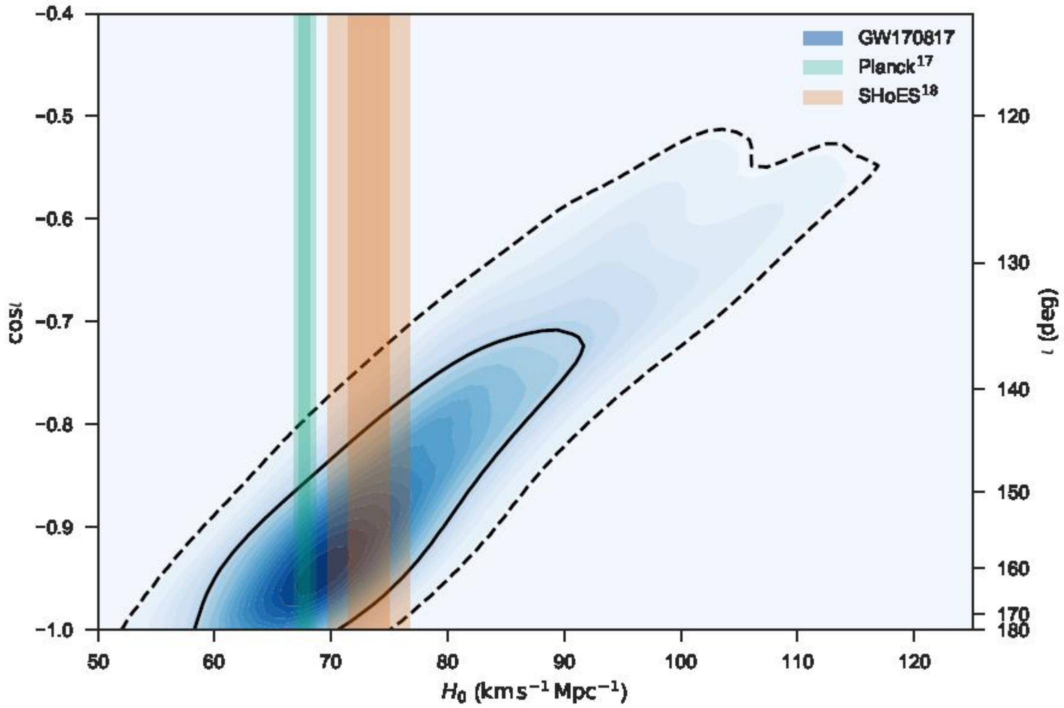

uncertainty almost dominated equally by

- Doppler shift contribution from the peculiar motion of NGC 4993
- inclination angle – distance degeneracy from GW information

COSMOGRAPHY

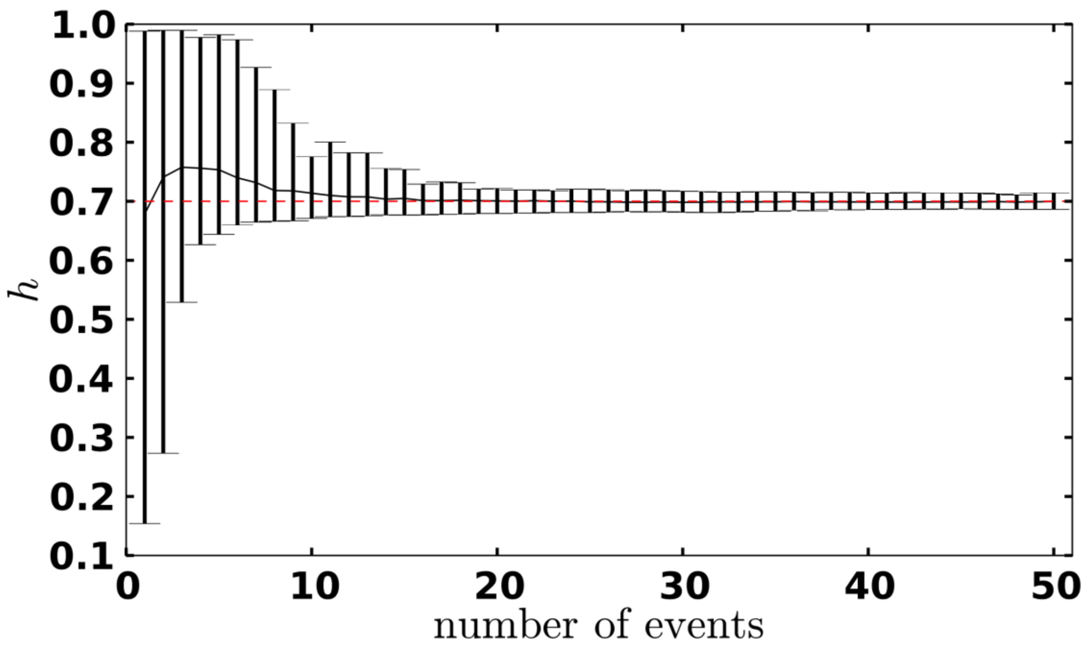

simulated improvement from statistical method
95% confidence

Del Pozzo PRD 86 043011

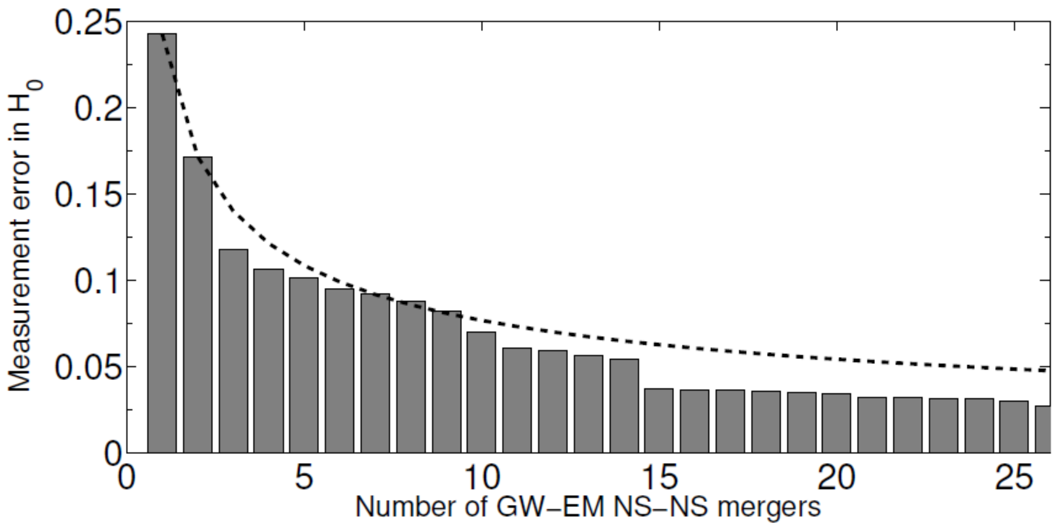

FIG. 2.— H_0 measurement error as a function of the number of multi-messenger (GW+EM) NS-NS merger events observed by a LIGO-Virgo network. The solid bars indicate the 68% c.l. measurement error in H_0 for the *joint* PDF of the independent binary mergers; the dashed line shows the 68% c.l. measurement error in H_0 derived assuming Gaussian errors for each GW-EM merger.

Nissanke+ 1307.2638

few % seems achievable on AdV+ time scale
likely limited to local universe

need ET to go to cosmological distances

EXTREME MATTER

NS equation of state improved LV results

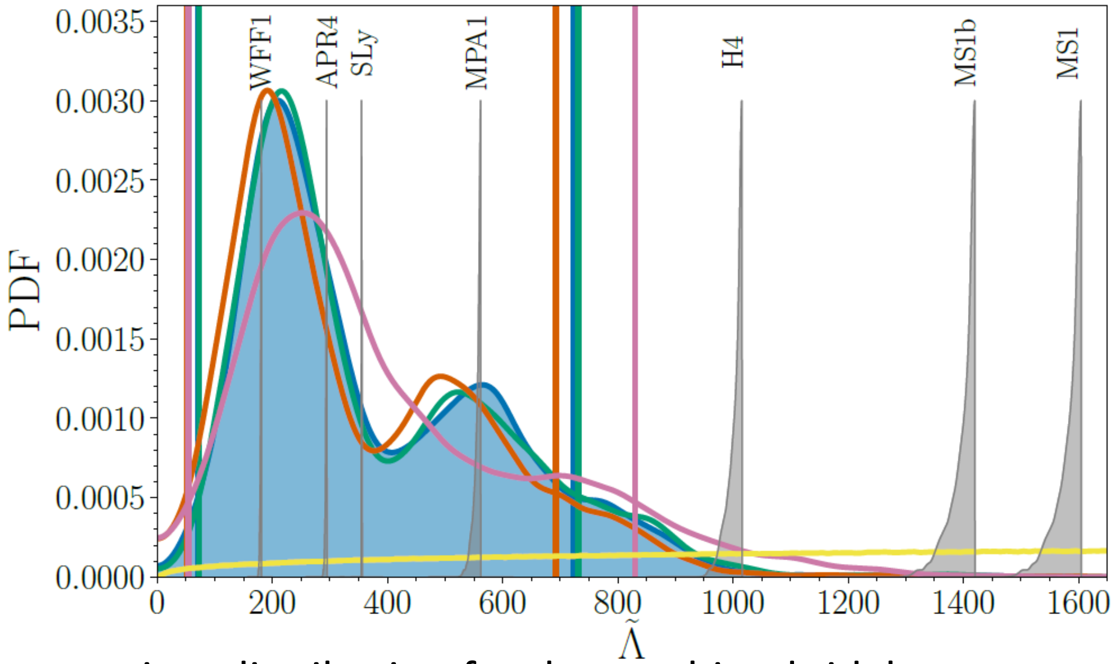

posteriors distribution for the combined tidal parameter
(low spin prior)
Phys. Rev. X 9, 011001 (2019)

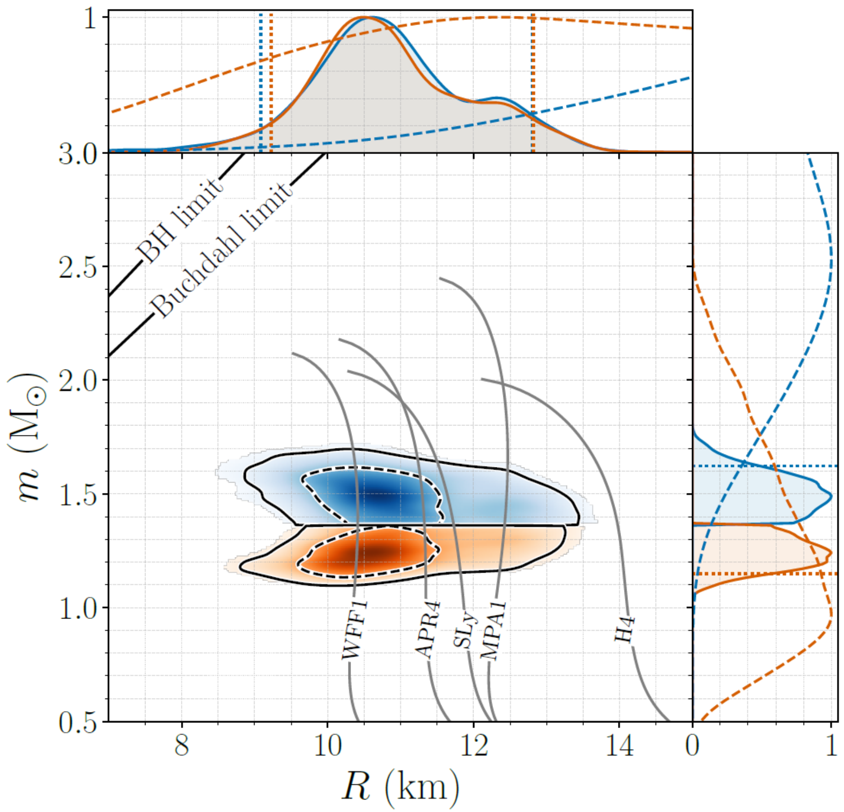

posteriors distribution for mass and radii
(most general)
Phys. Rev. Lett. 121, 161101 (2018)

the most crucial gain will come from more Signal-to-Noise Ratio at high frequency
late inspiral, merger and post-merger

GW190521: most massive BBH observed by LIGO-Virgo

Phys. Rev. Lett. **125**, 101102 (2020): the remnant is the first observed intermediate mass black hole

primary component in the forbidden mass range for BH production by supernova (pulsational pair instability mass gap)

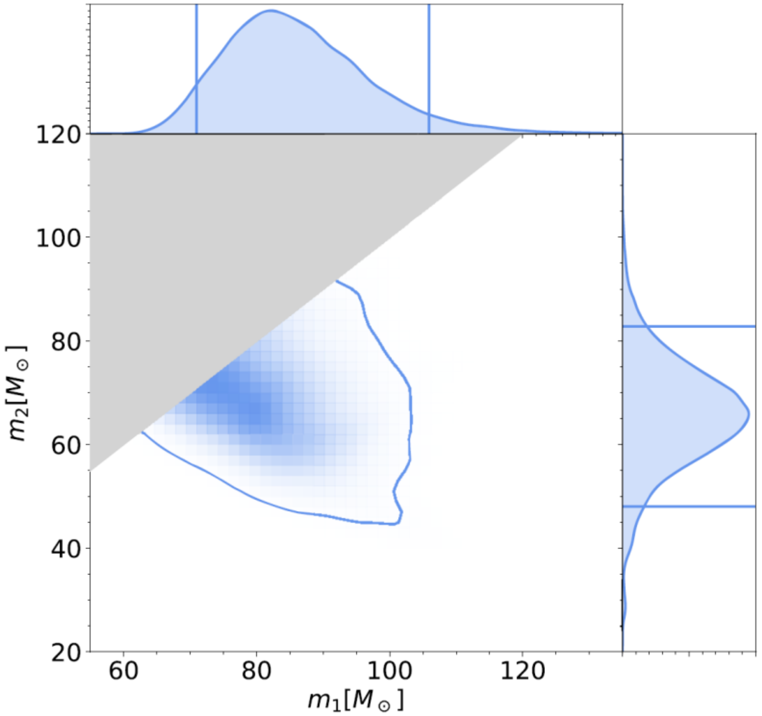

FIG. 2. Posterior distributions for the progenitor masses of GW190521 according to the NRSur7dq4 waveform model. The 90% credible regions are indicated by the solid contour in the joint distribution and by solid vertical and horizontal lines in the marginalized distributions.

Primary mass	$85^{+21}_{-14}\ M_\odot$
Secondary mass	$66^{+17}_{-18}\ M_\odot$
Primary spin magnitude	$0.69^{+0.27}_{-0.62}$
Secondary spin magnitude	$0.73^{+0.24}_{-0.64}$
Total mass	$150^{+29}_{-17}\ M_\odot$
Mass ratio $(m_2/m_1 \leq 1)$	$0.79^{+0.19}_{-0.29}$
Effective inspiral spin parameter $(\chi_{\rm eff})$	$0.08^{+0.27}_{-0.36}$
Effective precession spin parameter $(\chi_{\rm p})$	$0.68^{+0.25}_{-0.37}$
Luminosity Distance	$5.3^{+2.4}_{-2.6}$ Gpc
Redshift	$0.82^{+0.28}_{-0.34}$
Final mass	$142^{+28}_{-16}\ M_\odot$
Final spin	$0.72^{+0.09}_{-0.12}$
$P\ (m_1 < 65\ M_\odot)$	0.32%

GW190521: most massive BBH observed by LIGO-Virgo

10.1103/PhysRevD.103.082002

lowest frequency source detected, no evidence for the inspiral phase

minimally modeled analysis methods provided its statistical significance

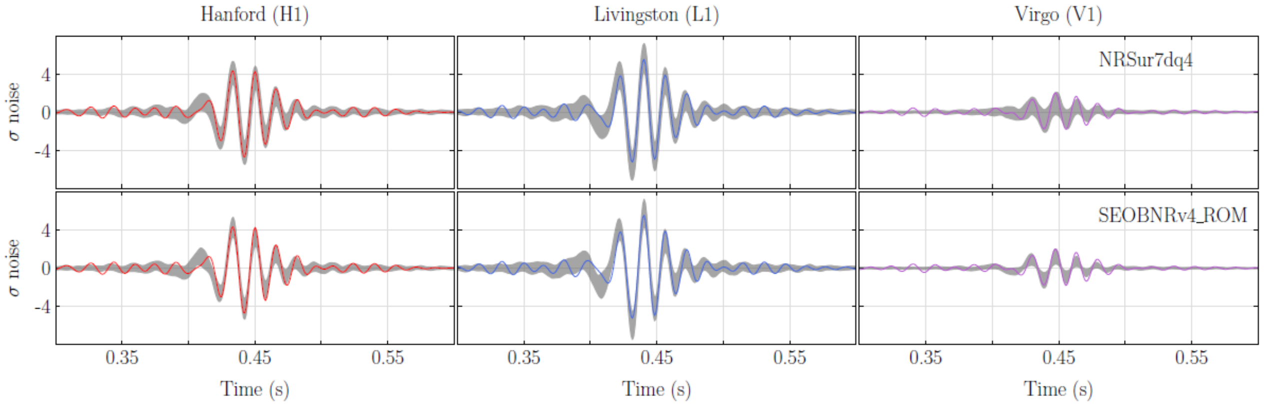

FIG. 5. Visualization of the consistency of the signal-agnostic measurement by cWB with two alternative models in time domain: upper panel NRSur7dq4 model, lower panel SEOBNRv4_ROM model. The colored curves are the whitened waveform for GW190521 as reconstructed by cWB for the LIGO Hanford (red), LIGO Livingston (blue) and Virgo (violet); they are a direct measurement and do not change from the upper to the lower panels. The shaded belts are 90% confidence intervals per each time sample at each detector and are model dependent.

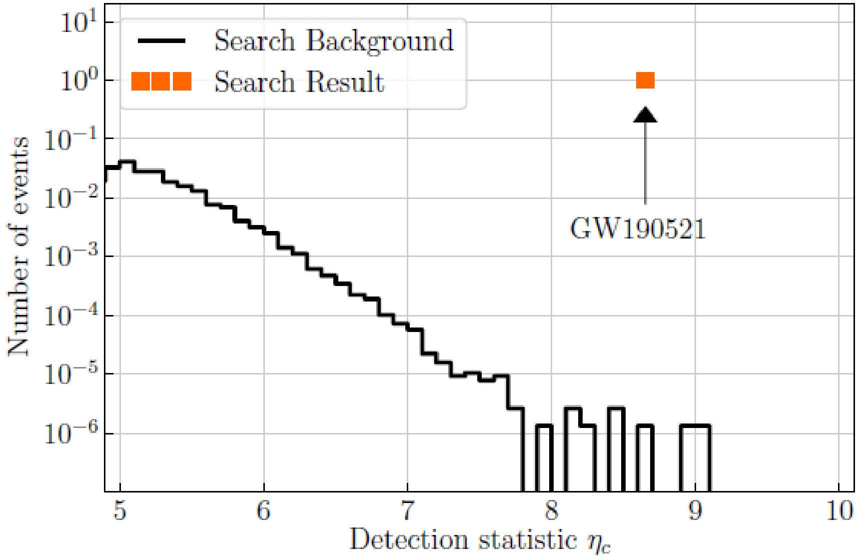

FIG. 4. The search background that established false-alarm rate of GW190521 to be 1 per 4900 years.

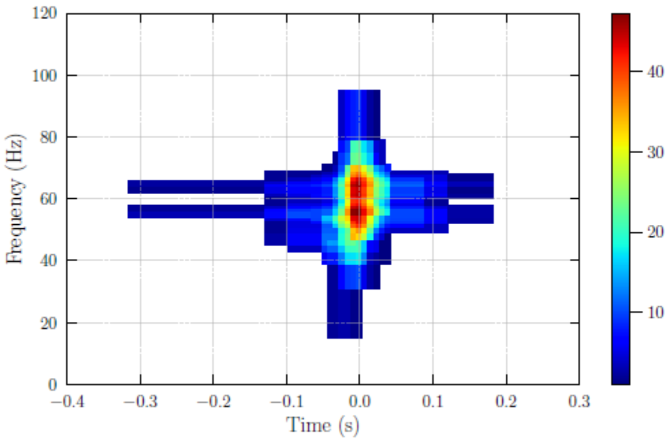

arXiv:2010.14529

Testing General Relativity on BBH

➢ selected tests of consistency with General Relativity:

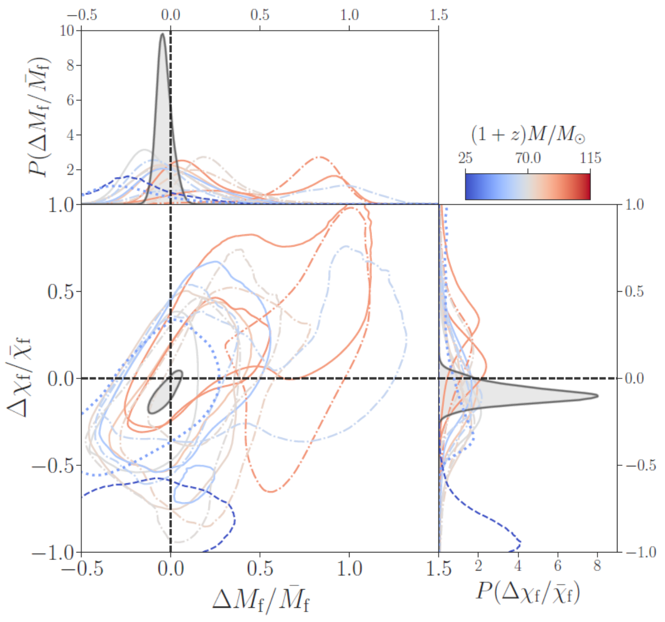

FIG. 3. Results of the IMR consistency test for the selected BBH events with median $(1+z)M < 100 M_\odot$ (see Table IV). The main panel shows the 90% credible regions of the posteriors for $(\Delta M_f/\bar{M}_f, \Delta\chi_f/\bar{\chi}_f)$ assuming a uniform prior, with the cross marking the expected value for GR. The side panels show the marginalized posterior for $\Delta M_f/\bar{M}_f$ and $\Delta\chi_f/\bar{\chi}_f$. The gray distribution correspond to the product of all the individual posteriors. O3a (pre-O3a) events are plotted with solid (dot–dashed) traces. Color encodes the redshifted total mass in solar masses, with a turnover between blue and red around the median of the $(1+z)M/M_\odot$ distribution for the plotted events. The results for GW190412 and GW190814 are identified by dotted and dashed contours, respectively. The two events with contours that do not enclose the origin are GW170823 (dot–dashed) and GW190814 (dashed). GW190408_181802 has a multimodal posterior that results in the small contour (blue) away from zero.

self-consistency test on reconstructed remnant mass and spin as inferred from different parts of the signal (inspiral and merger-ringdown phases)

upper bound on graviton mass

$$m_g \leq 4\ 10^{-23} eV \quad , 90\%$$

testing the dispersion relation

$$E^2 = p^2c^2 + Ap^\alpha c^\alpha \quad with\ \alpha \geq 0$$

GR A=0, massive graviton (α=0 , A>0), …

local Lorentz invariance tests in the Gravitational Sector

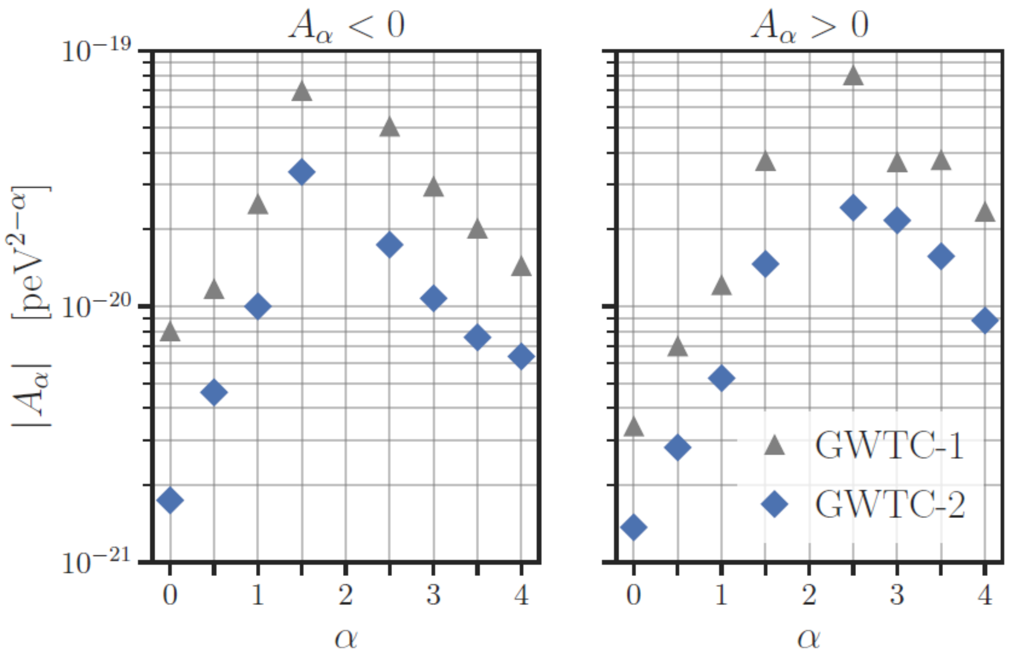

The main LIGO-Virgo searches for GWs

GW transients

- **Compact Binary Coalescences**
  - ✓ using stringent waveform models (phase evolution of signals)
- ...
- **Generic transient searches**
  - ✓ minimal assumptions on waveforms
- ...

Persistent GWs

- **Stochastic Background**
  - ✓ superposition of many unresolved cosmological and/or astrophysical sources
- **fast spinning NS**
  - ✓ quasi periodic signals

Probes of
- most extreme compact objects
- space-time dynamics
- early universe

Stochastic GW Background Searches

unresolved sources/processes:

- **cosmological origin:** from the earliest phases of the Universe
  vacuum fluctuations amplified by inflation, phase transitions, cosmic strings, pre-Big Bang models
- **astrophysical origin:**
  Binary BH coalescences (estimated from the observed mergers)
  other compact binary coalescences, Core Collapses to NS and BH, NS

✓ **search for isotropic SGWB: main target**
  optimally filtered correlations for the tensor GW polarizations

✓ **search for anisotropic SGWB: widest scope «hot spot» search**
  extended sources by spherical harmonic decomposition
  point sources by broadband radiometer
  point sources by narrowband radiometer vs frequency

✓ **search for non-GR polarizations** scalar and vector polarizations

Isotropic Stochastic GW Background

Phys. Rev. Lett. 118, 121101 (2017)

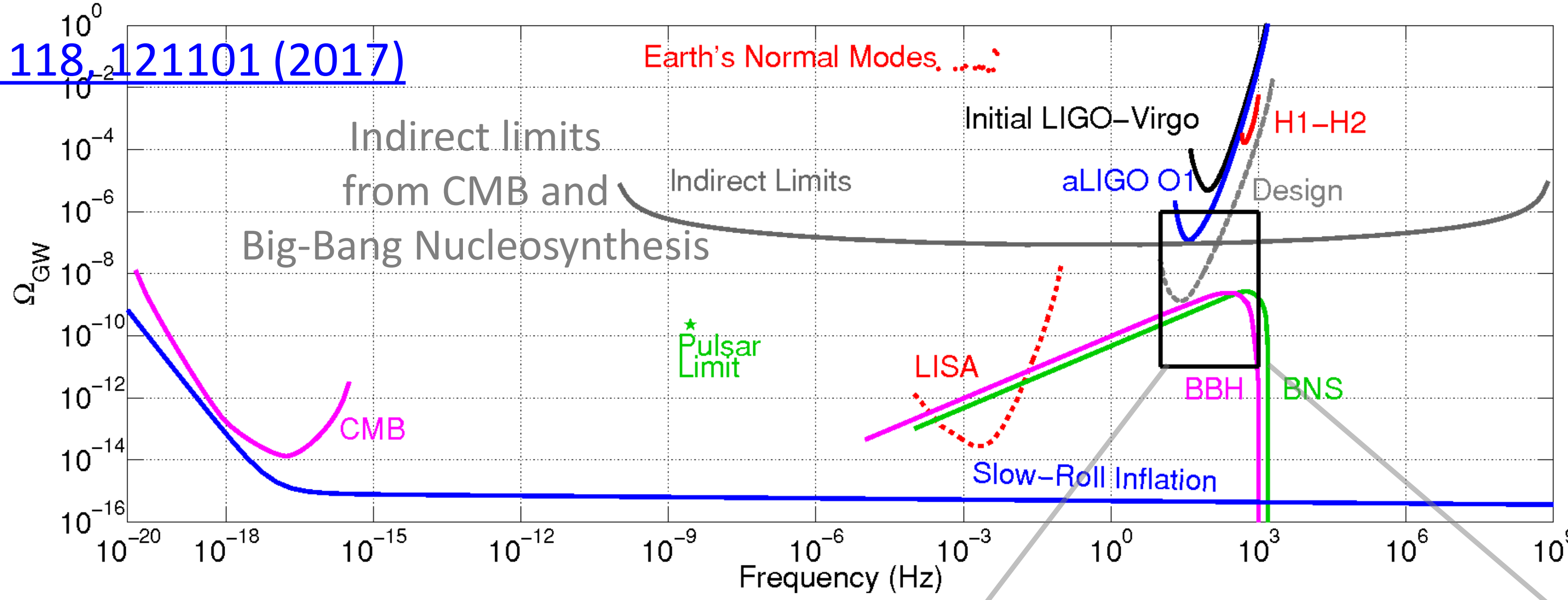

$$\Omega_{GW}(f) = \frac{f}{\rho_c}\frac{d\rho_{GW}}{df}$$

GW energy density per unit ln(f)

critical energy density

$$\rho_c = \frac{3c^2H_0^2}{8\pi G} \quad , \quad H_0 = 68\ \frac{km}{s\ Mpc}$$

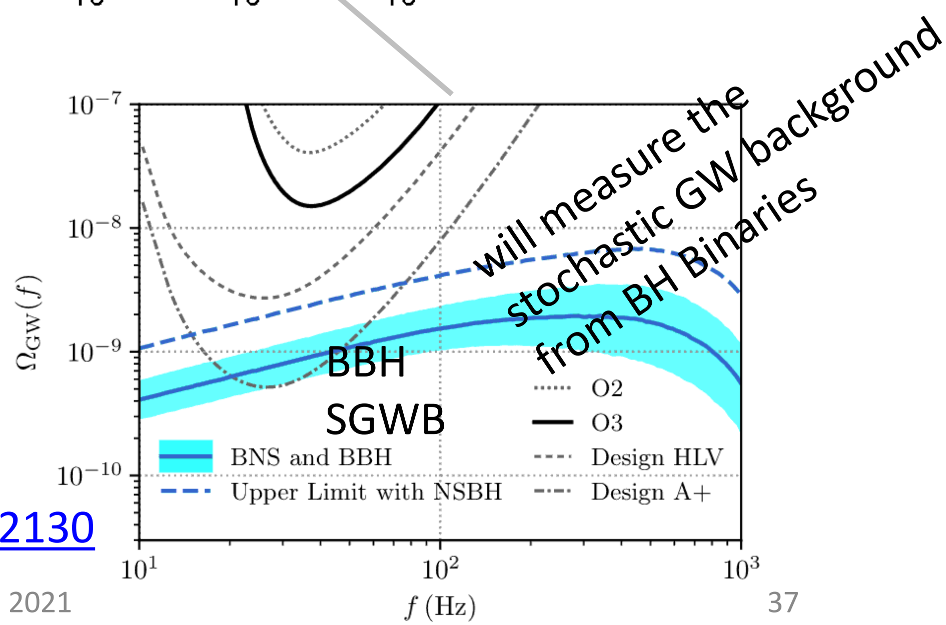

arXiv:2101.12130

Anisotropic Stochastic GW Background

arXiv:2103.08520

search for astrophysical background
GW energy flux [erg cm^{-2} s^{-1} Hz^{-1}] u.l. 90%

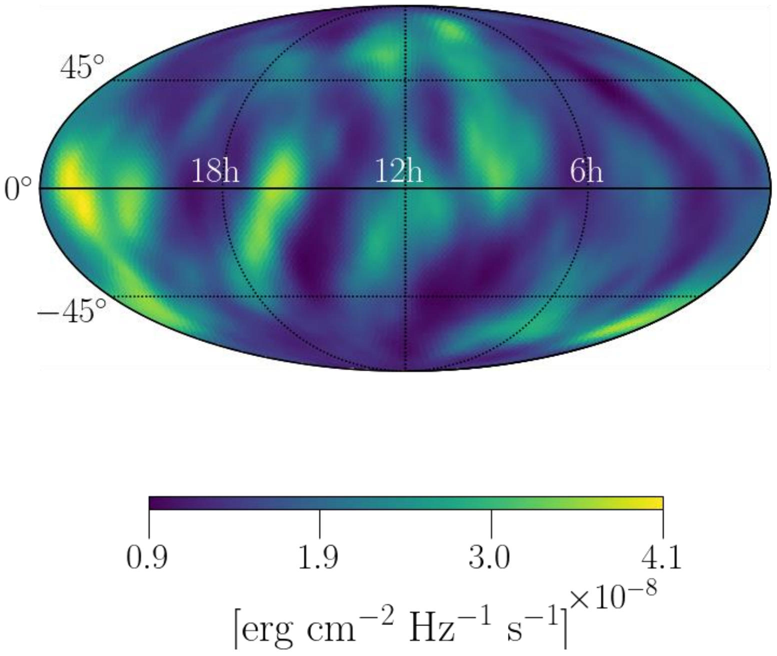

point-like sources
emitting narrowband
strain amplitude u.l. 90%

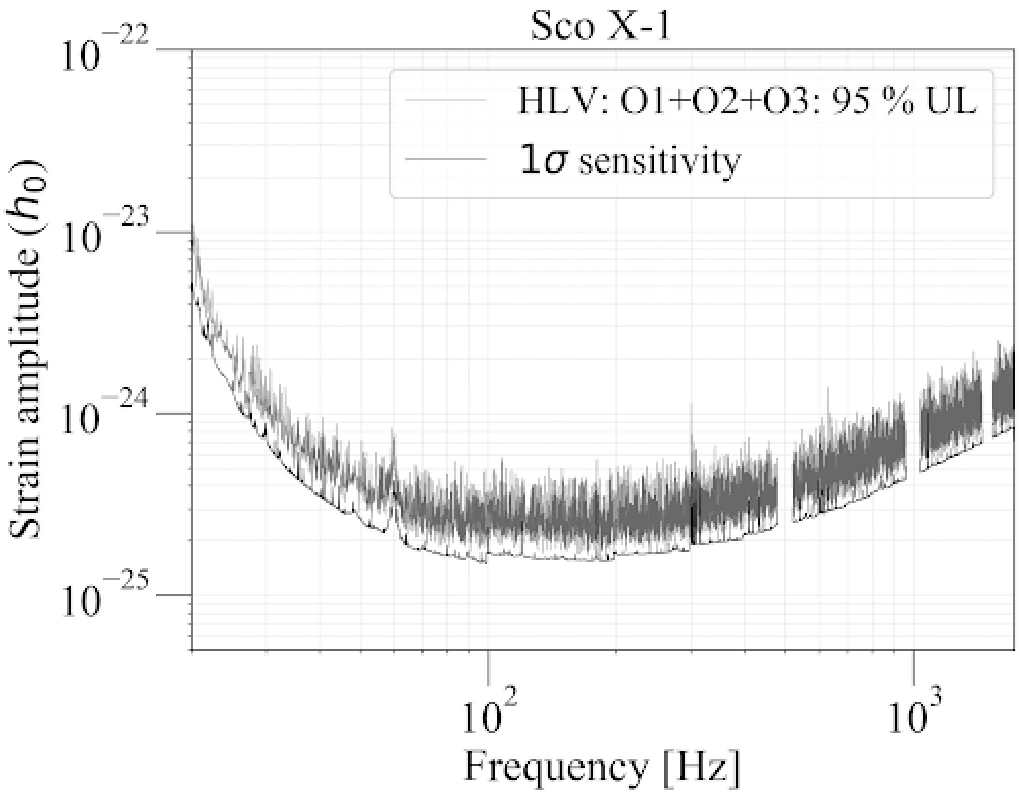

Stochastic GW Background Searches

Future sensitivity:

- scale as the energy PSD of detectors and $\sqrt{T_{observation}}$
- gains in terms of Ω_{GW} by extending PSD at lower frequencies

Future challenges: Schumann resonances

- correlated noise source at distant detectors $\Rightarrow$ bias on the results
- lightening strikes excite the global Schumann resonances at 8, 14, 20, ... Hz, correlated magnetic field variations (pT)
- noise cancellation strategy is possible

Virgo added value

- benefits the directional searches for persistent GWs

More detectors

- non-GR polarization search: easier to disambiguate the possible contributions from tensor, scalar and vector polarizations
- two detectors are however sufficient in principle to detect presence of non GR effects in persistent GWs

Periodic GW Searches

Search for persistent quasi-periodic GW emission from spinning NS:

- **> 2500 NS are known,** O(10^9) expected in our galaxy
- **GW emission from non-axisymmetry** originating from
  - deformation due to elastic stresses or magnetic field not aligned to the rotation axis ($f_{GW} = 2\, f_r$)
  - free precession around rotation axis ($f_{GW} \sim f_r + f_{prec}$; $f_{GW} \sim 2\, f_r + 2\, f_{prec}$)
  - excitation of long-lasting oscillations (e.g. r-modes; $f_{GW} \sim 4/3\, f_r$)
  - deformation due to matter accretion (e.g. LMXB; $f_{GW} \sim 2\, f_r$)

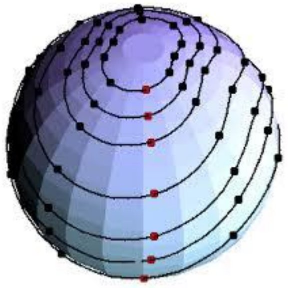

equatorial non-axisymmetry

ellipticity: $\boldsymbol{\varepsilon} = (I_{XX} - I_{YY}) \,/\, I_{ZZ}$

GW strain amplitude on Earth:

$$\boldsymbol{h_0} = 4\ 10^{-25} \left(\frac{\boldsymbol{\varepsilon}}{10^{-5}}\right) \left(\frac{I_{zz}}{10^{45}\, g\ cm^2}\right) \left(\frac{f_r}{100\ Hz}\right)^2 \left(\frac{1\ kpc}{d}\right)$$

Maximum ellipticity depends on NS composition:

normal NS: $\boldsymbol{\varepsilon} < 10^{-5}$ → hybrid NS: $\boldsymbol{\varepsilon} < 10^{-3}$ → quark NS: $\boldsymbol{\varepsilon} < 10^{-1}$ *PRD 87, 129903 (2013)*

Periodic GW Searches

- **known PSRs show a spin-down**

  $\dot{f}_r < 0.01 Hz / yr \quad \Rightarrow$ up to very high rotational energy losses

  - magnetic dipole radiation ...
  - possible GW emission ?

- **spin-down limit:**

  assuming all spin-down is by GW emission, one can set upper limits on the GW strain amplitude and on NS ellipticity from EM observations alone

✓ **Targeted Searches for GWs from known PSRs**

ephemeris available for all source parameters
search at EM ephemeris or in narrow bands
optimal analysis is computationally light

✓ **Directed Searches for GWs from NSs**

only sky location is available
optimal analysis requires computer farms

✓ **All-Sky Searches for GWs from yet unknown isolated NSs**

computationally limited (e.g. Einstein@home, GRID)
«semi-coherent» analysis to trigger a few coherent followups

Combination of single detector analyses

All-sky Searches for GWs from unknown isolated NSs

Phys. Rev. D **100**, 024004 (2019)

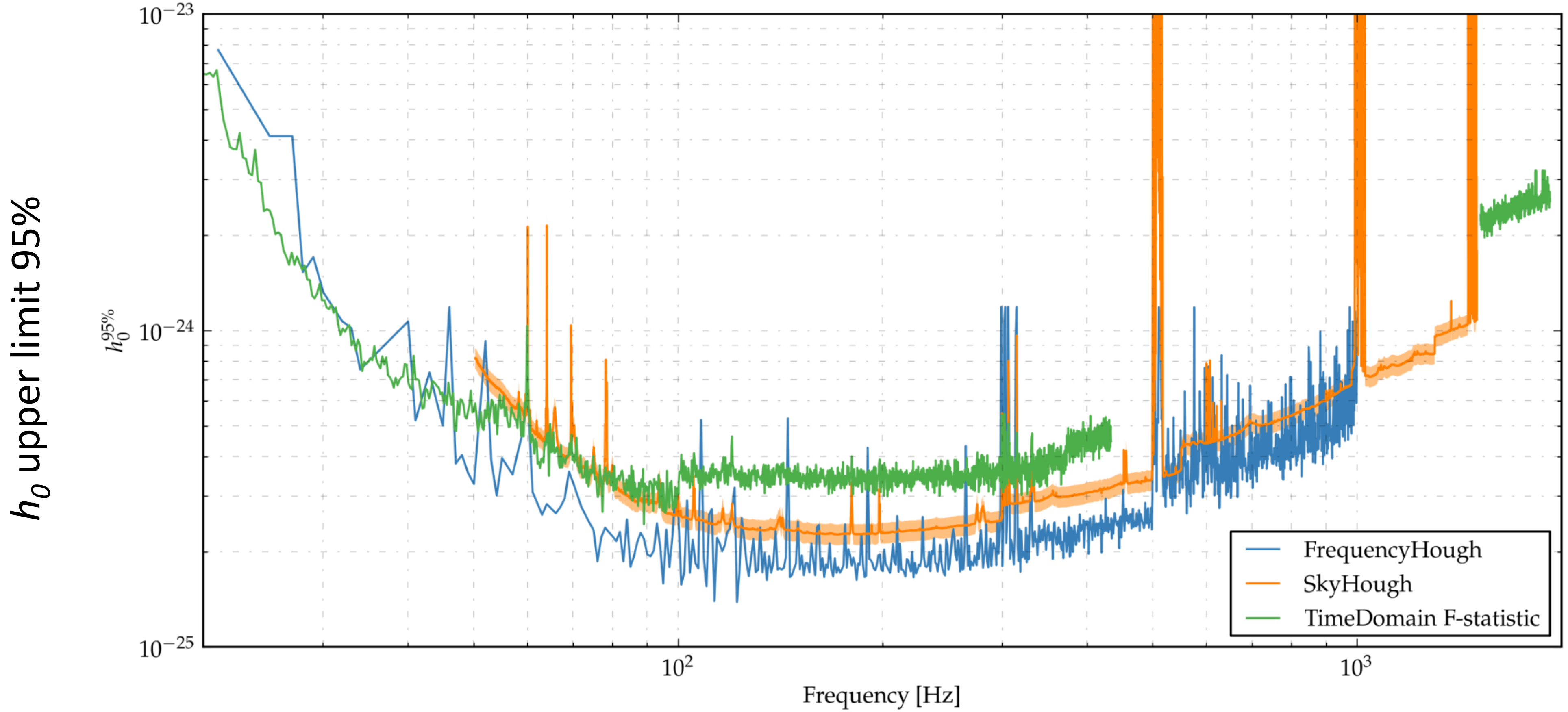

Targeted GW Searches from known PSRs

[Astrophys. J. **879**, 10 (2019)]

h_0 upper limit 95%

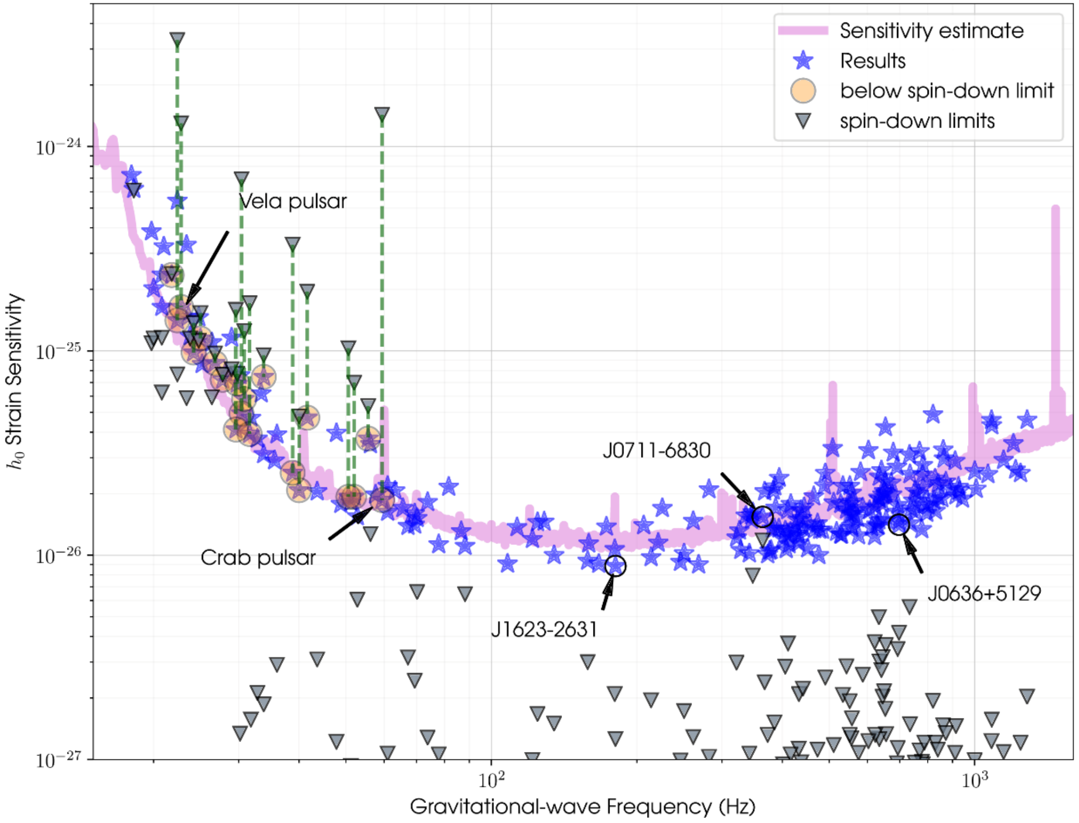

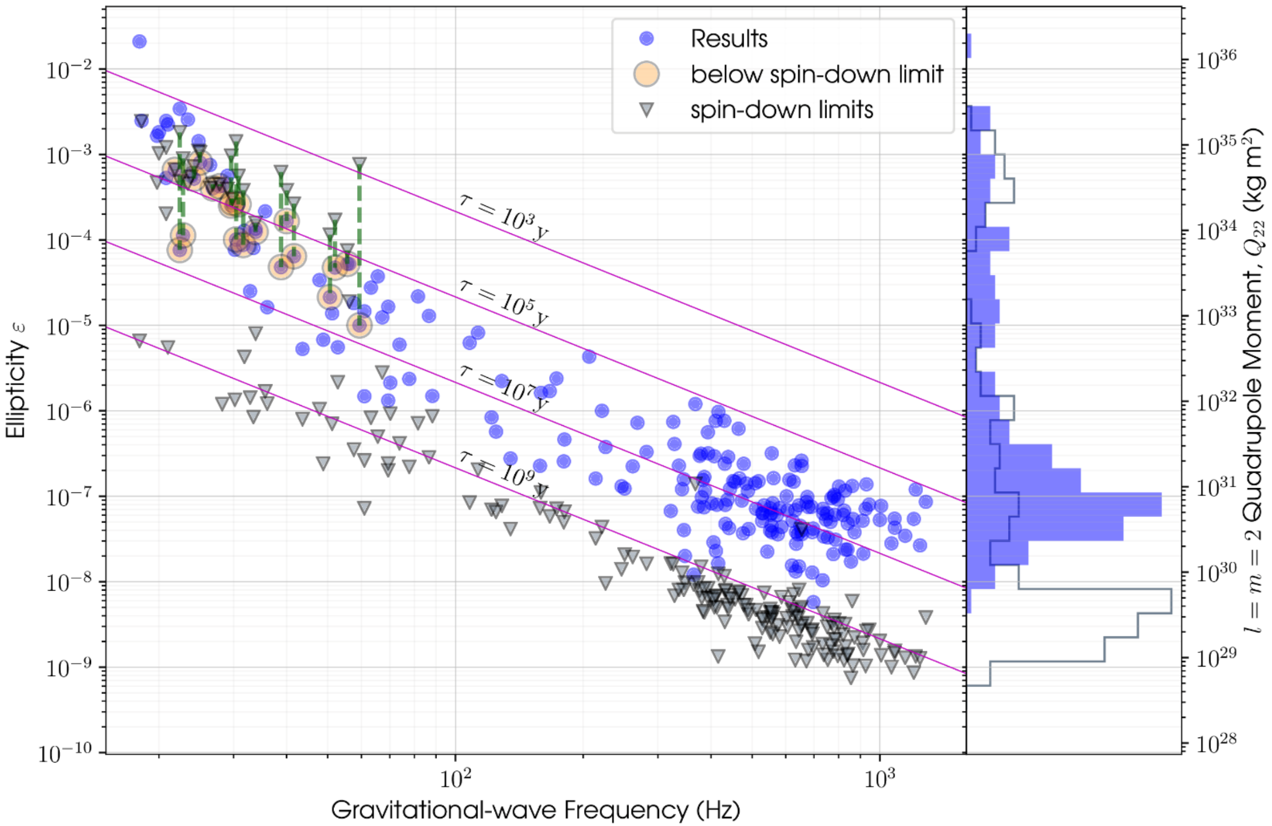

- ✓ **221 known PSRs**
- ✓ **20 spin-down limits beaten**

  Crab h_0 u.l. 70 times lower

  Vela h_0 u.l. 20 times lower

The filled circles show upper limits in terms of stars' ellipticities ε, whilst the triangles give the equivalent spin-down limits. The ellipticity can roughly be converted to a "mountain" size using $25\times(\varepsilon/10^{-4})$

Einstein Telescope

mid 2030 European underground infrastructure housing more detectors

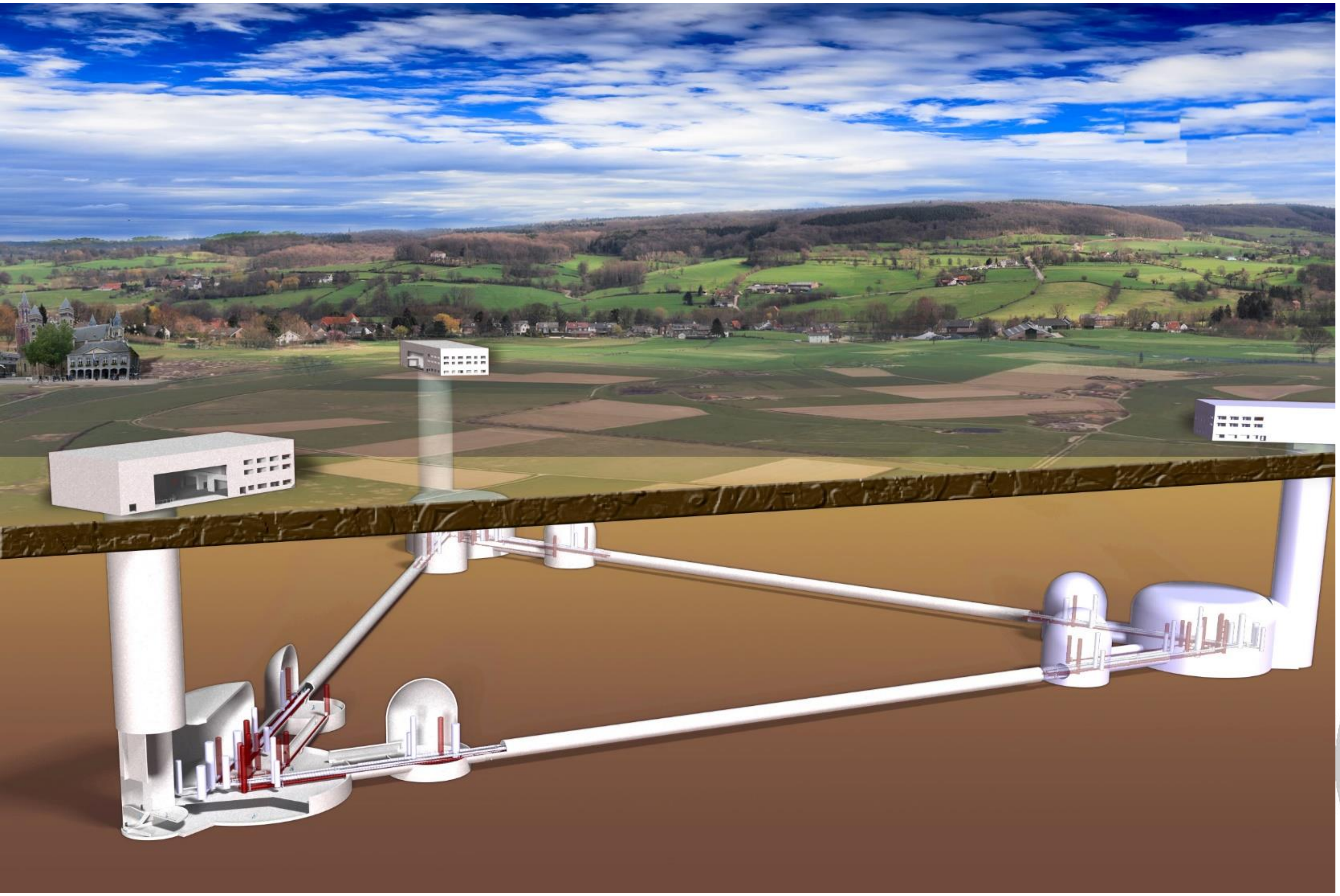

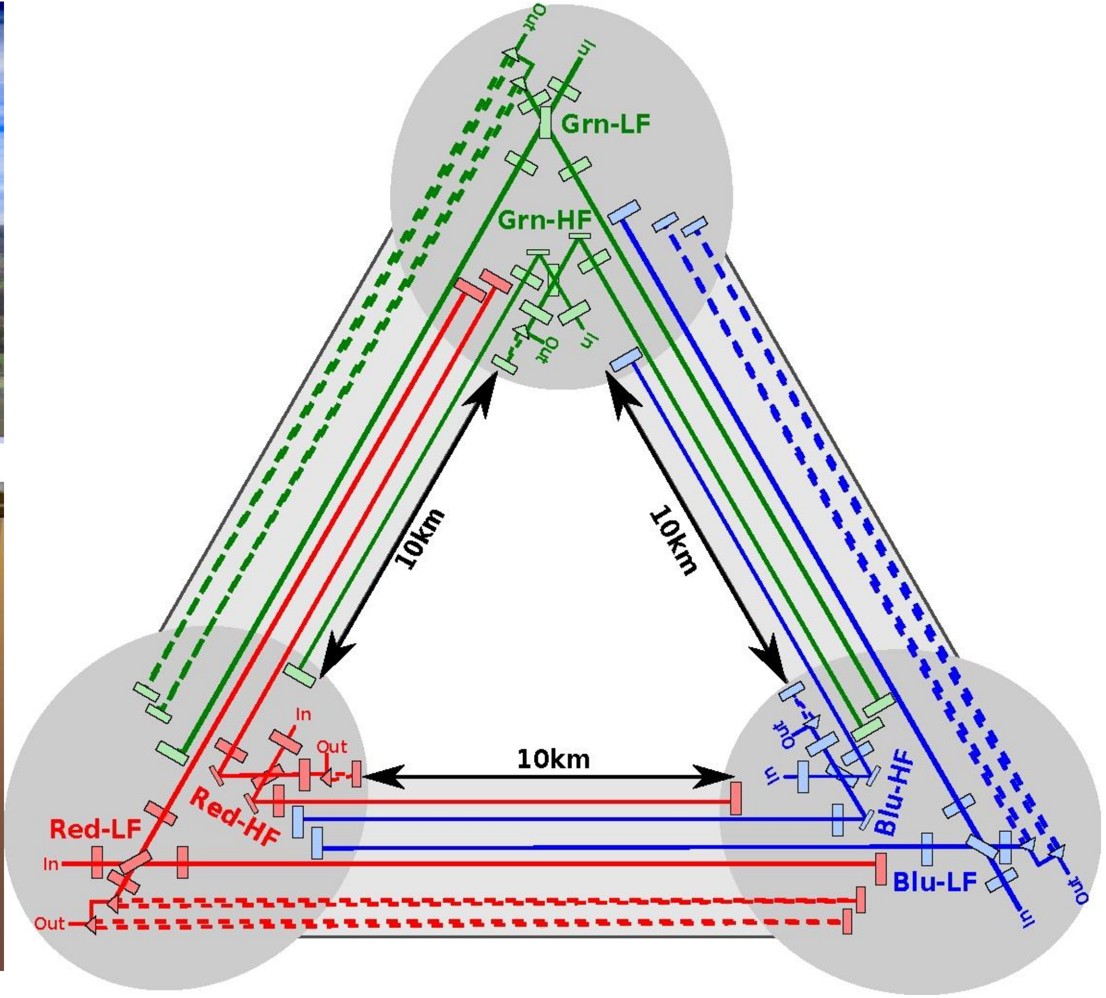

Einstein Telescope

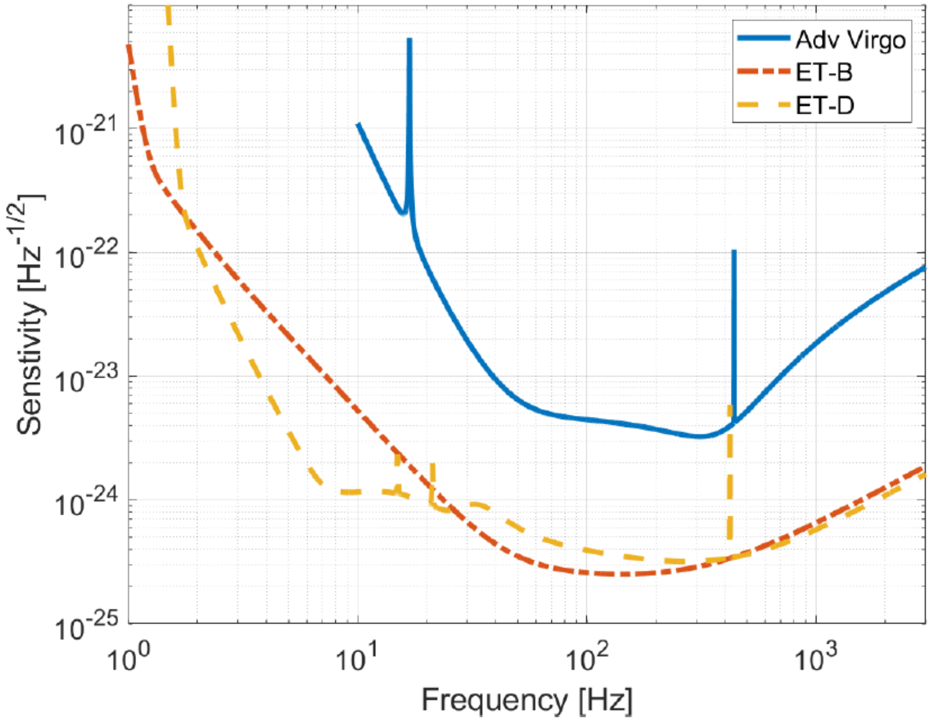

expand to lower frequencies by a factor 10

improve ASD by one order of magnitude

S.Hild et al., CQG 28, 094013 (2011)
Maggiore et al., arXiv:1912.02622

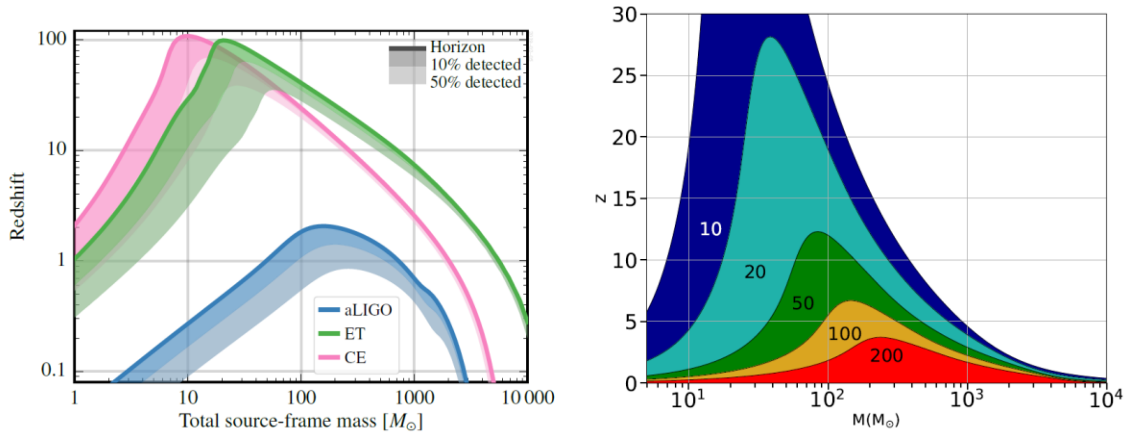

Figure 2. Left: astrophysical reach for equal-mass, nonspinning binaries for Advanced LIGO, Einstein Telescope and Cosmic Explorer (from ref. [26, 27]). Right: lines of constant signal-to-noise ratio in the (total mass, redshift) plane, for a network of one ET and two CE detectors. The curves shown assume equal-mass binary components (figure courtesy by M. Colpi and A. Mangiagli).

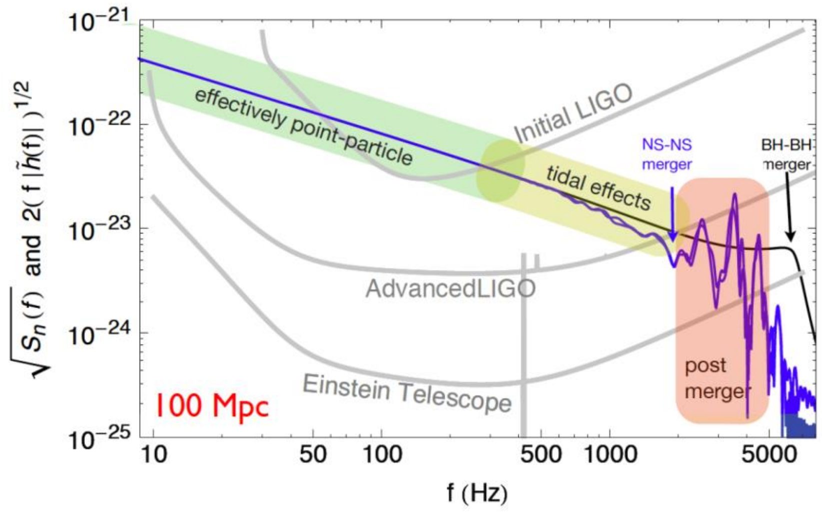

Einstein Telescope

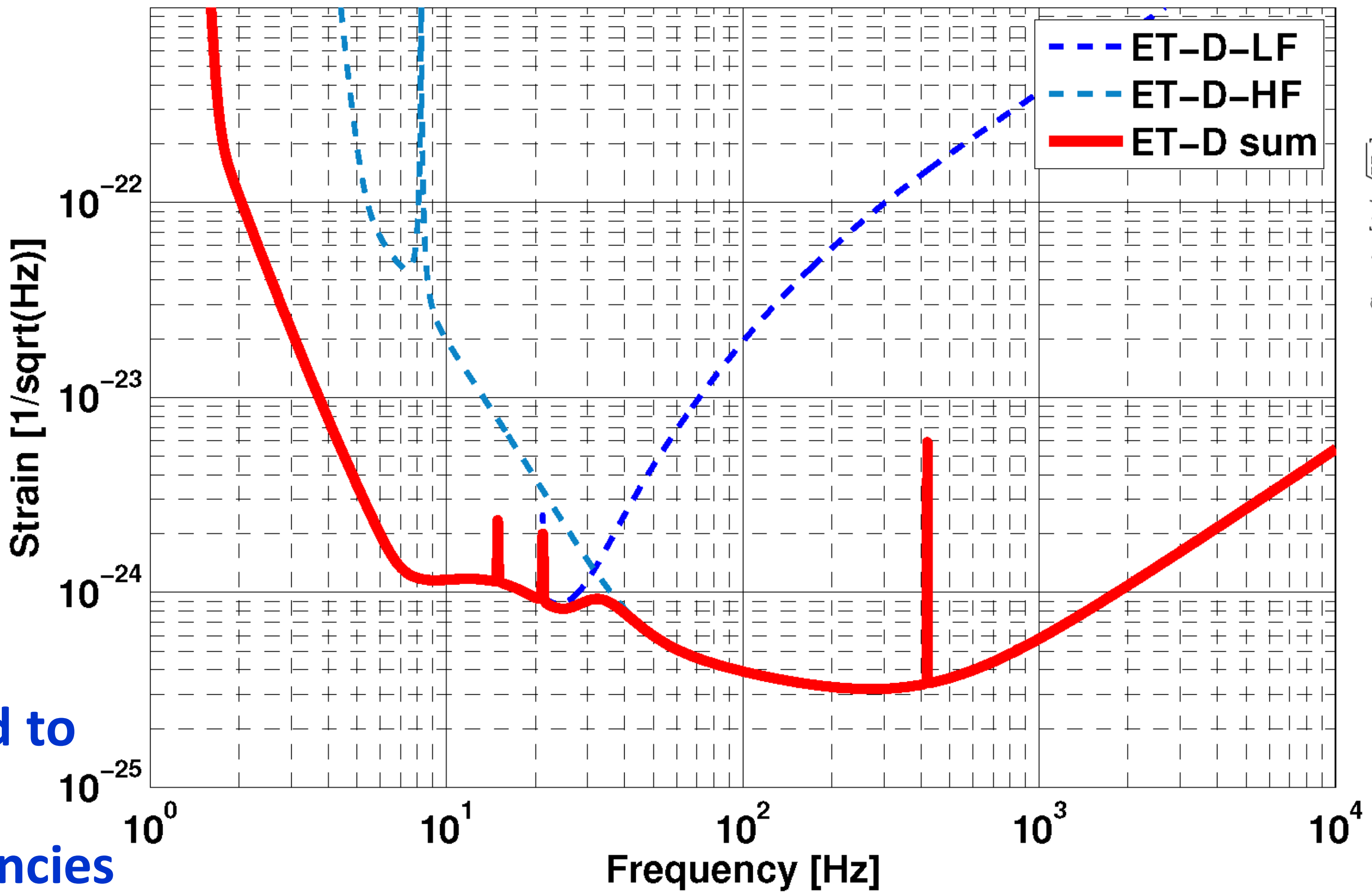

expand to lower frequencies

S.Hild et al., Classical and Quantum Gravity, Volume 28, Issue 9, pp. 094013, 2011

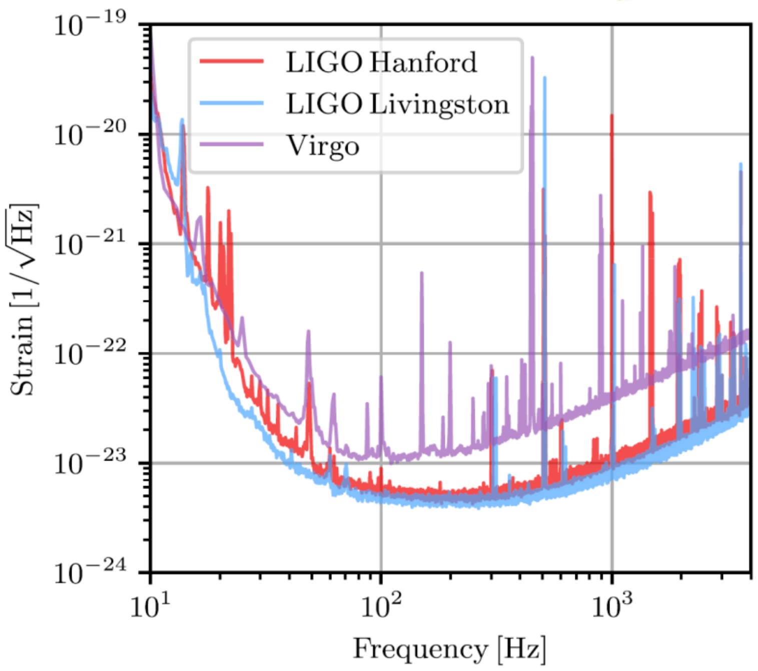

latest performances of LIGO-Virgo

LIGO-Virgo Black Holes and Neutron Stars

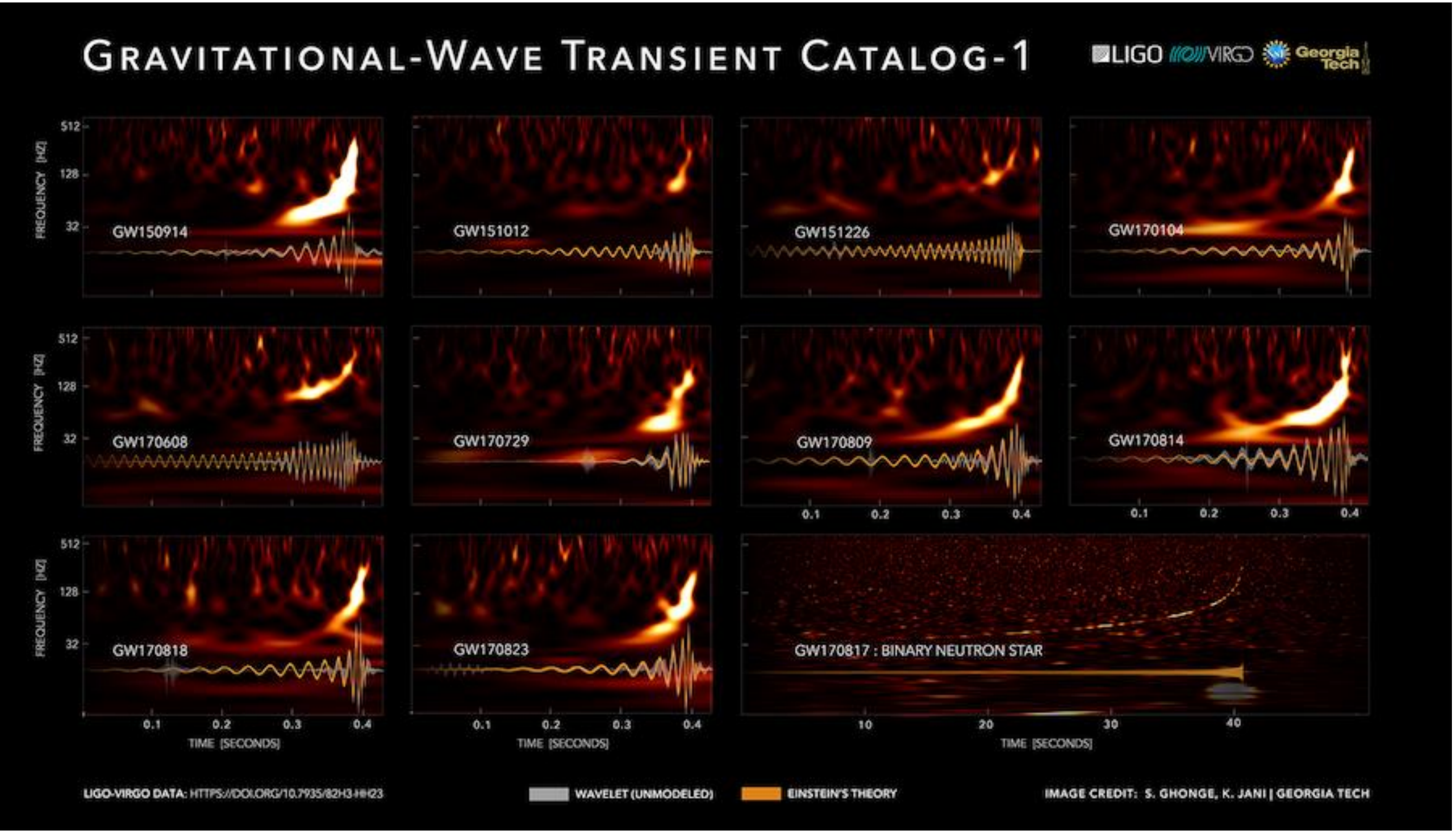

unexpected population of Binary Black Holes:

- higher mass

  x-ray binary BHs are lighter
- BBH merger rate compatible with highest expectations

  10-100 Gpc^{-3} yr^{-1}
- testbed for checking General Relativity
- no related electromagnetic emission found

one BNS coalescence: EM counterparts found

LVC arxiv:1811.12907

[more interactive plots: http://catalog.cardiffgravity.org/](http://catalog.cardiffgravity.org/)

GW170814 : Virgo is in the game!

On August 14, 2017 at 10:30:43 UTC, Virgo & LIGO detected the first triple coincidence BBH event

Primary black hole mass m_1	**30.5** $^{+5.7}_{-3.0}\,M_\odot$
Secondary black hole mass m_2	**25.3** $^{+2.8}_{-4.2}\,M_\odot$
Chirp mass $\mathcal{M}$	$24.1^{+1.4}_{-1.1}\,M_\odot$
Total mass M	$55.9^{+3.4}_{-2.7}\,M_\odot$
Final black hole mass M_f	**53.2** $^{+3.2}_{-2.5}\,M_\odot$
Radiated energy E_{rad}	**2.7** $^{+0.4}_{-0.3}\,M_\odot c^2$

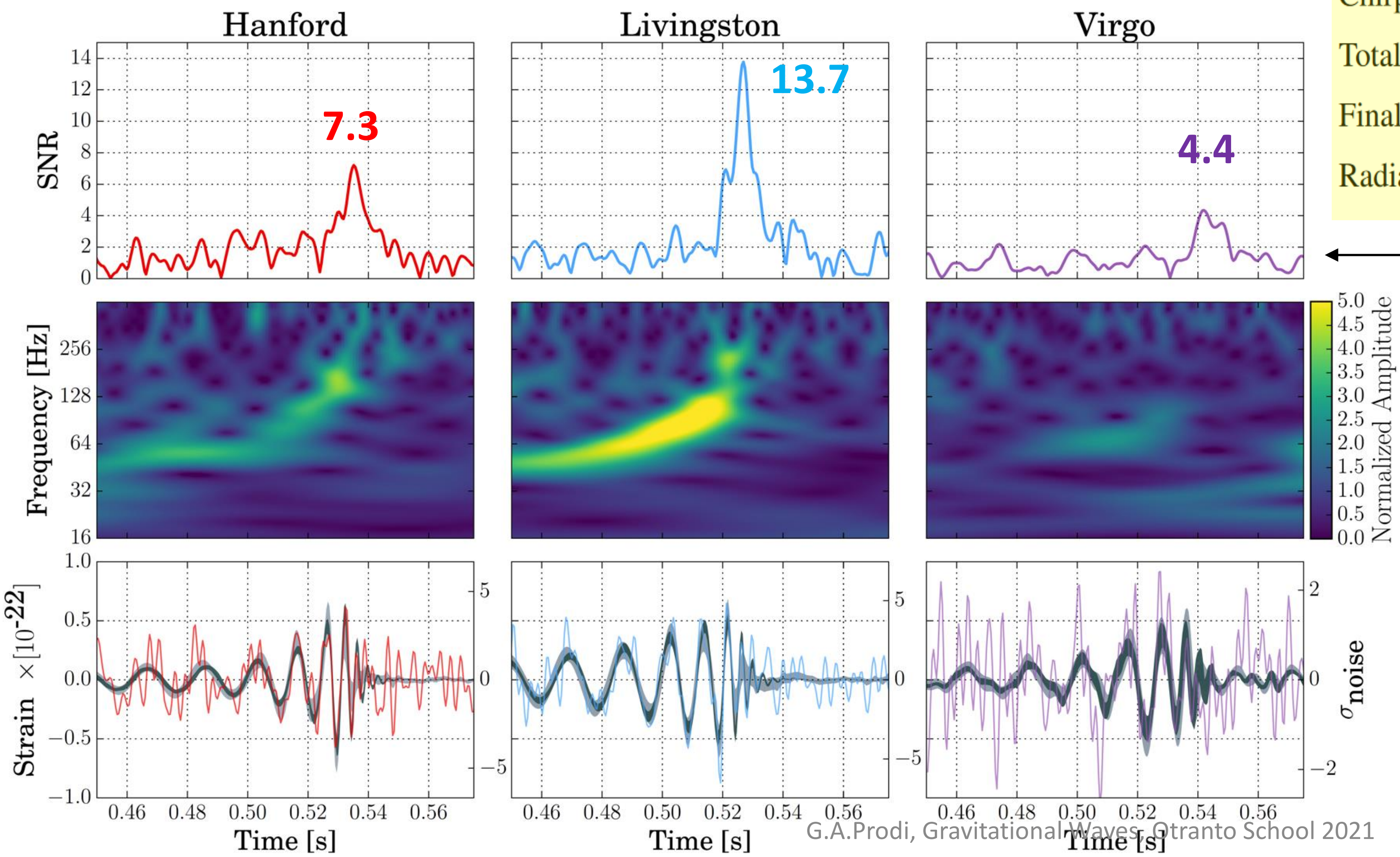

SNR time series using the best matching template

Time-frequency representation of the strain data around the time of GW170814

Reconstructed waveforms
- BBH model (dark gray)
- Unmodel (light gray)
- Whitened data (color)

Whitened Data domain

signal is projected at each detector according to its antenna pattern

LIGO-Virgo GWTC-1 Black Holes and Neutron Stars

- ***Chirp Mass*** $(m_1\, m_2)^{3/5}\,(m_1 + m_2)^{-1/5}$ *is well constrained.*
- ***Component masses ratio** is affected by degeneracy with **aligned spin components** with orbital momentum*

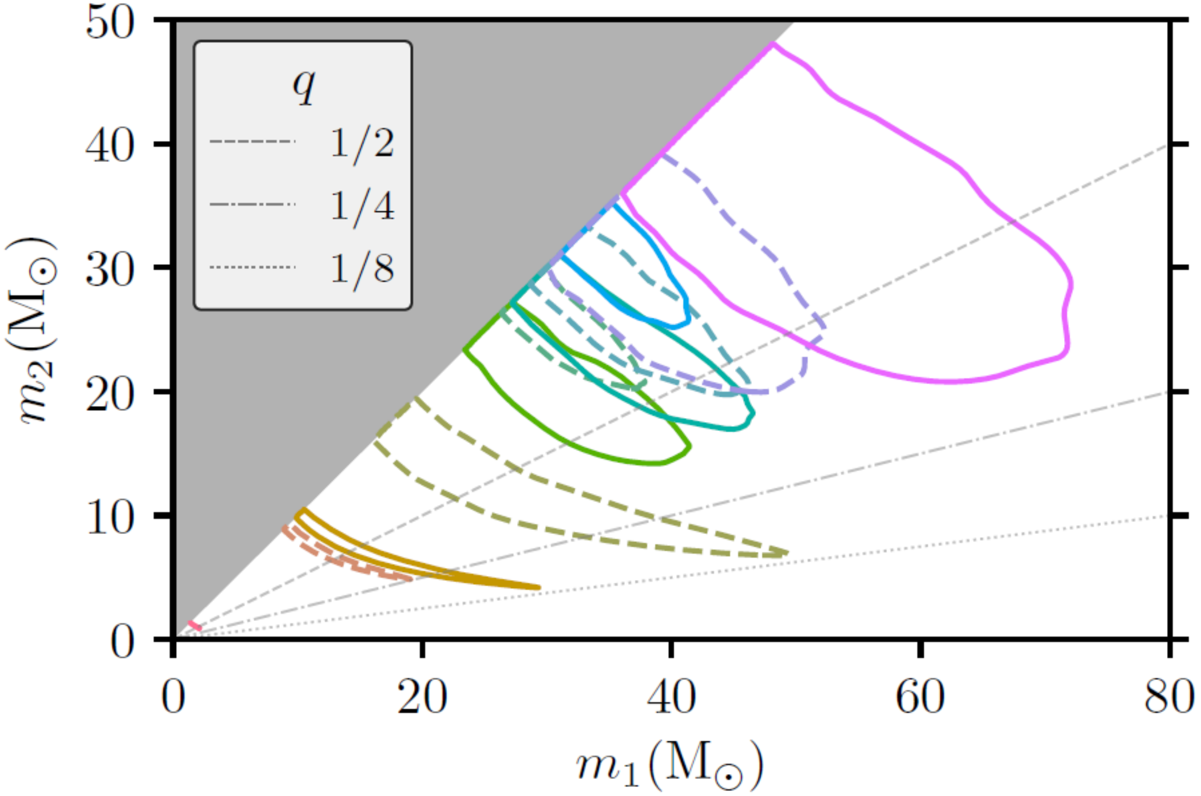

BNS GW170817:

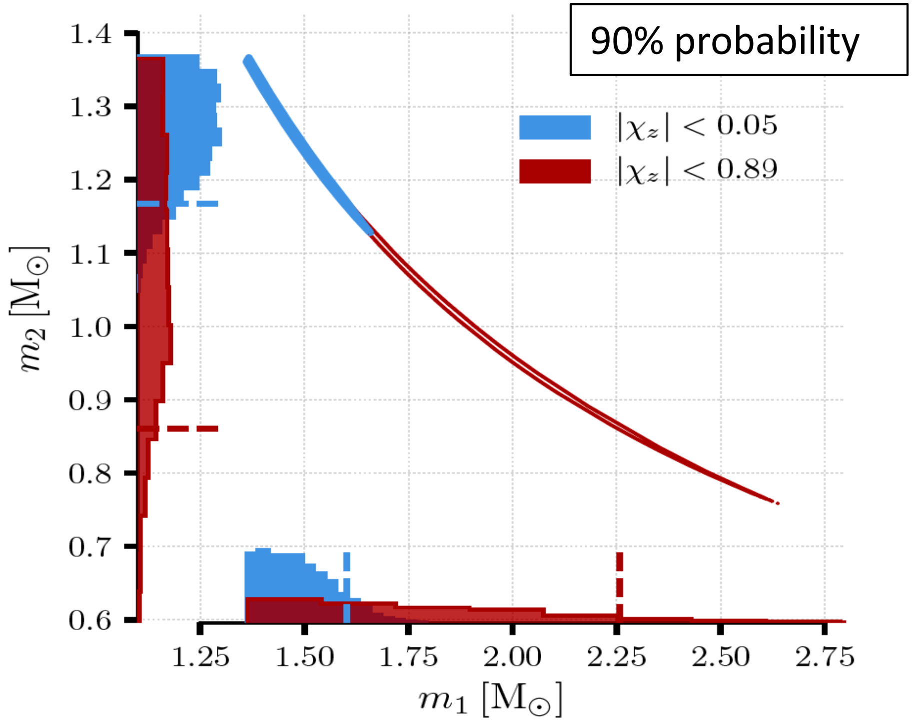

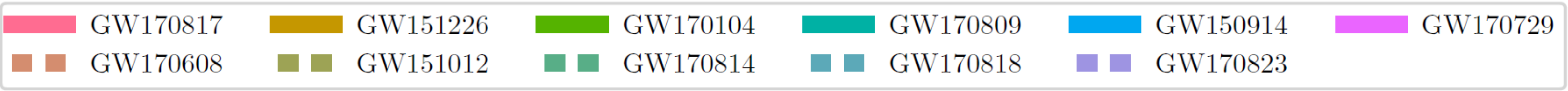

LIGO-Virgo GWTC-1 Black Holes and Neutron Stars

***Estimation of inclination angle** needs a better measurement of the polarization state of the GW*
=> estimation of distance show degeneracy

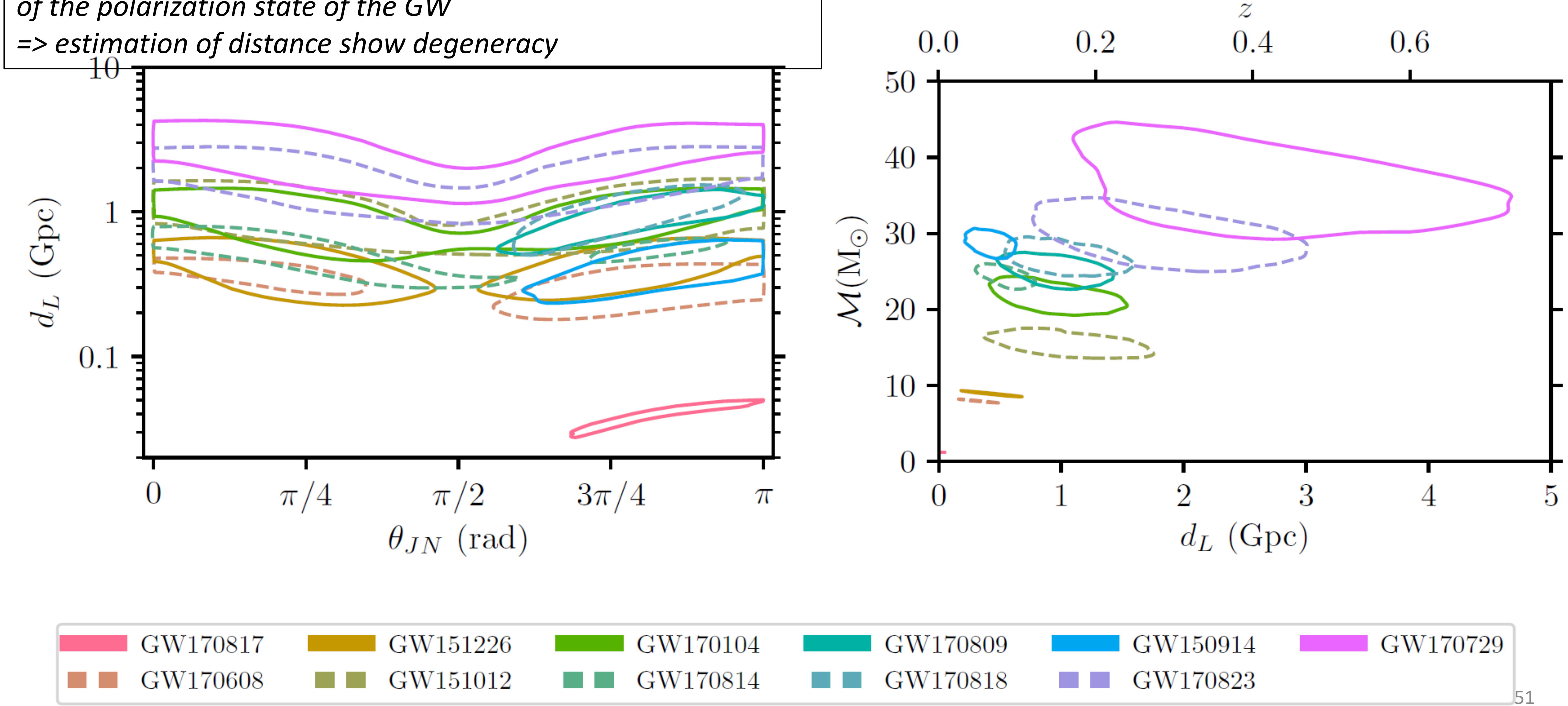

GW searches for stellar mass Compact Binary Coalescences

detection stage:

- **measurement of the detection significance** each search method ranks the findings against a reference distribution of the accidental background. The detection statistics is based on SNR but takes into account additional information.

Accidental background can be directly measured by creating independent copies of the experiment which cannot include astrophysical signals, e.g. by shifting the time of onde detector more than the maximum possible signal travel time or the filter autocorrelation time.

PyCBC

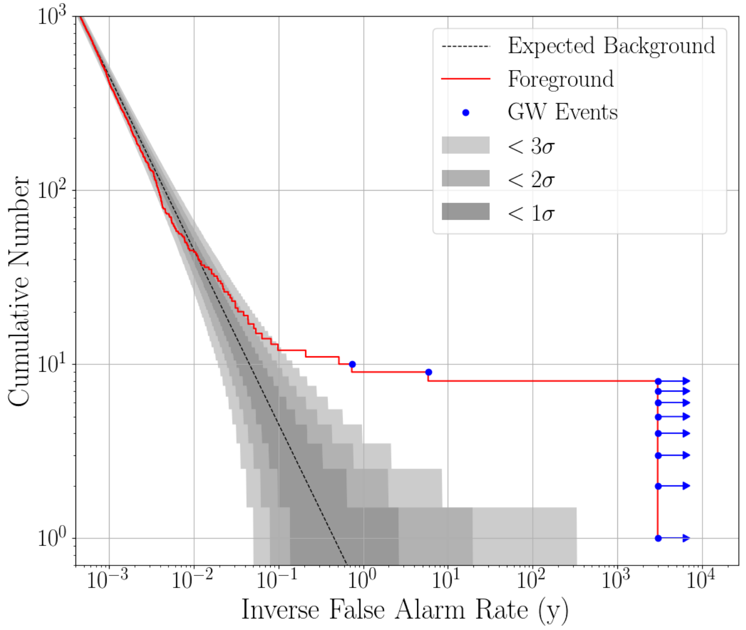

GstLAL

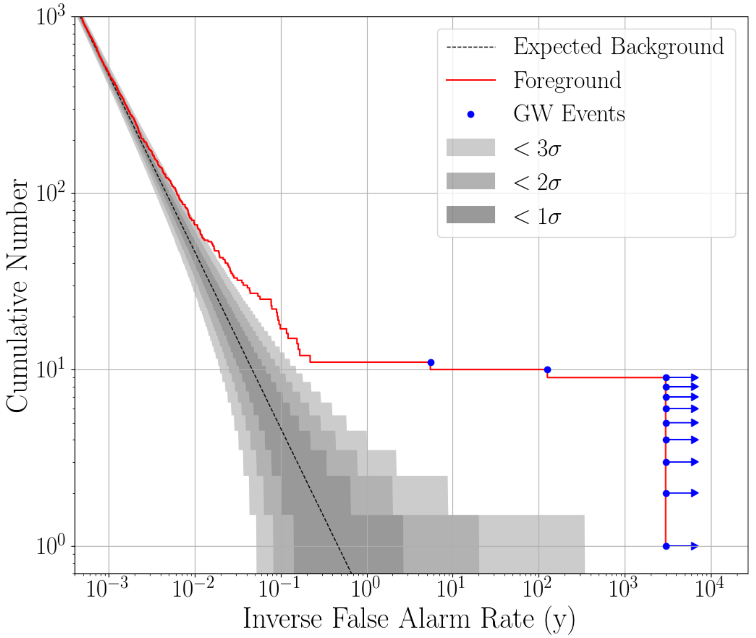

cWB

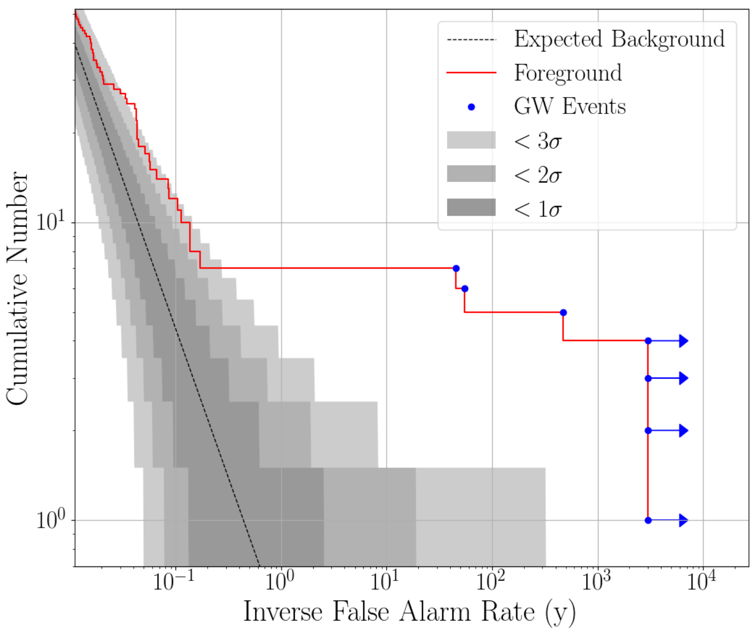

Identifyng noise source

- Transient noise outliers (**glitches**) in excess of Gaussian statistics are ubiquitous, and show non stationary characteristics
- More than **200000 auxiliary channels** are recorded to monitor instrument behaviour and environmental conditions
- In the case of clear correlation within glitches in gravitational wave channel and auxiliary ones, data are discarded from the analysis (**vetoed**)
- Burst methods in general and shorter template searches are more affected

Class.Quant.Grav. 33, 134001 (2016)

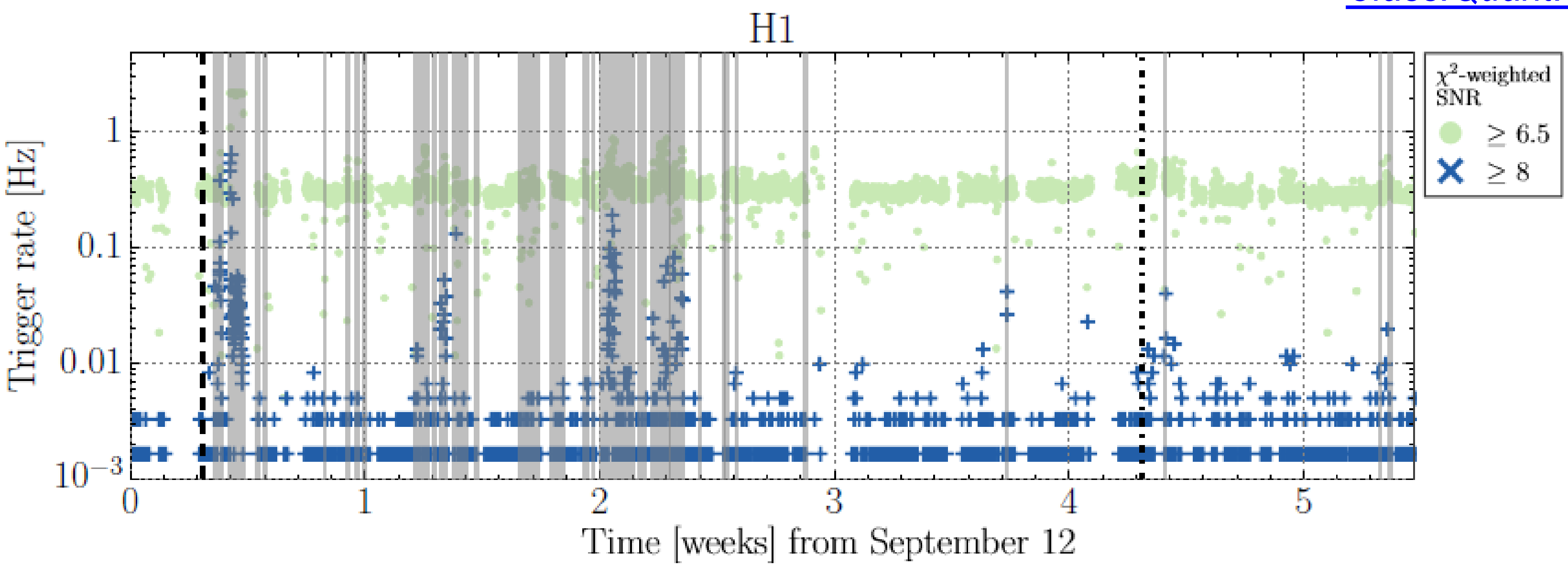

GW searches for stellar mass Compact Binary Coalescences

interpretation:

- **measurement of the detection efficiency** by performing MonteCarlo simulations of source population models.

The accessible spacetime volume, $\langle VT \rangle$, is estimated by injecting synthesized signals with parameters drawn from $\{\theta\}$ and recovering them using the search pipeline. For all $\{\theta\}$ the injections are assumed to be uniformly distributed in the comoving volume. Then the detection efficiency over redshift $f(z|\{\theta\})$ derived from the recovery campaign measures the fraction of the differential volume dV/dz which is accessible to the network:

$$\langle VT \rangle_{\{\theta\}} = T_{\rm obs} \int_0^\infty f(z|\{\theta\}) \frac{dV}{dz} \frac{1}{1+z} dz \,. \qquad (8)$$

The total $\langle VT \rangle$ is then the product of the accessible volume for a given population with the observational time $T_{\rm obs}$. The

- **classification of detected signals** into BBH, NS-BH, BNS, and «terrestrial origin» and related posterior probabilities.

e.g. estimate of the **rate of sources:** BBH mergers

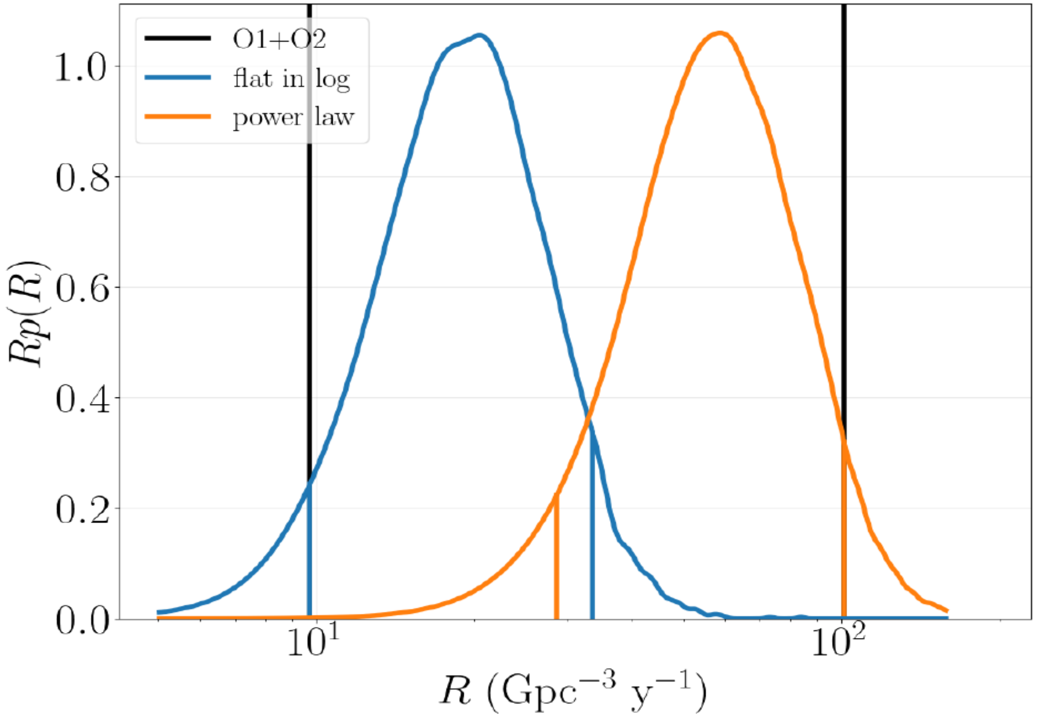

FIG. 12. This figure shows the posterior distribution — combined from the results of PyCBC and GstLAL— on the BBH event rate for the flat in log (blue) and power-law (orange) mass distributions. The symmetric 90% confidence intervals are indicated with vertical lines beneath the posterior distribution. The union of intervals is indicated in black.

primary mass m1 included in 5-50 Msun

extreme models as priors: $\propto \ln(m1)$ or $\propto m1^{-2.3}$

GW searches for stellar mass Compact Binary Coalescences

interpretation:

- **reconstructing the waveforms of signals using coherent analyses of the detector network** both by using detailed parametrized signal models and by more generic methods

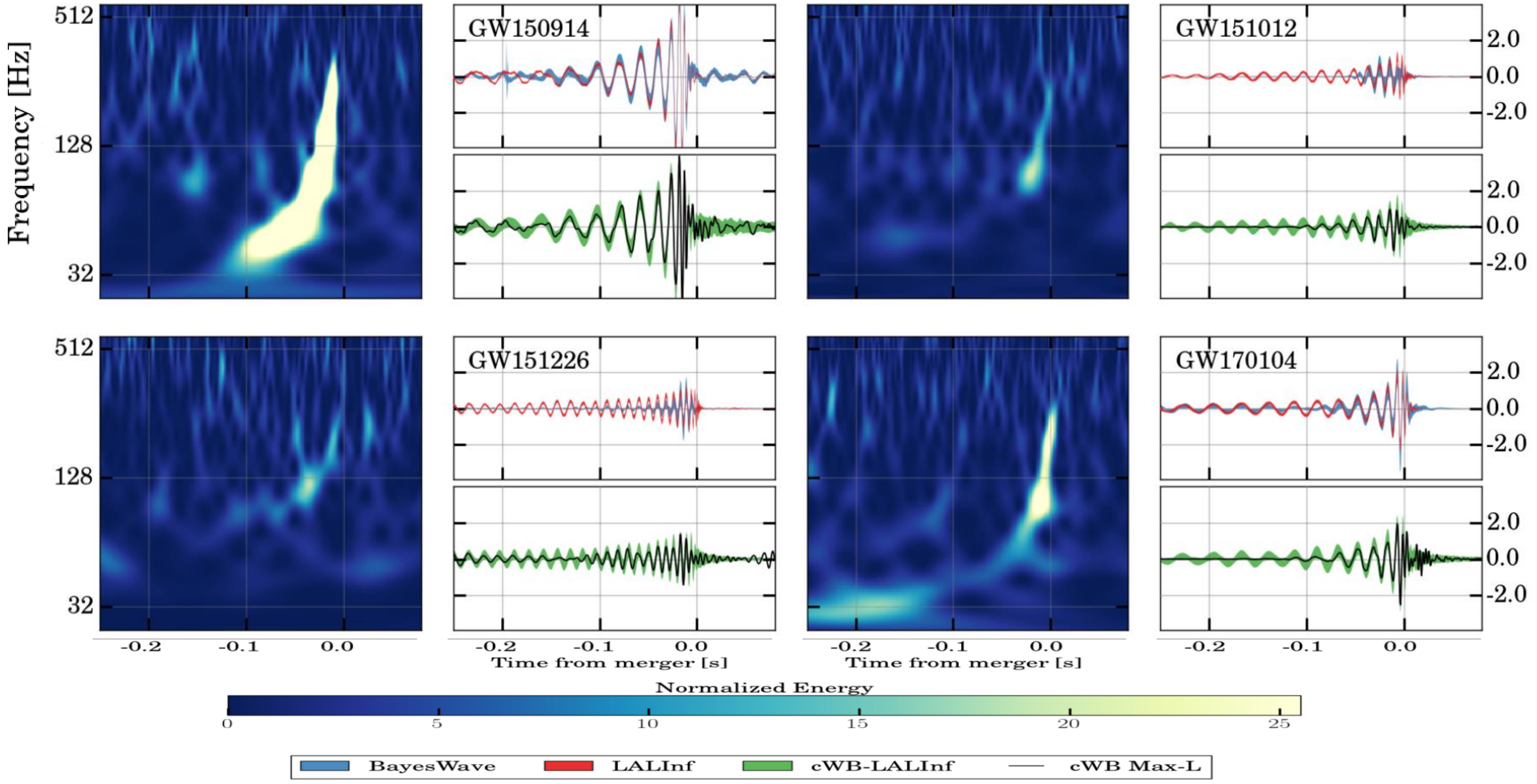

LIGO-Virgo Black Holes

Example prior and posterior distributions for GW170809

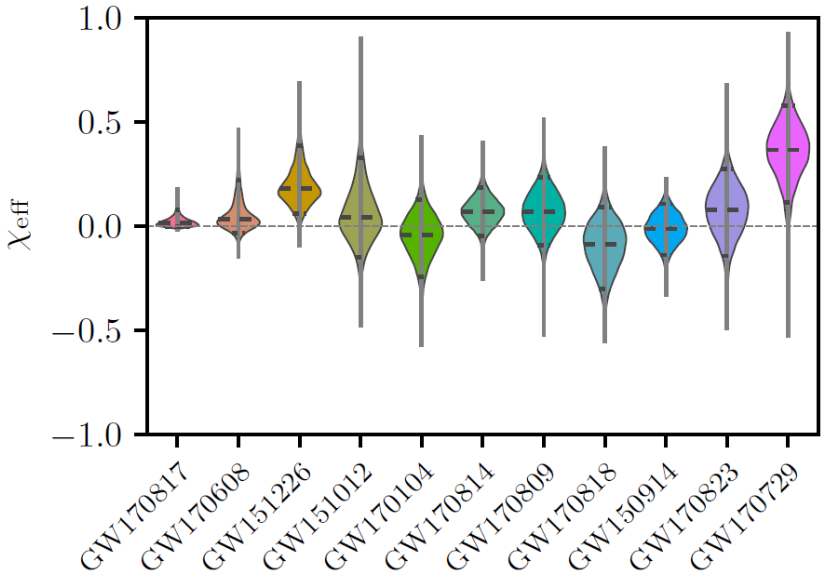

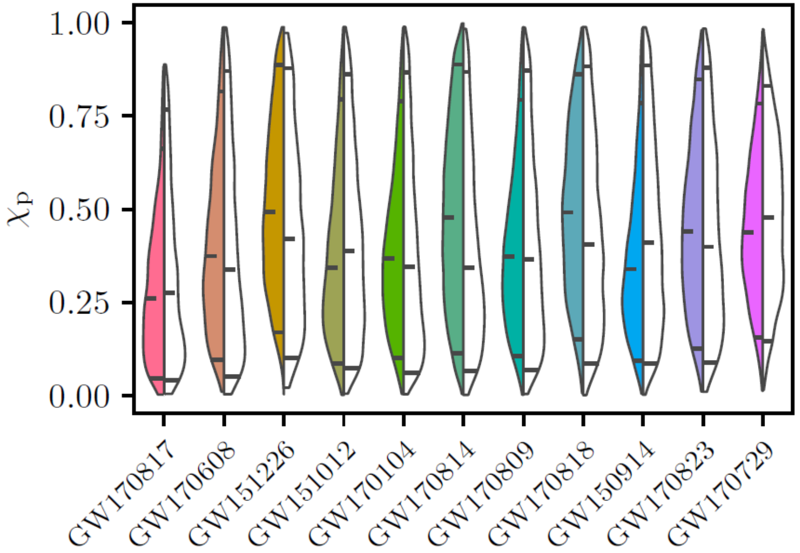

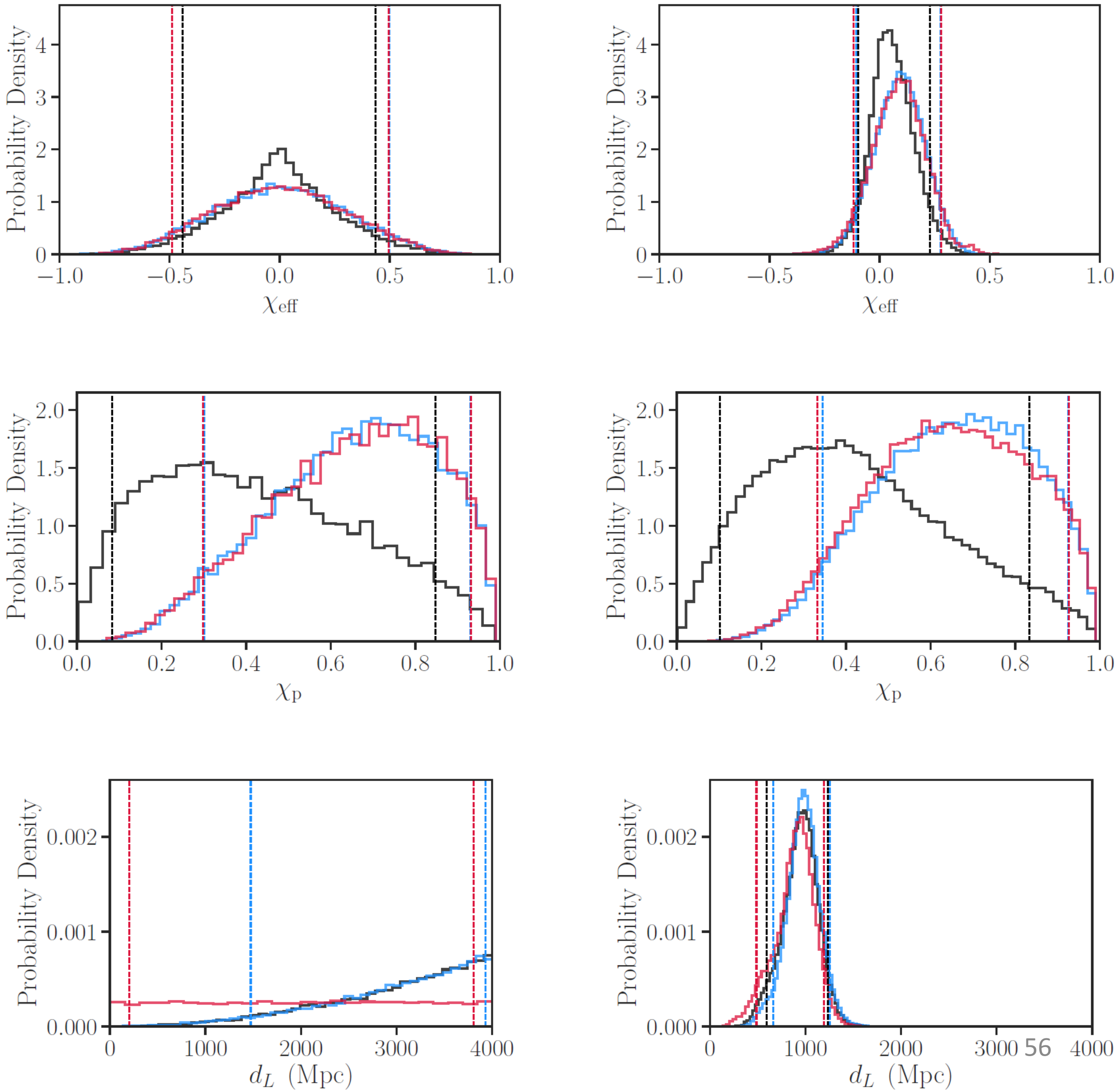

when early warning will be possible ?

GW170817

- Example values:

$$m_1 \sim 1.5\ M_\odot, \qquad m_2 = 1.25\ M_\odot, \qquad f_{gw,0} = 40\ Hz$$

$$R_0 \approx 290\ km, \qquad R_{ISCO} \approx 25\ km, \qquad \tau_0 \approx 25\ s$$

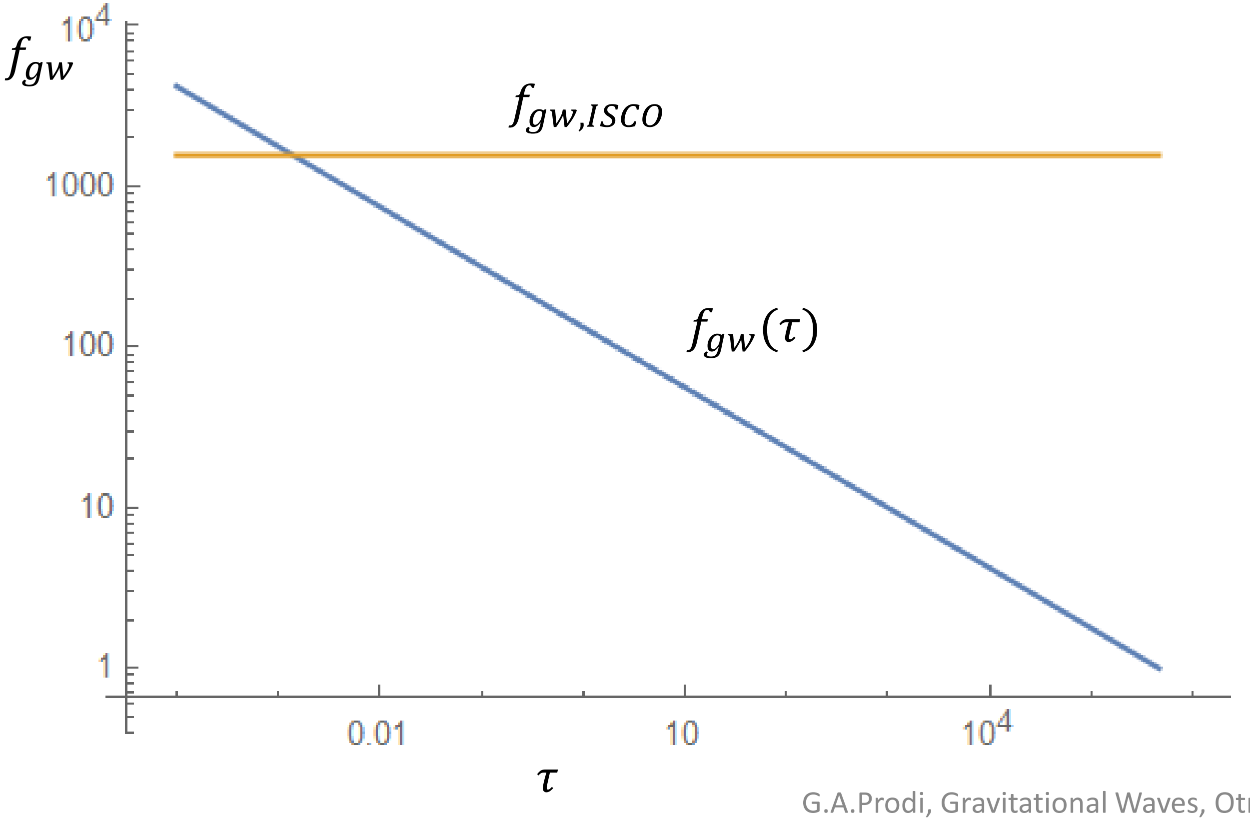

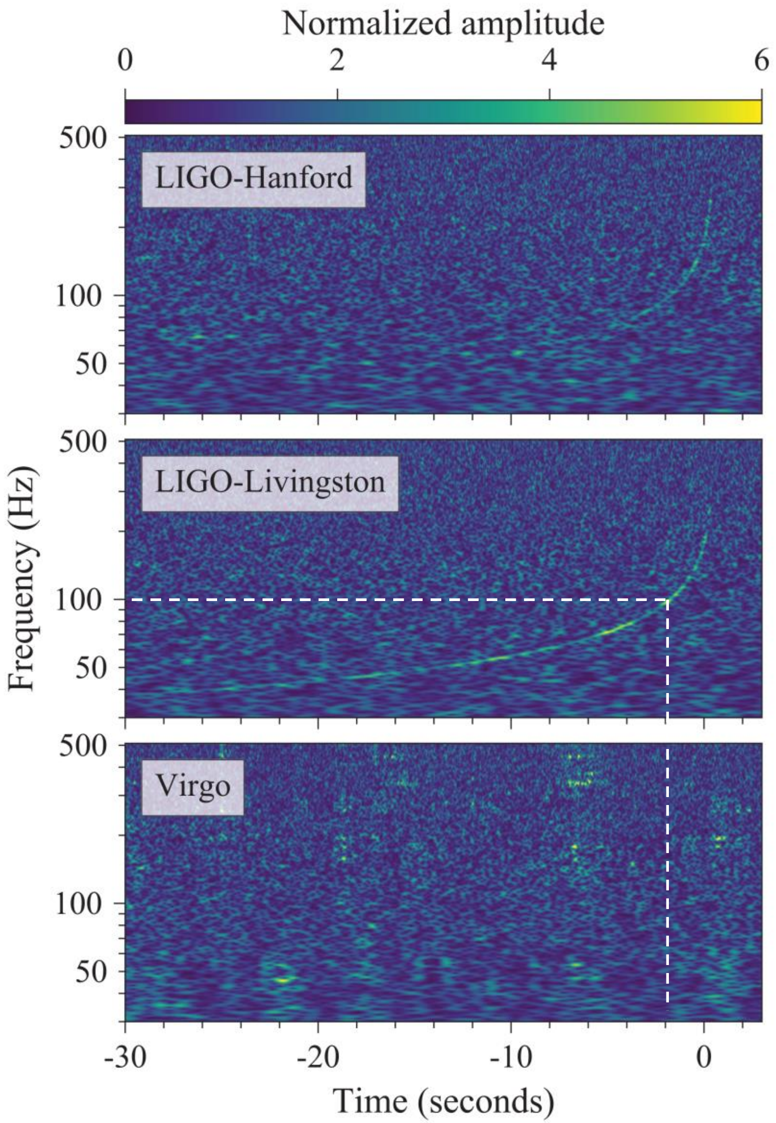

PRL 118, 221101 (2017)

GW170104 and previous

Data Release:
https://losc.ligo.org/events/GW170104/

➢ **Selected BH Binary Properties:**

matching templates comparison:

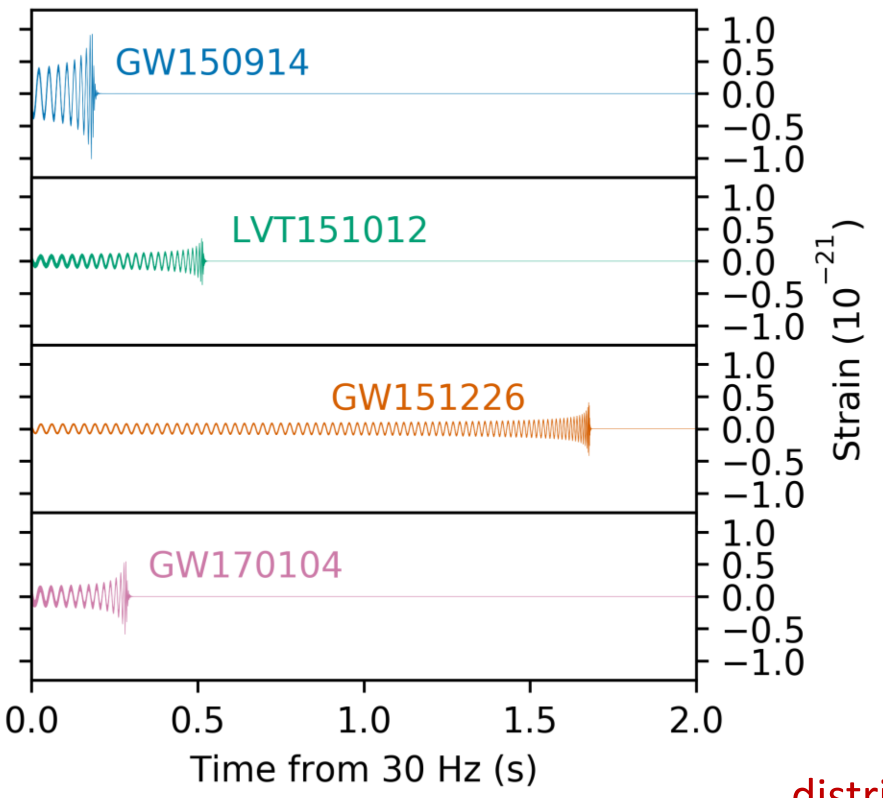

GW170608
Astrophys. J. Lett. 851, L35 (2017)
very similar to GW151226

distribution of primary BH component mass

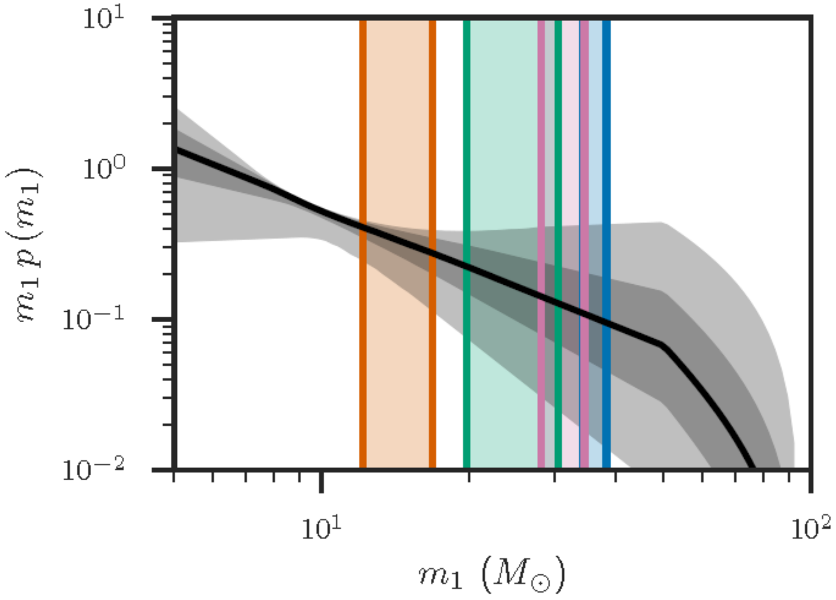

distribution of effective BH spin along orbital angular momentum

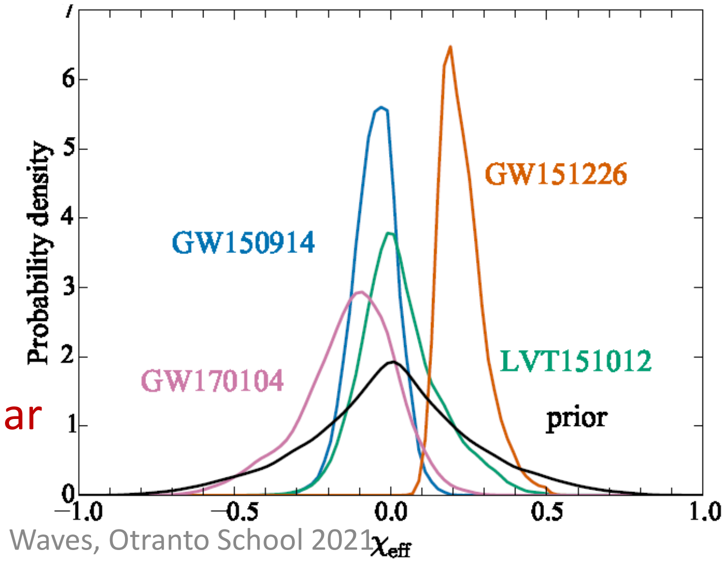

BBH Formation Models

dynamical interaction

isolated binary evolution

… ? primordial

Association of GW170817 and GRB170817A & Fundamental Physics

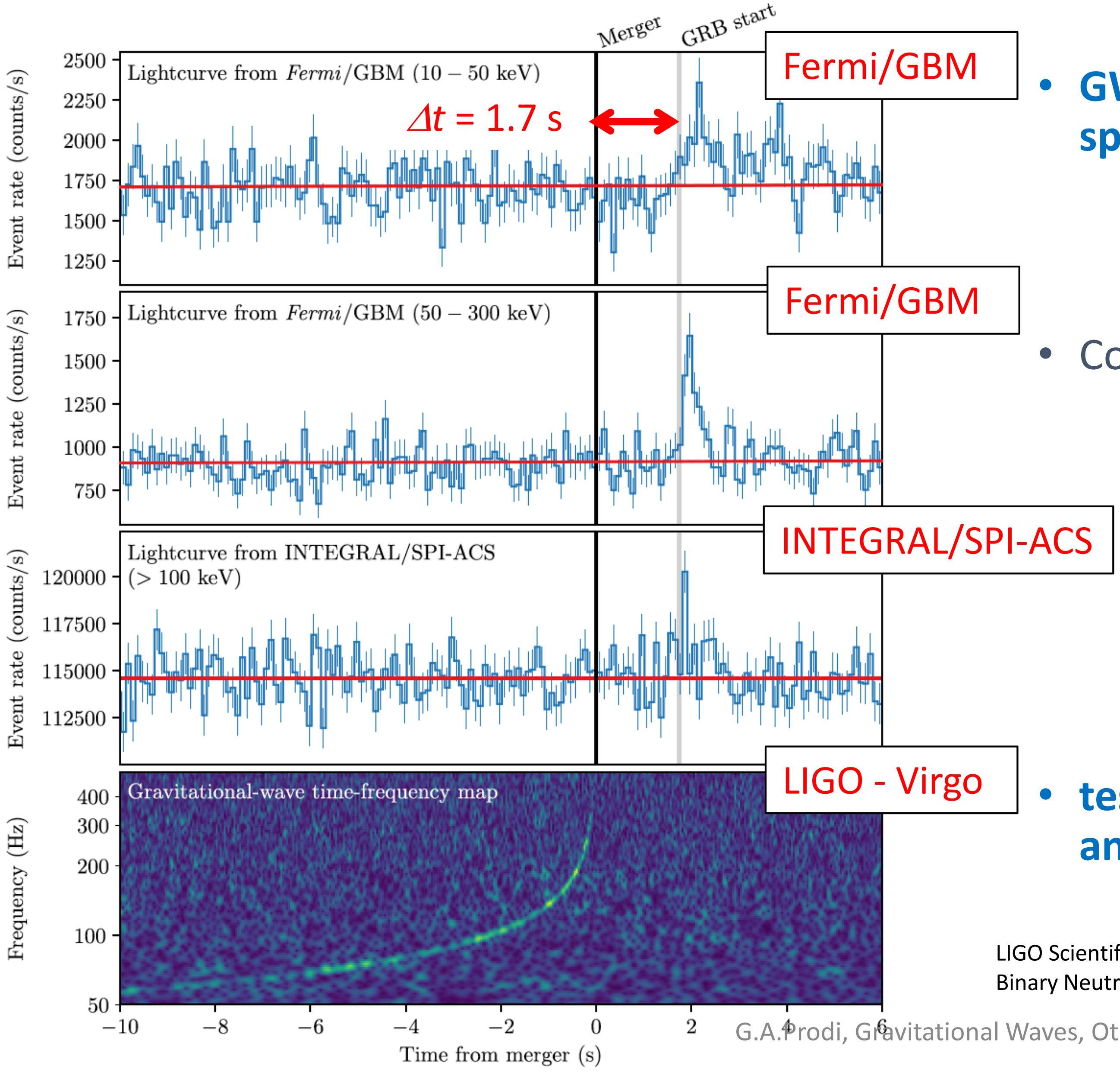

- **GW170817 provides a stringent test of the speed of gravitational waves**

$$\frac{v_{GW} - c}{c} \approx \frac{c\Delta t}{D}$$

- Conservative assumptions
  - t_{GW} - t_{EM} at emission in [-10, 0] sec
  - $D \approx$ 26 Mpc
    - Conservative limit – use 90% confidence level lower limit on GW source from parameter estimation

$$-3 \times 10^{-15} \leq \frac{\Delta v}{v_{\rm EM}} \leq +7 \times 10^{-16}$$

- ***testing violations of local Lorentz Invariance and Equivalence Principle***

LIGO Scientific Collaboration and Virgo Collaboration, Gravitational Waves and Gamma-Rays from a Binary Neutron Star Merger: GW170817 and GRB 170817A" Astrophys. J. Lett., 848:L13, (2017)

GW170104 and previous detections

First test of GR in strong field and highly relativistic speed

by checking the phase evolution of the inspiral

90% upper limits on $|\delta\varphi|$

$\delta\varphi$ describes possible deviations from GR prediction per each Post Newtonian order to the quadrupolar emission formula (considering one PN at a time)

New upper limits have been set for each PN order up to 3.5 except for 2.5 PN, unmeasurable with inspiral signal (degenerate with reference phase evolution)

limits from 10 years of double pulsar J0737-3039 are better only for the quadrupolar order 0PN

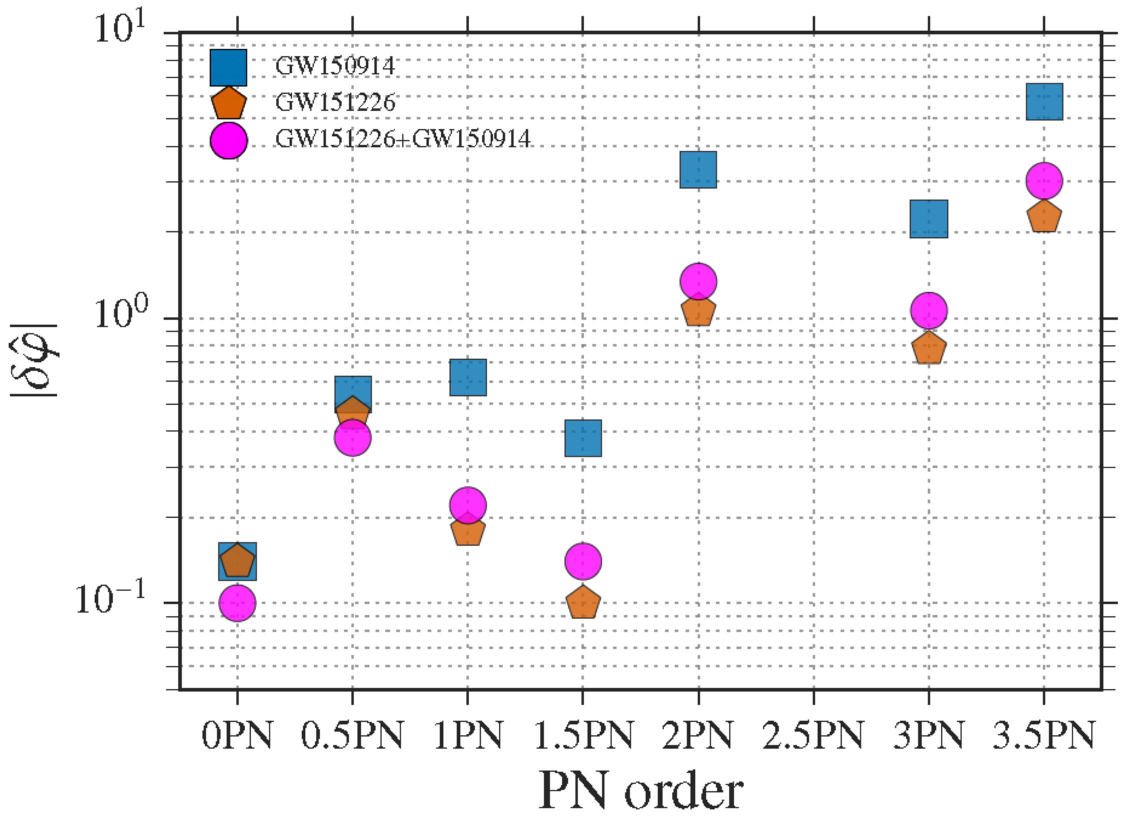

GW170104 and previous detections

First test of GR in strong field and highly relativistic speed

by checking the **phase evolution of the entire BBH coalescences**

posteriors on $\delta\varphi$

waveform regime	parameter	f–dependence
early-inspiral regime	$\delta\hat{\varphi}_0$	$f^{-5/3}$
	$\delta\hat{\varphi}_1$	$f^{-4/3}$
	$\delta\hat{\varphi}_2$	f^{-1}
	$\delta\hat{\varphi}_3$	$f^{-2/3}$
	$\delta\hat{\varphi}_4$	$f^{-1/3}$
	$\delta\hat{\varphi}_{5l}$	$\log(f)$
	$\delta\hat{\varphi}_6$	$f^{1/3}$
	$\delta\hat{\varphi}_{6l}$	$f^{1/3}\log(f)$
	$\delta\hat{\varphi}_7$	$f^{2/3}$
intermediate regime	$\delta\hat{\beta}_2$	$\log f$
	$\delta\hat{\beta}_3$	f^{-3}
merger–ringdown regime	$\delta\hat{\alpha}_2$	f^{-1}
	$\delta\hat{\alpha}_3$	$f^{3/4}$
	$\delta\hat{\alpha}_4$	$\tan^{-1}(af+b)$

post-Newtonian

effective

LVC, arXiv:1602.03841

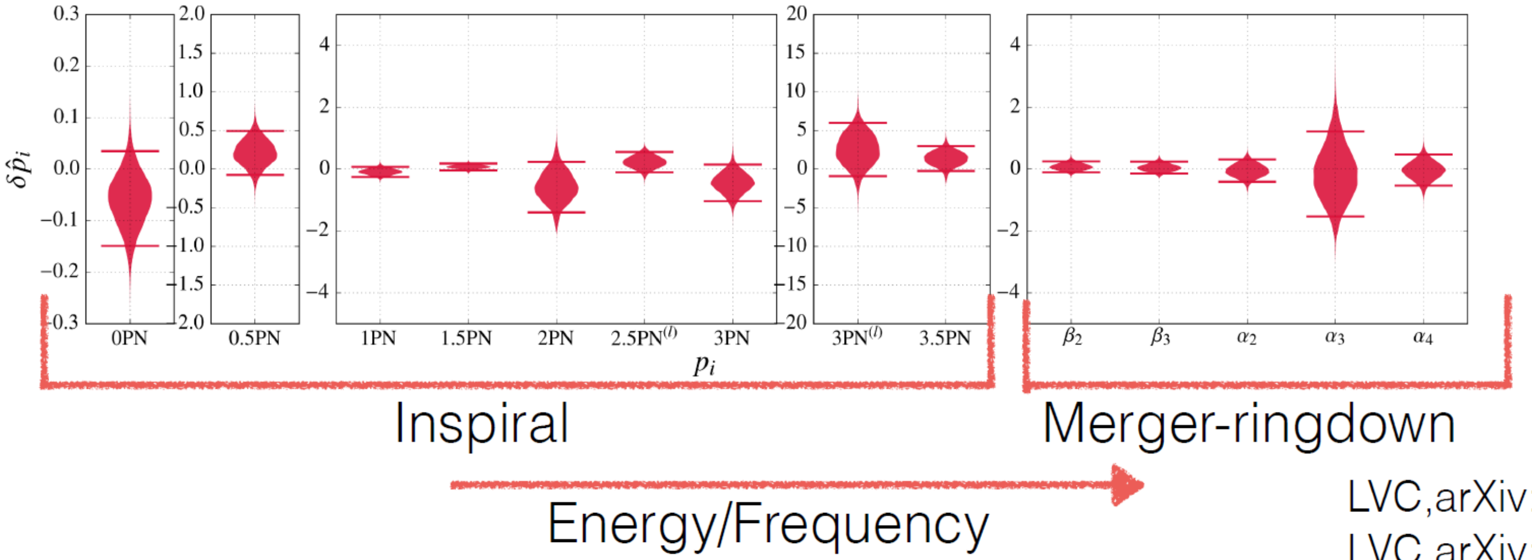

LVC,arXiv:1602.03841
LVC,arXiv:1606.04856

GW170814 : Sky localization & GW polarizations

Sky localization prediction greatly improved with Virgo
No electromagnetic or neutrino counterpart reported

PRL 118, 221101 (2017)

Rapid Analysis – 90% confidence
Only LIGO : 1160 deg^2
LIGO+Virgo : 100 deg^2

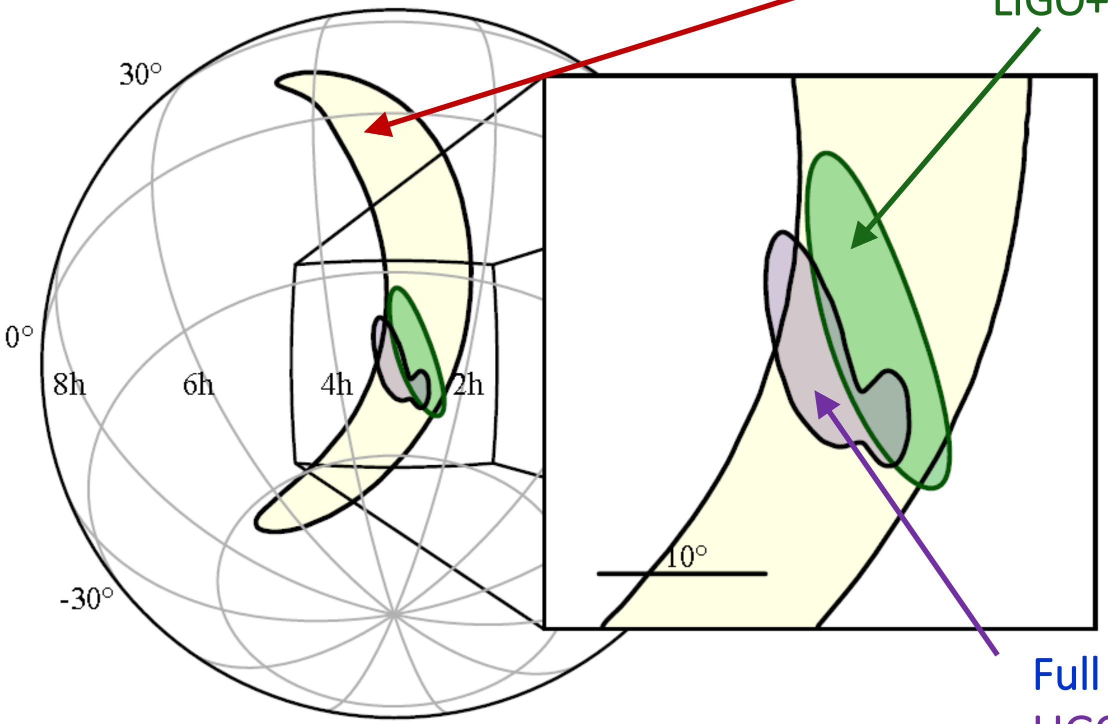

Estimated Distance
540 Mpc

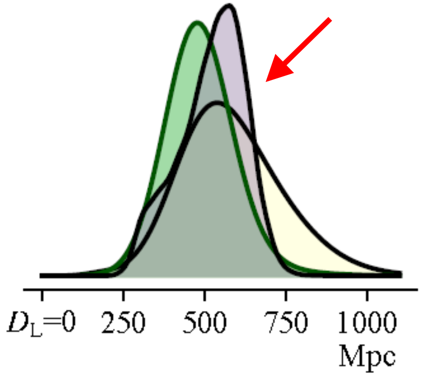

Full Analysis – 90% confidence
LIGO+Virgo : 60 deg^2

- **The volume** for GW170814 localization **is 30 times smaller** with the 3-detector network wrt the LIGO only network

GR polarization vs non-GR polarization

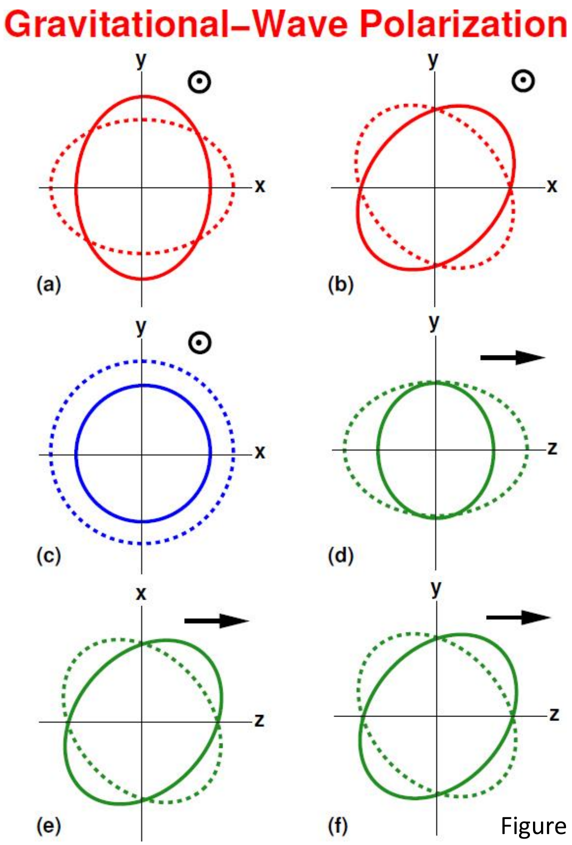

Tensor GR

Scalar non-GR

Vector non-GR

Figure 10 from Will (2014)

3 detector network enables investigations on GW polarizations.
The tensor polarizations are preferred

ENSURED SIGNALS

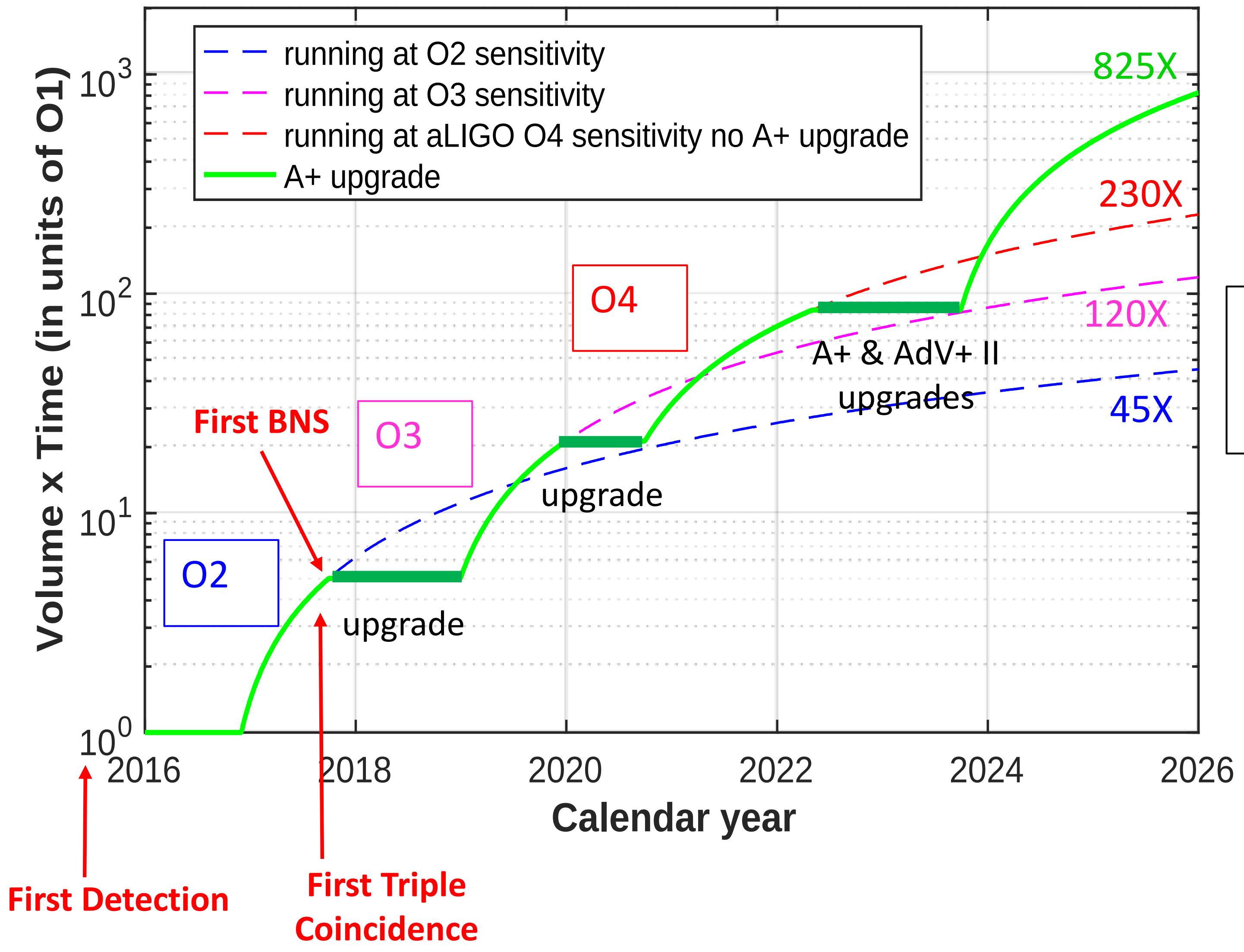

plotted values based on Binary Neutron Stars mergers

similar evolution for other compact object coalescences

N_{events} = <R>**VT** **VT *PRODUCTIVITY***

- <R> average astrophysical rate
- V volume of the universe probed → $(\text{Range})^3$
- T coincident observing time

expected ***rates of detections*** **with A+ AdV+**
≈ 100 x *rates of O2 detections*

a step-wise approach of upgrades interleaved by observation runs is the wisest strategy for exploiting the current infrastructures

NATURE OF GRAVITY

[PRL 118, 221101 (2017)]

Gravitational waves from binary black holes are the optimal probes to test

1) non linear regime of space-time dynamics: strongest field, highest curvature, fastest dynamics

self-consistency tests of GR predictions on reconstructed remnant mass and spin as inferred inspiral vs merger-ringdown phases)

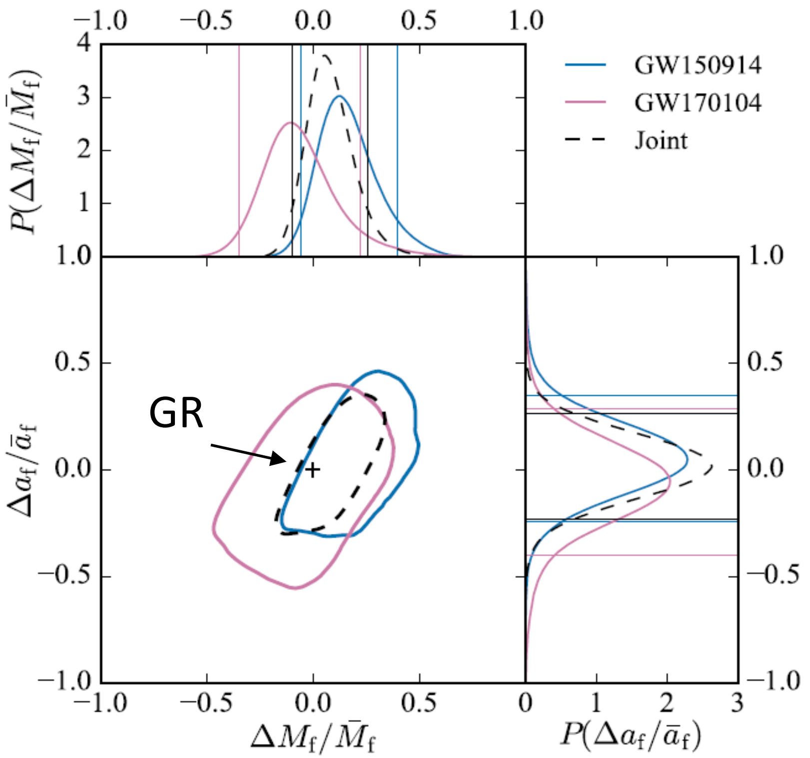

null tests on parametrized deviations of the phase evolution of the GW wrt General Relativity

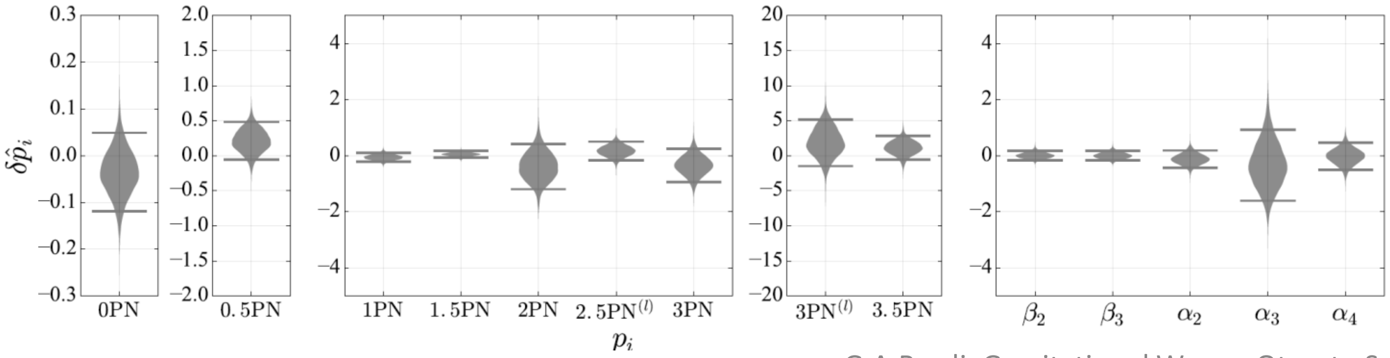

inspiral

merger ring-down

expected improvements in AdV+:

- longer inspiral duration (more cycles) in the detectors's band: x (a few)-10
- sqrt(number of detections) weighted by Signal-to-Noise Ratio

NATURE OF GRAVITY

nature of Black Holes, fundamental constituents in General Relativity

… link to quantum and Planck scale physics ?

- testing event horizon dynamics of Kerr Black Holes and no hair theorem

Berti+, Gen. Rel. Gravit (2018) 50:49

Black Hole spectroscopy (at least two Quasi Normal Modes) will be enabled by

- SNR $\approx$ 10 or greater in the ringdown for single events, e.g. 4 x SNR[GW150914]
- and/or stacking many measurements of ringdowns

$\Rightarrow$ both achievable by twin A+ & AdV+ II

Cardoso, Franzin, Pani, PRL 116, 171101 (2016)

Black Hole mimickers (exotic compact objects)

- GWs not fully absorbed by the "event horizon"

delayed "echoes" of the merger signal:

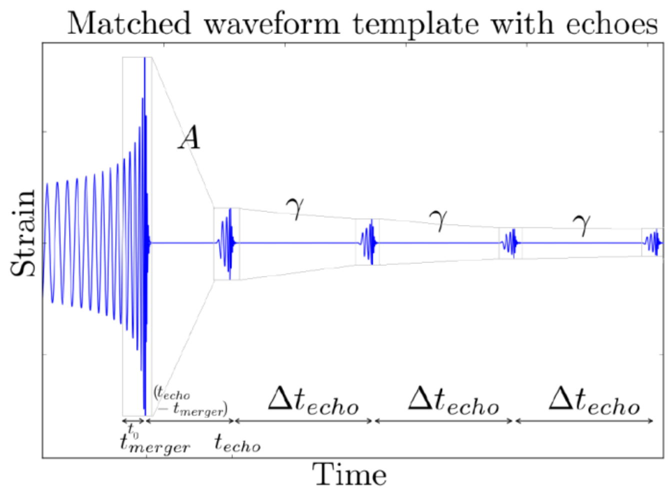

$\Rightarrow$ twin A+ & AdV+ will deeply invade parameter space of mimicker models

no evidence in LIGO-Virgo data: Westerweck+ PRD 97, 124037 (2018)

NATURE OF GRAVITY

nature of Gravitational Waves:

light speed propagation

- GRBs counterparts to test light speed (BNS or more distant NS-BH for the future)

GW and GRB170817 Astrophys. J. Lett. 848, L13 (2017)

conservative assumptions:
D=26Mpc
EM emission [-1.7,+10]s

$$\Delta v = v_{\mathrm{GW}} - v_{\mathrm{EM}}$$

$$\Delta v / v_{\mathrm{EM}} \approx v_{\mathrm{EM}} \Delta t / D$$

$$-3 \times 10^{-15} \leq \frac{\Delta v}{v_{\mathrm{EM}}} \leq +7 \times 10^{-16}$$

upper bound on graviton mass

$m_g \leq 7.7\ 10^{-23} eV$, 90%

testing the dispersion relation

$E^2 = p^2c^2 + Ap^\alpha c^\alpha \quad with\ \alpha \geq 0$

GR A=0, massive graviton (α=0 , A>0), …

first local Lorentz invariance test in the Gravitational Sector

testing against alternative models for CBC waveforms:

- dispersion relation equation, mass of graviton

- non GR polarizations (also in persistent signals)

based on the different directional sensitivity of detectors

GW information alone requires the 3 LIGO-Virgo unless the counterpart sky location is known

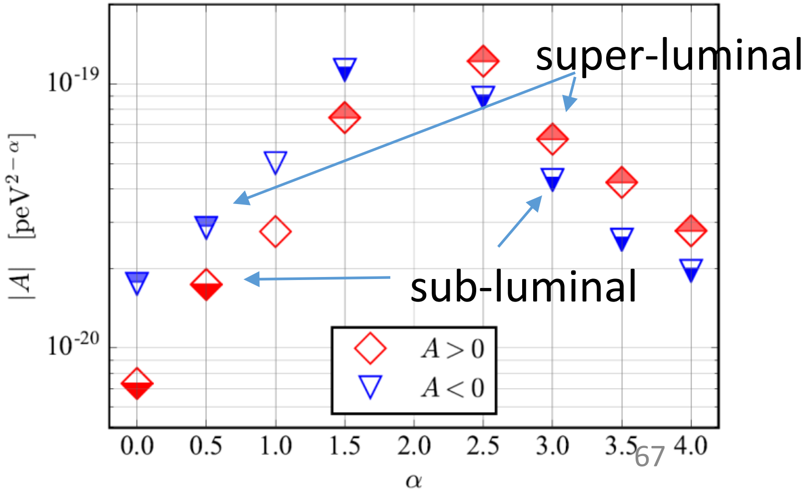

GW signal vs Noise Separation

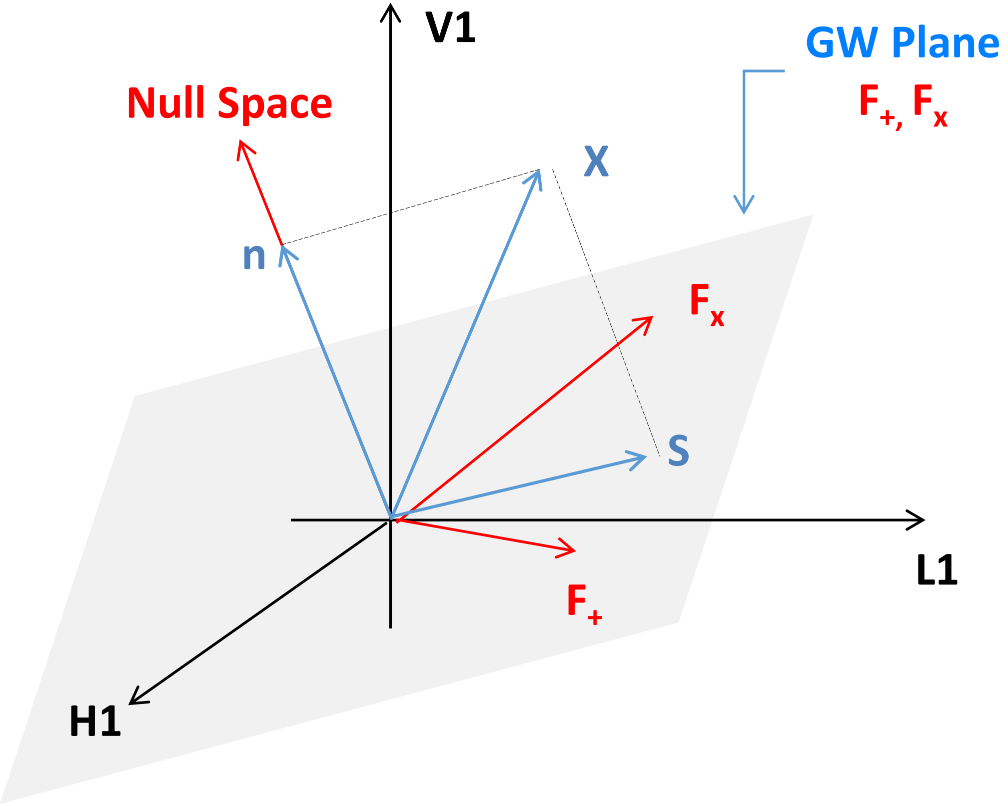

Basic principles of a **Coherent Network Data Analysis**:

- **H1,L1,V1,** … is the detector frame
- **X** is the data vector (H1,L1,V1, …) e.g. a time-frequency pixel
- F_{+}, F_{x} are the antenna pattern of the network of detectors for a given sky direction and spectral range, i.e.
- F_{+}, F_{x} define the **GW Plane** of all possible network responses to a GW from a given direction and at a given frequency
- **Null Space** is the noise contribution to the data **X** and is ⊥ to **GW Plane**

Each data X = S + n $\left\{ \begin{array}{l} \textbf{GW signal component S} \in \textbf{GW Plane} \\ \textbf{noise component n} \perp \textbf{GW Plane , i.e. n} \in \textbf{Null Space} \end{array} \right.$

this decomposition is a function of sky direction and frequency through the spectral and directional sensitivities of the detectors in the newtork.

With at least 3 detectors we can separate noise from signal components without relying on signal models